

AN ABSTRACT OF THE DISSERTATION OF

Sarah J. K. Frey for the degree of Doctor of Philosophy in Forest Science presented on December 9, 2014.

Title: Effects of Spatial Scale and Heterogeneity on Avian Occupancy Dynamics and Population Trends in Forested Mountain Landscapes

Abstract approved:

Matthew G. Betts

Population trends and patterns in species distributions are the major currencies used to examine responses by biodiversity to changing environments. Effective conservation recommendations require that models of both distribution dynamics and population trends accurately reflect reality. However, identification of the appropriate temporal and spatial scales of animal response, and then obtaining data at these scales present two major challenges to developing predictive models. In heterogeneous forested mountain landscapes I examined: A) the relative drivers of climatic variability at fine spatial scales under the forest canopy ('microclimate'), B) the influence of microclimate on local-scale occupancy dynamics of bird communities, and C) the effects of spatial scale and imperfect bird detection on long-term avian population trends.

Climate change has been predicted to cause widespread biodiversity declines. However, the capacity of climate envelope models for predicting the future of biodiversity has been questioned due to the mismatch between the scale of available data (i.e., global climate models) and the scales at which organisms experience their environment. Local-scale variation in microclimate is hypothesized to provide potential 'microrefugia' for biodiversity, but the relative role of elevation, microtopography, and vegetation structure in driving microclimate is not well known. If the microrefugia hypothesis is true, I expected to see areas on the landscape that

remained relatively cooler (i.e., buffered sites). To test this, I collected temperature data at 183 sites across elevation and forest structure gradients in complex terrain of the H. J. Andrews Experimental Forest in the Cascade Mountains of Oregon, USA (**Chapter 2**). I used boosted regression trees, a novel machine learning approach, to determine the relative influence of vegetation structure, microtopography, and elevation as drivers of microclimate and mapped fine-scale distributions of temperature across the landscape. Models performed extremely well on independent data – cross-validation correlations between testing and training data were 0.69 – 0.98 for ten selected climate variables. Elevation was the dominant driver in fine-scale microclimate patterns, although vegetation and microtopography also showed substantial relative influences. For instance, during the spring-summer transition, maximum monthly temperatures observed in old-growth sites were 2.6°C (95% CI: 1.8 – 3.3°C) cooler than plantation sites and minimum temperatures during winter months were 0.6°C (95% CI: 0.4 – 0.8°C) warmer. This suggests that older forest stands mediate changes in temperature by buffering against warming during summer months and moderating cold temperatures during the winter.

Climate is generally considered most influential on species distributions at large spatial scales; however much microclimate variability exists within regional patterns. I tested whether this high degree of microclimate variability has relevance for predicting species distributions and occupancy dynamics of the Andrews Forest bird community. I collected bird occurrence data in 2012 and 2013 at all 183 sites with fine-scale temperature measurements. I used dynamic occupancy models to test the effects of temperature on occupancy and apparent within-season bird movement while statistically accounting for vegetation effects and imperfect bird detection (**Chapter 3**). Most species (87%) exhibited within-season shifts in response to local-scale temperature metrics. Effects of temperature on within-season occupancy dynamics were as large or larger (1 to 1.7 times) than vegetation. However, individual species were almost as likely to shift toward warmer sites as toward cooler sites, suggesting that microclimate preferences are species-specific. My results emphasize that high-resolution temperature data provide valuable insight into avian distribution dynamics in montane forest environments and that microclimate is an important variable in breeding season habitat selection by forest birds. I hypothesize that microclimate-associated distribution shifts may reflect species' potential for behavioral buffering from climate change in complex terrain.

Factors influencing population trends often differ depending on the spatial scale under consideration. Further, accurate estimation of trends requires accounting for biases caused by imperfect detection. To test the degree to which population trends are consistent across scales, I estimated landscape-scale bird population trends from 1999-2012 for 38 species at the Hubbard Brook Experimental Forest (HBEF) in the White Mountains of New Hampshire, USA and compared them to regional and local trends (**Chapter 4**). I used a new method – open-population binomial mixture models – to test the hypothesis that imperfect detection in bird sampling has the potential to bias trend estimates. I also tested for generalities in species responses by predicting population trends as a function of life history and ecological traits. Landscape-scale trends were correlated with regional and local trends, but generally these correlations were weak ($r = 0.12 - 0.4$). Further, more species were declining at the regional scale compared to within the relatively undisturbed HBEF. Life history and ecological traits did not explain any of the variability in the HBEF trends. However, at the regional scale, species that occurred at higher elevations were more likely to be declining and species associated with older forests have increased. I hypothesize that these differences could be attributed to both elevated rates of land-use change in the broader region and the fact that the structure of regional data did not permit modeling of imperfect detection. Indeed, accounting for imperfect detection resulted in more accurate population trend estimates at the landscape scale; without accounting for detection we would have both missed trends and falsely identified trends where none existed. These results highlight two important cautions for trend analysis: 1) population trends estimated at fine spatial scales may not be extrapolated to broader scales and 2) accurate trends require accounting for imperfect detection.

© Copyright by Sarah J. K. Frey

December 9, 2014

All Rights Reserved

Effects of Spatial Scale and Heterogeneity on Avian Occupancy Dynamics and Population
Trends in Forested Mountain Landscapes

by
Sarah J. K. Frey

A DISSERTATION

submitted to

Oregon State University

in partial fulfillment of
the requirements for the
degree of

Doctor of Philosophy

Presented December 9, 2014
Commencement June 2015

Doctor of Philosophy dissertation of Sarah J. K. Frey presented on December 9, 2014.

APPROVED:

Major Professor, representing Forest Science

Head of the Department of Forest Ecosystems and Society

Dean of the Graduate School

I understand that my dissertation will become part of the permanent collection of Oregon State University libraries. My signature below authorizes release of my dissertation to any reader upon request.

Sarah J. K. Frey, Author

ACKNOWLEDGEMENTS

This research was possible with support from multiple grants and awards including: an NSF-IGERT fellowship awarded to Sarah Frey (from NSF-0333257), a Department of the Interior Northwest Climate Science Center graduate fellowship awarded to Sarah Frey, an HJ Andrews Forest LTER⁶ graduate research assistantship awarded to Sarah Frey (from NSF-0823380), a Catherine Bacon Memorial graduate fellowship awarded to Sarah Frey, and a James Duke Memorial fellowship awarded to Sarah Frey. Additional support and resources were provided by US National Science Foundation LTER program at Hubbard Brook and the HJ Andrews Experimental Forests, National Science Foundation grants awarded to Matthew Betts, Julia Jones, and Weng-Keen Wong (NSF-ARC 0941748), and Julia Jones (NSF-1005175), and the Smithsonian Migratory Bird Center.

This dissertation has benefitted immensely from the profound insight and creativity of my advisor, Matt Betts. A simple thanks does not even come close to expressing my gratitude and appreciation for his input and advice over the last six years. I thank Matt for showing me that I am not the only (crazy) one willing to conduct high-resolution, landscape-scale field studies and that there are always more things to discover no matter how much data we collect. Matt's drive to conduct the highest quality research possible is truly inspiring.

I am grateful to my committee members, Julia Jones, Dave Hibbs, Weng-Keen Wong, and Douglas Robinson. Their diverse insight has enhanced the quality of my research.

The members of the Andrews Forest phenology group (Mark Schulze, Sherri Johnson, Judy Li, and Bill Gerth) deserve a special thanks for providing valuable input and support for my work at the Andrews Forest. They have done a great job of helping me think beyond birds. Jay Sexton also deserves special thanks. Without his bright demeanor and logistical genius, my project may not have gotten off the ground.

My work and professional development has benefitted greatly from all of the interactions and discussions with the Betts Lab group. I am humbled to stand on the shoulders of the Hubbard Brook giants Dick Holmes, Scott Sillett, and Nick Rodenhouse.

Field assistance at the Andrews Forest was provided by Adam Hadley, Iris Koski, Evan Jackson, Ari DeMarco, Lauren Smith, Joshua Stagner, April Bartelt, Sean Ashe, Marcel Villar, Sveta Yegorova, Katelin Stanley, Andrea Mott, Grace Milanowski, Bryan Doyle, Kellen Mortensen, and Erik Kreiensieck. I commend all of the field crews that collected field data in the rugged mountainous terrain of the Andrews Forest; field work at the Andrews Forest is anything but easy. I will never forget Joshua Stagner relating one of the most densely vegetated point count routes to “being filtered by a whale’s mouth”. I would like to extend a special thanks to Robin Miron who helped us see the forest from top to bottom.

My family and friends are a constant source of light in my life. Their love and support are unmatched; thank you all for believing in me. Muchísimas gracias a mi familia en Costa Rica por apoyarme tanto durante este proceso; Mau Paniagua y Tocho Sandí siempre me hacen sonreír con su luz. Most importantly, I could not imagine a better partner in life than my husband Adam. His contributions to making my life richer are unquantifiable.

CONTRIBUTION OF AUTHORS

Chapter 2: Dr. Matthew G. Betts provided critical insight on the sampling methods and assisted with the writing and analysis. Dr. Adam S. Hadley contributed to sampling design and writing. Drs. Sherri L. Johnson, Mark Schulze, and Julia Jones contributed to temperature sampling, processing of temperature data, and provided many thoughtful discussions about analysis and interpretation of results.

Chapter 3: Dr. Matthew G. Betts provided assistance with the experimental design, methods and analysis. Dr. Adam S. Hadley assisted with data collection, analysis and writing.

Chapter 4: Dr. Matthew G. Betts provided critical assistance with the formulation of this chapter and input on the writing throughout. Drs. Nick L. Rodenhouse, T. Scott Sillett, and Richard T. Holmes, contributed to data collection and interpretation. Dr. Adam S. Hadley contributed to writing and interpretation of results.

TABLE OF CONTENTS

	<u>Page</u>
1 GENERAL INTRODUCTION.....	2
2 UNDER-CANOPY TEMPERATURE PATTERNS IN A MOUNTAINOUS LANDSCAPE REVEAL BUFFERING CAPACITY OF VEGETATION STRUCTURE AND MICROTOPOGRAPHY.....	7
2.1 Abstract.....	7
2.2 Introduction.....	8
2.3 Methods.....	11
2.3.1 Environmental predictor variables.....	12
2.3.3 Response variables.....	13
2.3.4 Statistical analysis – Boosted Regression Trees.....	14
2.3.5 Statistical analysis – Principal Component Analysis.....	15
2.4 Results.....	16
2.4.1 Model performance & spatial autocorrelation.....	16
2.4.2 General temperature patterns.....	16
2.4.3 Variable-specific results.....	17
2.4.4 Principal Component Analysis.....	20
2.4.5 Scale effects.....	21
2.4.6 Temporal consistency.....	21
2.5 Discussion.....	21
2.5.1 Management implications.....	24
2.5.2 Conclusions.....	25
3 MICROCLIMATE PREDICTS WITHIN-SEASON DISTRIBUTION DYNAMICS OF MONTANE FOREST BIRDS.....	42
3.1 Abstract.....	42
3.2 Introduction.....	42
3.3 Methods.....	45
3.3.1 Study site.....	45
3.3.2 Site selection.....	45
3.3.3 Point counts.....	46
3.3.4 Environmental covariates.....	47
3.3.5 Vegetation structure and composition.....	47
3.3.6 Occupancy models.....	48
3.3.7 Model selection.....	50
3.3.8 Relative importance of microclimate and vegetation on occupancy dynamics.....	52
3.3.9 Model fit.....	52
3.4 Results.....	53
3.4.1 Detection & initial occupancy.....	53

TABLE OF CONTENTS (CONTINUED)

3.4.2 Apparent movement.....	54
3.4.3 Model fit.....	56
3.4.4 Annual temperature consistency	56
3.5 Discussion	57
3.5.1 Implications.....	60
3.5.2 Conclusions.....	61
4 THE IMPORTANCE OF SAMPLING SCALE AND IMPERFECT DETECTION IN ESTIMATING LONG-TERM AVIAN ABUNDANCE TRENDS	73
4.1 Introduction.....	74
4.2 Methods.....	76
4.2.1 Study site.....	76
4.2.2 Watershed-Scale Avian Surveys.....	76
4.2.3 Estimating abundance trends with binomial mixture models for open populations....	77
4.2.4 Linear regression with raw counts	78
4.2.5 Comparison of trends by spatial scale	79
4.2.4 Life history traits.....	79
4.3 Results.....	81
4.3.1 Effects of spatial scale	81
4.3.2 Effects of imperfect detection on population trends	82
4.4 Discussion	82
5 CONCLUSION.....	98
BIBLIOGRAPHY	104
APPENDICES	117

LIST OF FIGURES

<u>Figure</u>	<u>Page</u>
2.1. Maps showing A) the elevational gradient (meters) and microtopography, and B) Canopy height (meters) based on LiDAR from 2008 at the H. J. Andrews forest, Oregon, USA (Watershed Sciences 2008). Black dots show the 183 temperature sampling locations.	27
2.2. Relative importance of variables describing elevation, microtopography and vegetation for each temperature metric in both years A) 2012, B) 2013. Relative importance values were derived from the number of times each variable was selected in the process of model building using BRTs.....	28
2.3. Spatially predicted temperature metrics of cumulative degree days at the H. J. Andrews Experimental Forest based on BRT models. Response variables are: (A) Cumulative degree days >0°C January-March (CDD0JM), (B) CDD >0°C April-June (CDD0AJ), and (C). CDD >10°C April-June (CDD0AJ). Vegetation and microtopography had a high relative influence on degree days in January-March (A), but degree days in April-June were primarily a function of elevation.	29
2.4. Partial dependence plots of key microtopographic (TOPO) variables. The fitted functions generated using boosted regression show the effect of the variable on the response after accounting for all other variables in the model. (A) Sites with a larger range in elevation within 25m (i.e., steep slopes) and (B) more exposure accumulate more degree days January-March (CDD0JM 2013). C) Sites located in exposed areas also are more variable in temperature during this period (SDwTJM 2013). (D) Aspect played a large role in determining the maximum temperature of sites with north-facing slopes being coolest (MxTWM 2012). Relative variable importance is indicated in parentheses (RI%).	30
2.5. Key interactions identified from BRT models testing the effects of elevation, microtopography, and vegetation structure on microclimate. A) Exposed sites with low variability in biomass (e.g., plantation stands) accumulated the most degree days >0°C from January-March (CDD0JM 2013). B) Higher elevations (above ~1000m) were less variable in January-March (SDwTJM 2013), particularly if they had low topographic exposure. C) Mean monthly maximum temperature from April-June (MonMnMaxAJ 2013) was lowest at high elevations in high amounts of canopy cover in the surrounding landscape. D) An interaction between elevation and microtopography indicated that high elevation sites in areas of gentle slopes had the lowest minimum temperatures in April-June (MonMnMinAJ 2013).	31
2.6. Spatially predicted variability in weekly temperature at the H. J. Andrews Experimental Forest based on BRT models. Response variables are: (A) Standard deviation (SD) of weekly temperature January-March (SDwTJM), and (B) SD of weekly temperature April-June (SDwTAJ). Elevation, vegetation and microtopography all had large relative influences on variability in weekly temperature in 2012 (A). In 2013 variability in January-March had a high	

LIST OF FIGURES (CONTINUED)

component of vegetation and microtopography, but variation in April-June was primarily a function of elevation (B).....	32
2.7. Partial dependence plots of key vegetation (VEG) variables. (A) Sites with a higher coefficient of variation in canopy height and (B) more variable biomass showed less variability in January-March (SDwTJM 2013). Proportion of canopy >10m (C) and increasing biomass (D) both reduce monthly maximum temperatures. Sites with a higher proportion of the canopy over 10m in height (E) and higher values of median return (HOME) (F) had the highest minimum temperatures (MiTCM 2012). Sites with a high proportion of the canopy >10m (G) and taller canopies (H) reduced the variability in temperature April-June (SDwTAJ 2013). Relative variable importance is indicated in parentheses (RI%).....	34
2.8. Principal component analysis showing how vegetation structure metrics differ between old-growth/mature forest sites (OG-MAT) and plantations (PLANT). See Appendix 3 for vegetation structure predictor variable definition.....	35
2.9. Comparison of temperature metrics measured in both 2012 and 2013. The majority of temperature metrics (A, B, C, F, G, H) showed extremely consistent temperature patterns in the two years despite warmer overall temperatures in 2013. Temperature variability (D, E) showed less consistency. Maximum temperature of the warmest month and minimum temperature of the coldest month were omitted from this figure because they were only calculated for 2012 due to a complete year of data.	36
2.10. Spatially predicted temperature metrics showing monthly temperature at the H. J. Andrews Experimental Forest based on BRT models. Response variables are: (A) Mean monthly mean temperature April-June (MnMoMeanAJ), (B) Mean monthly maximum temperature April-June (MnMoMaxAJ), (C) Mean monthly minimum temperature April-June (MnMoMinAJ). Mean monthly temperatures were primarily a function of elevation (A), but maximum (B) and minimum temperatures (C) also had substantial relative influences of vegetation and microtopography.	37
2.11. Spatially predicted temperature metrics showing temperature extremes at the H. J. Andrews Experimental Forest based on BRT models. Response variables are: (A) Maximum temperature of the warmest month (MxTWM), and (B) Minimum temperature of the coldest month (MiTCM). Maximum temperatures were primarily a function of vegetation and topography (A), but minimum temperatures were primarily influenced by elevation.	38
2.12. Results from generalized linear regression models testing the effect forest structure (PC1) on A) MonMnMaxAJ and B) MiTCM after accounting for the effect of elevation. A) and B) show the modeled relationship between forest structure (PC1) and the residuals from an elevation-only model of MonMnMaxAJ (A) and MiTCM (B). Maximum monthly temperatures observed in old-growth sites were 2.6°C (95% CI: 1.8 – 3.3°C) cooler than plantation sites during the spring-summer transition (A) and minimum temperatures during winter months were 0.6°C (95% CI: 0.4 – 0.8°C) warmer in old-growth stands (B). Three-dimensional LiDAR-	

LIST OF FIGURES (CONTINUED)

generated images of old-growth forest (i = side, ii = top) and plantation forest (iii = side, iv = top) at H. J. Andrews Experimental Forest.....	39
2.13. Relative importance of variables measured at 25m and 250m scales for each temperature metric in both years. Relative importance values are derived from the number of times each variable is selected in the process of model building using BRT	40
3.1. The proportion of species in each year for each of the ecological parameters where the effect of 1) temperature alone (TEMP), 2) both vegetation and temperature (BOTH), or 3) vegetation alone (VEG) were significant (at $P < 0.05$) in the top model, or whether 4) neither vegetation nor temperature (NEITHER) were significant in the top model. Initial occupancy described the distribution in the first sample session (mid-May). Settlement and vacancy described patterns in ‘apparent movement’ between the second and sixth sample sessions (late-May until early-July).	65
3.2. Hermit warbler (HEWA, <i>Setophaga occidentalis</i>) is an example of a species where local site-scale dynamics are largely driven by temperature and vegetation structure to a lesser extent. Hermit warblers were both less likely to settle sites (A) and more likely to vacate sites (C) that were warmer. Vegetation structure was not a significant predictor of either vacancy (B) or settlement (D).	66
3.3. Pacific wren (PAWR, <i>Troglodytes pacificus</i>) is an example of a species where both temperature and vegetation were important in within season dynamics. Pacific wrens were more likely to settle warmer sites (A) and vacate cooler sites (E). Pacific wrens were more likely to settle sites with old-growth characteristics (B) and higher deciduous composition (C). Wrens were more likely to vacate even-aged vegetation stands such as plantations (D).	67
3.4. Predicted maps for hermit warbler (A) initial occupancy, (B) settlement, (C) vacancy and (D) final occupancy patterns at the end of the sampling period. By the end of the season (D) hermit warblers have shifted away from warmer sites towards cooler sites.....	68
3.5. Predicted maps for Pacific wren (A) initial occupancy, (B) settlement, (C) vacancy and (D) final occupancy patterns at the end of the sampling period. By the end of the season (D) hermit warblers have shifted away from plantation sites towards older forest sites sites. Predicted maps do not include proportion of deciduous basal area since it is a local-site vegetation variable.	69
3.7. Mean population trend estimates from BBS data grouped by species that showed cool vs warm associations in the H. J. Andrews dataset. We detected weak evidence for population declines in species we identified as being ‘cool-associated (mean trend [95% CIs] = -1.06 %/year [-1.96 – -0.16]) at the regional scale (BBS) relative to their warm-associated counterparts (-0.16 %/year [-0.99 – 0.68]). CIs for trends of cool-associated species did not include 0, where trends for warm-associated species did. Breeding Bird Survey 2002-2012 trends from the Northern Pacific Rainforest region (OR, WA, CA; (Sauer et al. 2014).	71

LIST OF FIGURES (CONTINUED)

- 4.1. Map of the 3400-ha Hubbard Brook Experimental Forest study area showing valley-wide 371 sample points (black dots), LTREB plot (star), and elevational distribution (in meters)..... 87
- 4.2. A) Abundance trend estimates (% change/year) for 38 bird species at Hubbard Brook Experimental Forest in the White Mountains of New Hampshire from 1999-2012. Trend estimates account for sampling error due to uneven detection rates. Error bars are 90% credible intervals. B) Breeding bird survey abundance trend estimates for 38 bird species in the state of New Hampshire, USA from 1999-2012. Error bars are 90% credible intervals. Filled circles represent significant trends (90% CIs do not overlap 0). Open circles are stable, or non-significant trends (90% CIs overlap 0). See Appendix 1 for definition of species codes. C) Direct comparison of abundance trends by species between HBEF and BBS. The solid line is 1:1 (intercept = 0, slope = 1). The dotted lines divide the plot into four quadrants: top right = both trends are positive, top left = HBEF hierarchical models predict positive trend, traditional models predict negative trend, bottom right = traditional models predict positive trend, hierarchical models predict negative trend, and bottom left = both trends are negative. 89
- 4.3. A) 1999-2012 abundance trends from the long-term (LTREB) 30x30m plot at Hubbard Brook. Error bars are 90% confidence intervals. Filled circles represent significant trends (90% CIs do not overlap 0). Open circles are stable, or non-significant trends (90% CIs overlap 0). See Appendix 1 for definition of species codes. B) Direct comparison of abundance trends by species between HBEF and LTREB plot. The solid line is 1:1 (intercept = 0, slope = 1). The dotted lines divide the plot into four quadrants: top right = both trends are positive, top left = HBEF hierarchical models predict positive trend, traditional models predict negative trend, bottom right = traditional models predict positive trend, hierarchical models predict negative trend, and bottom left = both trends are negative. 91
- 4.4. A) Effect size estimates for the influence of life history traits on patterns in abundance trends from Hubbard Brook Valley. Estimates are from univariate generalized mixed models with family as the random effect. Error bars are 95% confidence intervals. B) Effect size estimates for the influence of life history traits on patterns in abundance trends from the New Hampshire Breeding Bird Survey. Estimates are from univariate generalized mixed models with family as the random effect. Error bars are 95% confidence intervals. SSI = species specialization index (see methods for how this variable is calculated), low value indicates a generalist species and a high number indicates a specialist species. Elev., Canopy Ht., and Basal Area refer to the mean elevation, canopy height, and basal area at which the species is most abundant. Migration: LD = long distance, SD = short distance. 93
- 4.5. A) HBEF trend estimates using linear regression that assumes perfect detection of all species (uses raw counts to infer ecological state of interest, in this case abundance). Filled circles represent significant trends (90% CIs do not overlap 0). Open circles are stable, or non-significant trends (90% CIs overlap 0). See Appendix 1 for definition of species codes. B) Direct comparison of abundance trends by species between HBEF hierarchical models and traditional models using raw counts. The solid line is 1:1 (intercept = 0, slope = 1). The dotted lines divide the plot into four quadrants: top right = both trends are positive, top left = HBEF hierarchical

LIST OF FIGURES (CONTINUED)

models predict positive trend, traditional models predict negative trend, bottom right = traditional models predict positive trend, hierarchical models predict negative trend, and bottom left = both trends are negative. 95

4.6. Comparison of abundance trends between scales and modeling methods for four species. HBEF raw abundance and estimates from the hierarchical model are number of individuals in a point count circle (50-m radius around sample point). Abundance in the LTREB plot is the number of individuals within the 10-ha plot. The BBS produces an index of relative abundance per sampling route (25 miles in length). A) White-breasted nuthatch was increasing in BBS and HBEF datasets, but decreasing in the LTREB plot. B) Yellow-bellied flycatcher was declining in both BBS and HBEF. C) American redstart, was declining in all datasets and was almost absent from HBEF at the end of the 14-year period. D) Blackburnian warbler was relatively stable at HBEF, increasing in the LTREB and decreasing in the BBS dataset. 96

LIST OF TABLES

<u>Table</u>	<u>Page</u>
2.1. Generalized linear regression model results for the relationship between temperature metrics and the first component (PC1) of a principle component analysis representing a gradient in vegetation structure.	26
3.1. Species list for the 15 bird species we examined at the H. J. Andrews Experimental Forest.	62
3.2. Coefficients and standard errors for apparent settlement (γ) by species and year for top models.	63
3.3. Coefficients and standard errors for apparent vacancy (ε) by species and year for top models.	64

LIST OF APPENDICES

<u>Appendix</u>	<u>Page</u>
2.1. Details concerning deployment and maintenance of temperature sensors.....	117
2.2. Details about temperature data processing (cleaning, flagging, pruning, and filling).....	118
2.3. Predictor variables used to predict patterns in microclimate metrics.....	119
2.4 BRT model settings (Learning rate, No. trees), performance diagnostics (Deviance, Deviance SE, CV corr, CV SE), and tests for spatial autocorrelation in the BRT model residuals (Moran's I and P).....	120
2.5. Results from a PCA of all vegetation structure predictor variables and box plots comparing on the ground basal area measurements to forest type (plantation vs. old-growth/mature forest) categorizations.....	121
2.6. Summary statistics for all temperature metrics and results from Welch two-sample t-tests comparing temperature metrics measured in both 2012 and 2013.....	123
3.1. Map of the H. J. Andrews Experimental Forest, Blue River, Oregon with the 183 sample locations.....	124
3.2. Pearson's correlation coefficients between all predictor variables.....	125
3.3. Constant rates for all parameters.....	126
3.4. Coefficients and standard errors for detection probability.....	127
3.5. Coefficients and standard errors for initial occupancy.....	129
3.6. Comparison of effect sizes between fine-scale temperature and vegetation for settlement and vacancy probability in the top models by species and year.....	130
3.7. Predicted occupancy probability as a function of temperature and vegetation in the final sampling session of 2012 (session 6; late June to mid-July) for the warm-associated species...	131
3.8. Predicted occupancy probability as a function of temperature and vegetation in the final sampling session of 2012 (session 6; late June to mid-July) for the cool-associated species.....	132
3.9. Goodness-of-fit bootstrap results for top models of all species in 2012 and 2013.....	133
3.10. Results from tests for spatial autocorrelation in the residuals from the top models for all species in 2012 and 2013.....	134
3.11. Google docs site for AIC model selection tables.....	135
4.1. Species list and life history traits used in analysis.....	136

LIST OF APPENDICES (CONTINUED)

4.2. Map of the Hubbard Brook Experimental Forest study area showing forest cover types....	137
4.3. Prior distributions for model parameters.....	138

DEDICATION

To my dear mother, whose support and love was without limits. Thank you for teaching me that with hard work and dedication no dream is too big to attain.

Effects of Spatial Scale and Heterogeneity on Avian Occupancy Dynamics and Population
Trends in Forested Mountain Landscapes

1 GENERAL INTRODUCTION

Climate change is exerting a strong influence on species distribution dynamics and population trends (Parmesan and Yohe 2003, Thomas et al. 2004, Both et al. 2006, Hitch and Leberg 2007, Devictor et al. 2008, Gutiérrez Illán et al. 2014). Given that climate influences are expected to amplify over the coming century (IPCC 2014), a key question is the degree to which such trends will continue, and whether biodiversity will decline as a result (Thomas et al. 2004). Effective conservation recommendations in the face of future change require that models of both population trends and distribution dynamics accurately reflect reality (Bellard et al. 2012). However, identification of the appropriate temporal and spatial scales of animal responses (Wiens 1989), and data acquisition at these scales (Potter et al. 2013b) present two major challenges to developing predictive models (Betts et al. 2006).

Species abundance patterns are influenced by processes operating at multiple spatial scales. Therefore, distributions and trends may differ depending on the spatial scale investigated (Wiens 1989, Bohning-Gaese et al. 1994). Species distributions at large spatial scales are generally considered to be climate-driven (Thuiller et al. 2004a, Thomas 2010, Boucher-Lalonde et al. 2014) and at smaller scales, factors such as land cover and species interactions are hypothesized to be more influential (Brown et al. 1995, Luoto et al. 2007). For example, stochasticity in food resources or patchiness in vegetation structure can result in disparate abundance patterns at local versus regional scales. The scale at which measurements should be taken is a function of the ecological questions being asked (Seo et al. 2009). Failure to choose the appropriate scale for investigation may lead to misguided conclusions due to the mismatch between sample unit and the scale at which organisms interact with their environment (Wiens 1989). Despite this, many studies are conducted at smaller spatial scales yet aim to transfer these local patterns to the larger landscape (Urban 2005). The degree to which population trends are consistent across spatial scales has rarely been examined (but see Holmes and Sherry 1988).

The capacity of climate envelope models for predicting the future of biodiversity has been questioned due to the mismatch between the scale of available data (i.e., global climate models) and the scales at which organisms experience their environment (Bernardo 2014). Climate stations are typically placed in open areas and often are separated by large distances

(Scherrer et al. 2011). Therefore they provide little insight into small-scale drivers of microclimate patterns – particularly under forest canopies. In heterogeneous environments, such as complex mountainous systems, considerable variability in local-scale climate (i.e., microclimate) can exist within a relatively small area (Potter et al. 2013b). Patterns in microclimate across forested mountain landscapes likely arise from a combination of elevation, microtopography, and vegetation structure, but the relative roles of these three factors in driving microclimate are not well known.

The potential for local microclimate variability to influence species distribution patterns has largely been ignored (Potter et al. 2013b) due to both the logistical constraints in measuring temperature at fine resolutions over large spatial extents (Logan et al. 2013, Potter et al. 2013b) and the general assumption that factors other than climate are more dominant drivers at small spatial scales (Brown 1995, Boucher-Lalonde et al. 2014). However, local-scale variation in microclimate is hypothesized to provide potential ‘microrefugia’ for biodiversity (Ashcroft 2010).

The broad goal of this thesis was to understand how spatial scale differences influenced the ecological patterns we observed in forested montane systems. I started by comparing the relative drivers of climatic variability at fine spatial scales (i.e., ‘microclimate’). I modeled microclimate patterns under forest canopy in complex terrain of the HJ Andrews Experimental Forest (HJAEF) in the western Cascade Mountains of Oregon, USA (**Chapter 2**). Next, I explored the influence of microclimate on local-scale occupancy dynamics of bird communities in the HJAEF (**Chapter 3**). Finally I examined the effects of spatial scale and imperfect detection on long-term avian population trends at local, landscape and regional scales surrounding the Hubbard Brook Experimental Forest (HBEF) in the White Mountains of New Hampshire, USA (**Chapter 4**).

1. What drives patterns of understory microclimate variability in mountainous terrain? (Chapter 2)

I collected temperature data at 183 sites across elevation and forest structure gradients in complex terrain of the HJAEF. The HJAEF is larger (6400-ha) and consists of a forest mosaic of plantations, old-growth, and mature forests. The dramatic nature of the terrain (very steep slopes and narrow valleys) creates temperature inversions due to cold-air pooling—a common

occurrence on the landscape (Daly et al. 2010). This combined variability in microtopography and vegetation structure in the HJAEF provided an excellent opportunity to examine patterns of microclimate. I used boosted regression trees, a novel machine learning approach, to test the relative influence of vegetation structure, microtopography, and elevation as drivers of microclimate. I also mapped fine-scale distributions of temperature across the landscape. If potential for microrefugia existed within the HJAEF, I expected to see areas on the landscape that remained relatively cooler (i.e., buffered sites).

2. Can local microclimate variability influence distribution dynamics of forest birds? (Chapter 3)

I tested whether site occupancy dynamics of the bird community were influenced by the high degree of microclimate variability at HJAEF that I observed in **Chapter 2**. I collected bird occurrence data in 2012 and 2013 at all 183 sites with fine-scale temperature measurements. I used dynamic occupancy models to test the effects of temperature on occupancy and apparent within-season bird movement while statistically accounting for vegetation effects and imperfect bird detection.

3A. Are avian population trends consistent across scales? (Chapter 4)

To test population trend consistency, I estimated landscape-scale bird population trends from 1999-2012 for 38 species at the HBEF and compared them to both regional and local trends. HBEF is a 3160-ha bowl-shaped valley comprised of contiguous second-growth forest with a gradual transition from northern hardwood forest at lower elevations to softwood-dominated forests at upper elevations (elevation range 222 – 1015 m.a.s.l.). HBEF is relatively undisturbed, with no history of anthropogenic disturbance for a century (since 1915, (Holmes 2011), aside from small experimental watershed cuts in 1965 (Likens et al. 1970). In contrast, regional conditions are more fragmented, with higher levels of anthropogenic disturbance due to rural housing developments (Kluza et al. 2000) and timber harvest practices (Kittredge Jr et al. 2003). Three long-term datasets of avian population data were collected over the last 14 years at local (10-ha plot, (Holmes and Sherry 2001, Holmes 2011), landscape (3160-ha watershed, (Doran and Holmes 2005), and regional scales (Breeding bird survey data, (Sauer et al. 2014).

3B. Do detection biases affect trend estimates? (Chapter 4)

Sampling techniques often introduce biases that can make inferences about populations problematic. Raw counts arise from a combination of two interrelated processes, the ecological (state) process and the observation process (Kéry 2011). Not accounting for such biases through study design and analysis can lead to biased estimates or a lack of power to detect important demographic patterns (Tyre et al. 2003, Guillera-Aroita et al. 2010). By not accounting for detection probability in estimating abundance trends, researchers risk missing trends (type I error) or identifying trends that are not real and due to changes in detection over time rather than abundance (type II error). To test the hypothesis that imperfect detection in bird sampling has the potential to bias trend estimates, I used a new method – open-population binomial mixture models (Kéry et al. 2005) – to estimate detection-corrected trends.

3C. Can life history and ecological traits predict population trends? (Chapter 4)

Finally, I tested for generalities in species responses by predicting population trends as a function of life history and ecological traits (Hansen and Urban 1992, Clark and Martin 2007). Life history characteristics govern a species' capability to cope with environmental change therefore influencing the direction of population trends (Bennett and Owens 2002, Angert et al. 2011).

In the final section of my thesis (**Chapter 5**) I summarize findings from my work described above. I also address limitations and propose compelling new directions for future research.

UNDER-CANOPY TEMPERATURE PATTERNS IN A MOUNTAINOUS LANDSCAPE
REVEAL BUFFERING CAPACITY OF VEGETATION STRUCTURE AND
MICROTOPOGRAPHY

Sarah J. K. Frey, Adam S. Hadley, Sherri L. Johnson, Mark Schulze, Julia Jones, Matthew G. Betts

2 UNDER-CANOPY TEMPERATURE PATTERNS IN A MOUNTAINOUS LANDSCAPE REVEAL BUFFERING CAPACITY OF VEGETATION STRUCTURE AND MICROTOPOGRAPHY

2.1 ABSTRACT

Climate envelope models predict widespread declines in biodiversity in the face of future climate change. However, there is a mismatch between these global climate models and the scale at which organisms experience their environment. Local-scale variation in microclimate is hypothesized to provide potential microrefugia for biodiversity, but the relative role of elevation, microtopography, and vegetation structure in driving microclimate is not well known. We sampled fine-scale air temperature data at 183 sites under the forest canopy in mountainous terrain (elevation range 410 – 1630 m.a.s.l.) to examine the relationship between site characteristics and six temperature variables commonly used to predict species distributions (e.g., mean/max/min, degree days, variability in temperature). We used boosted regression trees (BRTs) to examine the relative contribution of variables describing elevation, microtopography and vegetation structure at two spatial extents (25 and 250m). BRTs offered several advantages over traditional regression methods including the capacity to: 1) examine multiple variables without risk of over-fitting or collinearity, 2) handle non-linear relationships, and 3) allow interactions among variables. Elevation explained the most variation in temperature (mean \pm SD = $63 \pm 24.9\%$) across all response variables, but vegetation and microtopography were also important predictors ($18.7 \pm 15\%$ and $18.3 \pm 12.6\%$ contributions respectively). Importantly, vegetation characteristics associated with older forest stands (e.g., taller canopies, with more complex vertical structure, and higher biomass) tended to mediate changes in temperature by providing an insulating effect – both buffering against warming during summer and against cooling during winter. For instance, maximum monthly temperatures observed in old-growth sites were 2.6°C (95% CI: $1.8 - 3.3^{\circ}\text{C}$) cooler than plantation sites during the spring-summer transition and minimum temperatures during winter months were 0.6°C (95% CI: $0.4 - 0.8^{\circ}\text{C}$) warmer in old-growth stands. Overall, the local scale (25-m radius) explained the majority of variation in temperature patterns; however the capacity of vegetation to buffer a site depended more on the vegetation structure at the 250-m scale. The importance of vegetation in mediating temperatures implies that forest management strategies to conserve old growth characteristics

have the potential to maintain microrefugia, thereby enhancing persistence of biodiversity in mountainous systems in a warming climate.

2.2 INTRODUCTION

Recent forecasts for the effects of climate change on biodiversity predict widespread extinctions (Thomas et al. 2004). However, most projections are based on climate envelope models, which relate species distributions to climate at large spatial scales averaging 10^4 -fold coarser resolution than the extent of animal territories (Bernardo 2014) and do not take into account local microclimatic variability (Pearson and Dawson 2003, Storlie et al. 2014). For logistical reasons temperature is usually measured at broad spatial scales representing macro-scale climate patterns. While macro-scale climate patterns are clearly important in determining range-wide suitability for biota, local-scale climate (hereafter microclimate) is often most relevant to animal behavior and demography (Potter et al. 2013b). Reconciling this mismatch between global climate models and the scale at which organisms experience their environment will improve our understanding of biodiversity responses to climate change (Wiens and Bachelet 2010, Storlie et al. 2014).

Generally climate models represent conditions found in the free air, which can differ substantially from the surface level (Pepin and Losleben 2002). It is widely known that, due to adiabatic lapse rates, altitude increases tend to be associated with cooler air temperatures. However, in mountainous terrain, processes such as cold air pooling and differences in topography can cause this relationship to break down (Dobrowski et al. 2009, Daly et al. 2010), resulting in highly variable, fine-scale spatial and temporal patterns in temperature. The decoupling of the surface temperature conditions from those of the free air is attributed to two main factors in mountainous areas: 1) local air-flow dynamics such as cold air drainage and pooling, and 2) variations in slope and aspect (i.e., microtopography; Dobrowski 2010). Vegetation structure can also interact with these abiotic factors to produce further variability in microclimatic conditions. However, the relative strength of each of these factors is not well understood (Fridley 2009, Vanwalleghe and Meentemeyer 2009) and potentially scale dependent (Wiens and Bachelet 2010).

Understanding the patterns and drivers of microclimate is required for predicting how species will respond to climate change in areas of heterogeneous topography and vegetation cover. Identification of areas on the landscape that may contain microrefugia will help focus conservation efforts of these areas and could lessen the impacts on biodiversity (Moritz and Agudo 2013). Mountains are identified as ideal locations for the existence and preservation of microrefugia due to their inherent heterogeneity at fine spatial scales (Luoto and Heikkinen 2008). These regions are also commonly biodiversity hotspots (Myers et al. 2000), perhaps partly due to the presence of such microrefugia (Botkin et al. 2007). In mountains, climate-sensitive species may have the potential to readily disperse to, and persist in small pockets of favorable microclimatic conditions (Sunday et al. 2014). In contrast, topographically homogeneous regions usually have consistent temperature patterns and require that individuals disperse farther to reach conditions present in their climate envelope (Loarie et al. 2009, Moritz and Agudo 2013).

In addition to microtopography, vegetation structure and composition can also vary dramatically over short distances due to disturbance, management history, and enduring features of a site (e.g., geology, soils). Vegetation has the potential to influence microclimatic patterns through solar radiation, wind exposure, interception of precipitation and retention of understory humidity (Oke et al. 1989). However, since most climate stations are placed in open areas, there is surprisingly little previous research on the influence of vegetation on local microclimates (but see Chen et al. 1993, Vanwalleghe and Meentemeyer 2009, Suggitt et al. 2011, Ewers and Banks-Leite 2013, Hardwick et al. 2015). To our knowledge, no existing studies have considered the relative influence of microtopography and vegetation structure in mediating microclimate.

If particular characteristics of vegetation structure can mediate the effects of regional climate change, human land use has the potential to amplify or buffer the effects of regional warming on biodiversity (Chen et al. 1999, De Frenne et al. 2013). In particular, vegetation characteristics and/or structures (e.g., canopy complexity, forest age, etc.) might sustain thermal conditions under which species persist (Oliver et al. 2010, De Frenne et al. 2013). For example, structural characteristics present in mature and old growth forests, such as taller and more variable canopies (Copeland et al. 1996), may increase the buffering capacity of a site. Alternatively, the closed canopy conditions of managed plantations could prevent rapid site-level warming, thereby moderating climate (Oke et al. 1989). However, if elevation and/or

microtopography are more influential in determining the spatial variability of air temperatures at fine spatial scales, fewer management opportunities are available.

Traditional approaches to temperature modeling typically use straightforward regression methods to determine the most important variables (Li et al. 2014). However, the assumption of linearity in response variables and the risk of overfitting limits the use of these approaches for examining the relative importance of microclimate drivers. Spatial interpolation is also limited in that it provides little information about the underlying processes and tends to perform poorly in complex terrain (Yao et al. 2013). Machine learning approaches such as boosted regression trees (BRTs) allow examination of a large number of predictor variables with built-in methods to eliminate overfitting (Elith et al. 2008). Machine learning also allows more flexible modeling interactions and non-linearities which one would expect for many ecological relationships (Elith et al. 2008).

Microclimate patterns may result from factors at multiple spatial scales (Dobrowski et al. 2009, Scherrer et al. 2011). The elevation and vegetation structure at a location are likely to influence its microclimate, but features in the surrounding area may also play a role. Topographic context within the broader landscape may influence microclimate by sheltering a site or through cold-air drainage (Daly et al. 2010, Dobrowski 2010). Effects of vegetation cover on microclimate can also extend for some distance (Chen et al. 1993, Baker et al. 2014) suggesting that vegetation adjacent to sites may also be important.

To better understand the variation in air temperature which drives habitat selection and phenology for many taxa, we collected understory air temperatures at high spatial resolution across a complex mountainous landscape at the H. J. Andrews Experimental Forest, Oregon, USA. We asked: 1) How much variation in surface air temperature can be explained by elevation, microtopography, and vegetation cover?; 2) Which of these variables are most important and what are their relative influences?; and 3) At what spatial and temporal scales are these drivers creating or influencing microclimates? Finally, we tested a new method for the spatial modeling of microrefugia at broad spatial scales.

2.3 METHODS

We collected fine-scale temperature data across the 6400-ha H. J. Andrews Experimental Forest (HJAEF) located in the Cascade Mountains of central Oregon, USA (44°12' N, 122°15' W). The HJAEF spans an elevational gradient from 410-1630 m.a.s.l. It is a forest mosaic composed of a mix of old-growth forests, mature forests, ~60-yr old Douglas-fir (*Pseudotsuga menziesii*) plantations, alpine meadows, sitka alder (*Alnus viridis*), red alder (*Alnus rubra*), and/or vine maple (*Acer circinatum*) shrub fields, and landslides. We placed temperature sensors at 183 locations across the entire study area. Our sample locations were set up as part of a multi-trophic study investigating the effects of climate on phenology of plants, insects, and birds. These locations were stratified across elevation, forest type, and distance to roads to ensure that the full environmental gradient was sampled (Fig. 1) with a minimum distance between sampling points of 300m. Sample points were categorized as transect, trail, or road. Transect points were selected by placing a random grid of points across a portion of the watershed using GIS. Individual transects were spaced 600m apart and points within each transect were placed 300m apart. Trail points were placed randomly along existing and abandoned trails at 300-m intervals using GIS. Selection of road points was a two-step process. First, points were placed randomly along maintained and abandoned gravel roads at 600-m intervals using Hawth's tools (Beyer 2004) in ArcGIS (ESRI 2011). Finally, from each of these starting points we chose a random direction and distance from the road (0, 50, or 100m).

At the majority of the sites (n=167) we used HOBO pendant data loggers (Onset HOBO Pendant Temperature/Light Data Logger 64K, model UA-002-64 [Fig. S1], see Appendix 1 for deployment of temperature sensors). At 16 sites we employed HOBO water temperature data loggers (Onset HOBO Water Temperature Pro v2 Data Logger, model U22-001). All units were calibrated using both 20.3°C hot water and 0°C cold ice-water baths prior to deployment.

We collected air temperature data at all 183 sample locations from Jan 2012 – July 2013. Occasional malfunctioning units and seasonal snow cover created gaps in our dataset. Additionally, extreme anomalous values were occasionally produced by the units. To address these issues in the dataset, we processed (i.e., cleaned, flagged, pruned, and filled; see Appendix

2 for details) the temperature data before any analyses were performed. In total we used 7,417,320 temperature loggings to calculate summary metrics.

2.3.1 Environmental predictor variables

All environmental variables were derived from GIS layers available for the Andrews Forest. We included a total of 19 predictor variables to model temperature metrics (see Appendix 3 for a complete list of predictor variables used in the models). We selected variables that we hypothesized to be important for influencing air temperatures in forested mountain landscapes and categorized these into three main categories: 1) elevational (ELV), 2) microtopographic (TOPO), and 3) vegetation (VEG).

The ELV category consisted of the mean elevation at each of two spatial scales (25-m, and 250-m; see “*Spatial scale*” below). The TOPO category included predictors that represent variability in elevation, slope, aspect, and a topographic index that describes the relative position of the sample point in relation to the surrounding area at the two spatial scales (25 and 250-m). This was calculated by subtracting the mean elevation within both radii from the elevation value at the sample point (after Daly et al. 2010). Negative numbers indicate that a point is lower than the surrounding area and positive numbers indicate the reverse. The VEG category variables described vegetation structure using metrics relating to: 1) canopy height, 2) cover at multiple strata, and 3) vertical distribution of canopy elements.

We derived all vegetation variables from Light detection and ranging (LiDAR) data collected at the Andrews Forest in August of 2008 during the leaf-on period (Watershed Sciences 2008). LiDAR is a relatively new technology that allows for fine-scale mapping of forest structure across broad spatial extents (Lefsky et al. 1999, Means et al. 2000). Variables derived from the LiDAR dataset include: 1) Canopy height (CH), 2) % cover mid-canopy (2-10m) and upper canopy (>10m), 3) Biomass, 4) Coefficient of variation in canopy height, 5) Height of median return (HOME) and 6) Vertical distribution ratio (VDR). HOME describes the height at which the bulk of the canopy exists (Goetz et al. 2010). VDR is an index of vertical distribution of intercepted canopy components (Goetz et al. 2010). It is calculated as follows: $[CH - HOME]/CH$. Lower VDR values represent a shorter distance between CH and HOME, indicating a larger understory canopy component (Goetz et al. 2010). We used Principle Component

Analyses (see PCA methods below) to examine the association of these vegetation characteristics with old-growth forest sites and even-aged plantation sites which represent the predominant forest management technique in the region.

2.3.2 Spatial and temporal scales

Regional climate data are typically collected at coarse resolutions, although the scale at which drivers of microclimate act is largely unknown (Bernardo 2014). We assessed the importance of the predictor variables at two spatial extents around each sample point: 1) 25-m radius that represents site- or stand-level predictors and 3) 250-m radius that represents both local and landscape conditions surrounding the site. The relative roles of biotic and abiotic aspects of the environment could influence microclimates differently at these two spatial scales (Wiens and Bachelet 2010).

2.3.3 Response variables

Our response variables were: 1) Cumulative degree days $>0^{\circ}\text{C}$ January – March (CDD0JM), 2) CDD $>0^{\circ}\text{C}$ April – June (CDD0AJ), 3) CDD $>10^{\circ}\text{C}$ April – June (CDD10AJ), 4) Standard deviation (SD) of weekly temperature January – March (SDwTJM), 5) SD of weekly temperature April – June (SDwTAJ), 6) Mean monthly mean temperature April – June (MnMoMeanAJ), 7) Mean monthly maximum temperature April – June (MnMoMaxAJ), 8) Mean monthly minimum temperature April – June (MnMoMinAJ), 9) Maximum temperature of the warmest month (MxTWM, 2012 only), and 10) Minimum temperature of the coldest month (MiTCM, 2012 only). We chose the two time periods of January – March (winter) and April – June (spring) because they are relevant to phenology of many organisms on our landscape. CDD are linked closely to timing of spring plant bud burst, leaf out, and flowering as well as insect emergence, and therefore have potential to influence higher trophic levels (Both et al. 2009a). In temperate regions, such as in Oregon, phenological events during spring also have direct implications for reproduction and growth in both plants and animals. Further, Daly et al. (2010) found that cold-air pools are more persistent in winter than in spring and summer when there is more energy and more consistent mixing of the vertical air profile. The variability in weekly temperature in both time periods (as measured by standard deviation [SD]) may also determine

the quality of sites by affecting its temperature stability (Stralberg et al. 2009, Dunstan et al. 2012).

2.3.4 Statistical analysis – Boosted Regression Trees

We used a machine learning approach (BRTs) to explore the relationship between our suite of predictor variables and air temperature at our 183 sample locations. BRTs have recently been used extensively in species distribution modeling due to their capacity for uncovering non-linear relationships between predictors and response variables as well as flexibility in testing interactions among predictors (Elith et al. 2008). BRTs can also handle large numbers of predictor variables and collinearity between them (Elith et al. 2008), which is advantageous in studies such as ours where there are many categorized predictor variables, but little prior information about which are most important or at which spatial scales. This modeling method allowed us the flexibility needed to explore multiple potential correlates of microclimate without arbitrarily restricting our predictor set.

We used program R (R Development Core Team 2011) version 3.0.1 in combination with the ‘dismo’ package version 0.8-17 (Hijmans et al. 2013) for all analyses. When using BRTs, there are settings for tree complexity, learning rate, and bag fraction. Tree complexity determines the number of interactions fitted in the modeling process. Learning rate (also known as the shrinkage parameter) controls the contribution of each tree added to the model. Reducing the learning rate will increase the number of trees used in the model. Bag fraction determines the number of observations used for the training set (without replacement) for each tree fitted. This adds a stochastic component to the modeling process, which improves model performance by reducing variance in the final model. We used the following default settings for each of our BRT models: tree complexity = 5, learning rate = 0.01, bag fraction = 0.75. We chose a bag fraction on the upper end of the suggested range (0.5 – 0.75) because of the relatively small number of sites in our dataset. When these settings did not result in 1000 or more trees, we decreased the learning rate incrementally until 1000 or more trees were obtained (following Elith et al. 2008; See Appendix 4 for model settings and diagnostics).

We used the function ‘gbm.step’ which has a built in 10-fold cross-validation to determine the ideal number of trees (Elith and Leathwick 2014). Predictive deviance is measured

as the mean deviance from the held-out data in all folds. We used this as our primary measure of model performance. Deviance is a likelihood-based metric that describes the loss in predictive performance as a result of a suboptimal model and is relative to the scale of the response variable and therefore not directly comparable between temperature metrics. We also tested the correlation between predicted and observed temperature metrics using 10% independent ‘test’ data. These tests thus represent an entirely independent test of model performance. If overfitting occurred, these tests should show low correlations between predicted and observed values.

We assessed the contribution of each category of predictor variables (ELV, TOPO, VEG) to explained variance in temperature metrics by summing the relative importance (RI) values of the variables in each category. Relative importance values are based on the frequency that a predictor variable is chosen for splitting (weighted by the squared improvement to the model) while growing trees. Non-informative predictors have minimal influence on prediction (Elith et al. 2008). To determine the direction and nature of the relationships between the temperature metrics and the most influential individual predictor variables (>2% RI), we examined the partial dependence plots for visualization of the fitted functions. Partial dependence plots show the effect of a predictor variable on the temperature response after the average effects of all other variables have been accounted for (Elith et al. 2008). We created a predicted spatial map for each temperature metric using the final BRT models and raster layers for each predictor variable. Finally, we identified important interactions between predictors.

Spatial autocorrelation is a common attribute of most ecological datasets (Legendre 1993), particularly those characterized by broad-scale environmental gradients. In order to test whether spatial autocorrelation was present in our dataset we calculated Moran’s I on the residuals for each BRT model using the correlog function in the ‘ncf’ package in R (Bjornstad 2013). We chose an interval of 500m and resampled 1000 times. We report these values (which vary between -1 and 1) along with their associated P -values.

2.3.5 Statistical analysis – Principal Component Analysis

We performed a principal component analysis (PCA) on all of our LiDAR-derived vegetation variables at the 25-m scale (19 variables, Appendix 4) to test if we could reliably differentiate between plantations and older forests. This also aided in determining whether our

vegetation structure variables captured the gradient in forest structure present across the landscape, which then facilitated our interpretation of their individual effects on the microclimate variables. A weakness of BRTs is that they do not produce effect sizes that can be easily related to differences in response variables (here °C or degree days). Therefore, we used generalized linear models (GLMs) to examine the relationship between PC1 values (gradient in forest structure) and temperature metrics. In this fashion, we were able to quantify differences in temperature across the range of variability in forest structure (PC1).

2.4 RESULTS

2.4.1 Model performance & spatial autocorrelation

All models performed very well when tested on independent data; low deviance values indicated minimal differences between modeled and observed values (Appendix 4). The cross-validation correlations were high showing high congruence between training and test data (2012 mean \pm SD [range] $r = 0.87 \pm 0.09$ [0.69 – 0.98]; 2013 mean $r = 0.87 \pm 0.10$ [0.69 – 0.96], Appendix 4). Further, there was no evidence of spatial autocorrelation in our model residuals; the Moran's I values were all small (mean \pm SD [range] across all models = -0.01 ± 0.007 [-0.026 – 0.003], Appendix 4 and none were statistically significant (mean \pm SD [range] of P -value for all models = 0.20 ± 0.05 [0.14 – 0.28], Appendix 4). This indicates that after modeling temperature using our predictors, no variance remained to be explained by spatial structure (Legendre 1993).

2.4.2 General temperature patterns

As expected, elevation had a large relative influence ($63 \pm 24.9\%$) on patterns in fine-scale air temperature, but for many temperature metrics, vegetation and microtopography had a major effect ($18.7 \pm 15\%$ and $18.3 \pm 12.6\%$, respectively; Fig. 2). Elevation was the dominant predictor for the majority of our temperature metrics: CDD0AJ (2012: 84.9%, 2013: 87.5%), CDD10AJ (2012: 64.9%, 2013: 70.6%), MnMoMeanAJ (2012: 86.2%, 2013: 88%), MnMoMaxAJ (2012: 67%, 2013: 71%), MnMoMinAJ (2012: 77%, 2013: 68%), and MiTCM (2012: 92.9%).

For the remainder of the temperature metrics (2012: 4/10 temperature metrics, 2013: 2/8 metrics), elevation was less important than vegetation and microtopography combined. In 2012,

vegetation structure showed the largest influence on variability in weekly temperature from April to June (SDwTAJ: 36.7%) and maximum temperature of the warmest month (MxTWM: 35.5%). Vegetation structure was also an important predictor of our winter temperature variability metric (SDwTJM 2012: 28.9%, 2013: 31.6%) and cumulative degree days during winter (CDD0JM 2012: 31.2%, 2013: 34.3%). Vegetation was also important for maximum temperature of the warmest month in 2012 (MxTWM 35.5%). Topographic features were more important than elevation for CDD0JM in both years (2012: 45.9%, 2013: 53.9%) but surprisingly had little importance on cumulative degree days in the spring and summer months (2012: 9.0%, 2013: 7.0%). The maximum temperature of the warmest month in 2012 similarly had a large microtopographic component (37.9%).

2.4.3 Variable-specific results

Cumulative degree days >0°C from January to March – In both years, topographic variables had the highest relative influence values (2012: 45.9%, 2013: 53.9%), followed by vegetation (2012: 31.2%, 2013: 34.3%, Figs. 2 & 3A). The overall patterns were nearly identical in both years. As with all temperature metrics we investigated, elevation explained at least some of the variation in CDD0JM (Σ RI at both scales [unless otherwise indicated, all % values are RI summed across both scales] – 2012: 23%, 2013: 11.9%, Fig. 2). Overall, higher elevations had fewer CDD0JM. Larger ranges in elevation at a site (Fig. 4A; 2012: 17.9%, 2013: 24.6%), more exposed topographic position (Fig. 4B; 2012: 6.8%, 2013: 8%), and steeper slopes (2012: 7.2%, 2013: 8.4%) all led to increases in CDD0JM. Additionally, intermediate slope variability (2012: 5.6%, 2013: 3.2%) and northern exposure (2012: 3.2%, 2013: 3.7%) decreased CDD0JM. However, dense forest cover can accentuate the effect of topographic position (Fig. 5A). Exposed sites with low variability in biomass (e.g., plantation stands) accumulated the most degree days (interaction strength = 0.68).

Cumulative degree days >0°C and >10°C from April to June – In both 2012 and 2013, elevation was identified as the main apparent driver of both CDD0AJ (Figs. 2 & 3B; 2012: 85.7%, 2013: 88.1%) and CDD10AJ (Figs. 2 & 3C; 2012: 65.9%, 2013: 70.2%). Higher elevations showed lower CDD0AJ and CDD10AJ, and there appeared to be a threshold of 1000m at the local scale after which CDD0AJ remained low and constant. There was a larger

topographical influence on CDD10AJ (Figs. 2 & 3C; 2012: 20.5%, 2013: 18.2%). A wider elevation range in the surrounding area (2012: 7.7%, 2013: 6.7%), more exposure (2012: 3.2%, 2013: 2.4%), and steeper slopes (2012: 3.2%, 2013: 2.6%) all increased CDD10AJ.

Variation in mean weekly temperature – A) January to March – The variability in weekly temperature from January to March (SDwTJM) was similar in both years. On average, mean weekly temperatures across the Andrews Forest varied 1.6°C (0.8 – 2.7°C) in 2012 and 2.6°C in 2013 (from 1.2 to 3.6°C). However, the effect of elevation on variation in mean weekly temperature was not consistent in the two years (Fig. 6). In 2012, the lowest elevations varied least, and above ~1000m, variability was maximized (Fig. 6A). In 2013 contrarily, higher elevations (above ~1000m) were less variable (Fig. 6A), particularly if they had low topographic exposure (i.e., located in valleys or depressions; Fig. 5B; interaction strength = 1.34). We observed similar patterns in topographic influence in both years (2012: 24%, 2013: 28.6%); more exposed areas (Fig. 4C, 2012: 8.2%, 2013: 11.6%), sites with larger ranges in elevation (2012: 5%, 2013: 6.3%), and steeper slopes (2012: 2.6%, 2013: 1.8%) showed more variable temperatures than sites in low topographic positions during the late winter/early spring. In 2012, north-facing slopes appeared to be more stable (2.6%). Vegetation effects were also similar between years; old forest traits including higher relative variation in canopy cover (Fig. 7A; 2012: 6.7%, 2013: 8.7%) and more mid-canopy cover (2-10m; 2012: 4.2%, 2013: 3.1%) both reduced variability in mean weekly temperature. In 2013, areas with the lowest biomass variability (e.g., even-aged stands such as plantations; Fig. 8) showed more variability (Fig. 7B; 5.4%).

Variation in mean weekly temperature – B) April to June – Standard deviation in mean weekly temperature from April to June (SDwTAJ) was quite different between years (Figs. 2 & 4). The main difference was in the category of predictor variables that had the highest relative influence; in 2012, vegetation was most important (2012: 36.7%, 2013: 10.2%) and in 2013, elevation explained the majority of the variation (2012: 45.5%, 2013: 79.2%) in SDwTAJ. The effect direction of elevation also differed in the two years with high elevations being less variable in 2012 and more variable in 2013 (Fig. 4). In both years, topographically protected areas (low topographic exposure; 2012: 3.6%, 2013: 4.7%) were least variable. The overall

amount of variability was slightly higher in 2013 (2012 mean [range] = 3.78°C [3.34 – 4.53°C]; 2013 = 4.86°C [4.20 – 5.54°C], Fig. 9).

Mean monthly mean temperature from April to June –In both years, mean temperatures during the spring-summer transition were largely a function of elevation (2012: 49.7%, 2013: 66%); MnMoMeanAJ was cooler with increasing elevation, but showed a threshold at 1000m (Fig 10A). The relationship between elevation and MnMoMeanAJ was more gradual at the broad spatial scale (2012: 36.5%, 2013: 22%). Elevation range (microtopographic) was also influential for MnMoMeanAJ (2012: 2.2%, 2013: 1.4%), with local sites with wider ranges in elevation (and likely steeper slopes) were warmer.

Mean monthly maximum temperature from April to June –Increasing elevation decreased MnMoMaxAJ more or less linearly and was more important at the local scale (2012: 42%, 2013: 52.6%; Fig. 10B). Increasing canopy cover >10m (2012: 3.0%, 2013: 2.8%), higher VDR values (2012: 2.2%, 2013: 2.9%), and biomass >500 Mg/ha (2012: 2.1%, 2013: 2.1%) lowered MnMoMaxAJ. East- (2012: 2.1%, 2013: 1.3%) and north-facing slopes (2012: 1.8%, 2013: 1.6%) had lower maximum temperatures. A vegetation-elevation interaction revealed that MnMoMaxAJ was lowest at high elevations with high amounts of canopy cover surrounding a site (250-m radius, Fig. 5C).

Mean monthly minimum temperature from April to June – MnMoMinAJ was higher at lower elevations with more influence at the finer spatial scale (2012: 48.8%, 2013: 40.3%; Fig. 10C). At the broad spatial scale, elevation was less effective in lowering minimum temperatures below ~1000m (2012: 28.7%, 2013: 27.6%). MnMoMinAJ dropped sharply from it's highest to lowest values at a VDR value of ~0.5, indicating a potential threshold (2012: 3.9%, 2013: 7.1%). In 2013, more canopy cover >10m increased MnMoMinAJ (2012: 1.3%, 2013: 2.2%). Minimum temperatures did not get as low at sites with more dramatic elevation ranges over a small area (local scale; 2012: 2.5%, 2013: 2.5%) and in steeper landscapes (broad scale; 2012: 1.7%, 2013: 2.2%). An interaction between elevation and microtopography indicated that high elevation sites in areas of gentle slopes had the lowest minimum temperatures in April-June (Fig. 5D).

Maximum temperature of the warmest month (2012) – Monthly temperatures during the warmest part of 2012 were on average 25.2°C and could range from 20 – 33.1°C depending on

position within the landscape (Fig. 11). There was a large vegetation and microtopography influence on MxTWM (Fig 2A). Overall, higher elevations (26.7%), north (18.9%; Fig 4D) and east-facing (6.6%) aspects, and gentle slopes (4.3%) showed lower MxTWM. Forest areas with less of an understory canopy component (7.5%) showed increased MxTWM. Old forest characteristics (Fig. 8) such as more canopy cover >10m (5.1%) and taller canopies (6.6%) reduced MxTWM.

Minimum temperature of the coldest month (2012) – Elevation was the main apparent driver for MiTCM (93.3%); higher elevations showed lower MiTCM (Fig. 11). At both spatial scales, as elevation increased the MiTCM decreased, more or less linearly. Although decreases were generally seen between 800-1000m, which was scale dependent.

2.4.4 Principal Component Analysis

The first two principal components of the PCA explained 74.7% of the variability in our forest structure variables (PC1 = 44.7%, PC2 = 30%, Fig. 8, Appendix 5). PC1 described the gradient in forest structure from plantation to mature and old-growth forests (Figs. 8 & 12). Sites with low PC1 values had less biomass (mean and SD), lower canopies (mean and SD), less cover 2-10 and >10m, higher variability in cover 2-10 and >10m, higher HOME values, lower CV in canopy height, and lower VDR (Appendix 5). The most influential variables were mean biomass, mean canopy height, and HOME (contributions ~0.4), followed by SD of biomass and canopy height and mean cover >10m (contributions ~0.3; Appendix 5).

Based on our results demonstrating the dominant role of elevation in determining fine-scale temperature patterns, we included elevation as a predictor in our linear regression models testing the influence of PC1. This is a more conservative approach because we could determine the effect of our vegetation structure gradient after accounting for the large elevation-based variability in temperature patterns. We found that for 7/10 temperature metrics in 2012 and 5/8 metrics in 2013, PC1 had a significant effect (Table 1) even after controlling for elevation. Effects were largest for temperature extremes (minimums and maximums) and cumulative degree days in the spring and summer months for both years (Table 1). Temperature differences were substantial across the gradient in forest structure: maximum monthly temperatures observed in old-growth sites in 2012 were 2.6°C (95% CI: 1.8 – 3.3°C) cooler than plantation sites during

the spring-summer transition (Fig. 12A, Table 1) and minimum temperatures during winter months were 0.6°C (95% CI: 0.4 – 0.8°C) warmer in old-growth stands (Fig. 12B, Table 1).

2.4.5 Scale effects

In both years, the local scale (25-m radius) comprised the majority of the relative influence for most temperature metrics (overall average RI of local scale [25m] across all metrics – 2012: $60.7 \pm 10\%$, 2013: $62.3 \pm 9.5\%$, Fig. 13). However, vegetation metrics tended to be more influential at the broad spatial scale (Fig. 13C & F).

2.4.6 Temporal consistency

The number of degree days that a site accumulated showed a very consistent pattern from year-to-year during both winter and spring-summer periods (Fig. 10 A-C; CDD0JM $r^2 = 0.84$, $P < 0.0001$; CDD0AJ $r^2 = 0.99$, $P < 0.0001$; CDD10AJ $r^2 = 0.98$, $P < 0.0001$) despite warmer overall temperature in much of 2013 (Fig. 9). However, variability in temperature during key periods of the year showed less consistency. Variability in temperature from January – March was the only temperature variable that was not significantly correlated in both years (Fig. 9D; SDwTJM $r^2 = 0.01$, $P = 0.18$). Variation in temperature from April – June was significantly and positively correlated between the years, however the correlation was weaker in comparison to the majority of the temperature metrics we investigated (Fig. 9E; SDwTAJ $r^2 = 0.56$, $P < 0.0001$). The mean monthly mean ($r^2 = 0.99$, $P < 0.0001$), maximum ($r^2 = 0.97$, $P < 0.0001$), and minimum ($r^2 = 0.98$, $P < 0.0001$) temperatures from April – June were all highly significantly and positively correlated between the years (Fig. 9F-H). Overall, 2013 was warmer (Fig. 9). The difference between years was significant for all metrics based on Welch two-sample t-tests (Appendix 6).

2.5 DISCUSSION

As would be expected due to adiabatic lapse rate alone, elevation was the most powerful predictor of air temperatures across years, variables, and scales. Higher elevations were typically cooler across both seasons. For example, the minimum monthly winter temperatures were almost exclusively a function of elevation. Our results are consistent with other data that show a relatively large role of elevation in fine-scale temperature patterns (Vanwalleghem and

Meentemeyer 2009, Dobrowski 2010). However, for four of ten temperature variables in 2012 and two of eight in 2013, the combined effects of microtopography and vegetation were greater than for elevation. Elevation predicted the most general temperature metrics well, but seemed to have less of an influence on the variables characterizing variability in temperature, and early-season degree day accumulation which are both likely to be important in determining the conditions experienced by organisms and in influencing their fitness (Bernardo 2014).

Vegetation had a strong effect on fine-scale temperature patterns in our system, equal to that of microtopography. On average, nearly 20% of the variation in temperature patterns was attributable to vegetation; this was consistent in both years. Vegetation characteristics associated with older forest stands (Fig. 6) appeared to mediate changes in temperature by providing a buffering effect. Taller stands with more complex vertical structure and higher biomass tended to be both warmer during winter months and cooler during summer months; open areas and stands with shorter canopies were colder in the winter and warmer in summer. This insulating effect resulted in differences as large as 3°C between plantations and old-growth sites (Fig. 12, Table 1). Other studies are congruent with vegetation influences on microclimate. However, the majority of these show differences between dramatically different vegetation types such as forest and grassland (Suggitt et al. 2011) or forest and young plantations (Chen et al. 1993, Baker et al. 2014, Hardwick et al. 2015). Forest patch size can generate different microclimates in montane landscapes (Vanwalleghe and Meentemeyer 2009) and tropical systems (Ewers and Banks-Leite 2013). To our knowledge, this is the first time that fine-scale differences across seral stages – particularly the importance of old-growth structure – have been shown to mediate temperature regimes. We observed mean monthly differences of several degrees when comparing >60 year old plantations with old-growth forest stands.

Microtopographic variables including slope, aspect, and relative topographic position (valley vs. topographically exposed sites) influenced temperature patterns. North- and east-facing sites and gentler slopes were associated with cooler temperatures during both summer and winter. Sites with more exposure (higher topographic position than its surroundings) and steeper slopes were typically warmer during spring/summer months. Depressions and other topographically-sheltered areas are thought to contribute to the decoupling of surface temperatures from regional patterns thereby potentially generating microrefugia in complex terrain (Dobrowski 2010). Our

findings at the Andrews Forest are consistent with these patterns; topography creates potential microrefugia with sheltered sites generally being cooler in summer and warmer in winter.

Overall, the local scale (25-m radius) explained the majority of variation in temperature patterns suggesting that factors at the immediate site are critical determinates of microclimate conditions (Fig. 13). However, the capacity of vegetation to buffer a site against changes in temperature depended more on the vegetation structure at larger scales (250-m radius). Other studies have shown that edge effects on microclimate can extend well into forest patches (Baker et al. 2014) and that smaller forest patches tend to be more susceptible to changes in temperature (Vanwalleghe and Meentemeyer 2009). Chen et al. (1993) showed that microclimate characteristics between old-growth Douglas-fir forests and clear cuts differ markedly, with forests areas always being cooler during the growing season, and edges showing the higher variability than the interior. Such edge effects also limit microclimatic buffering of tropical forests (Ewers and Banks-Leite 2013).

Our results suggest that effects of topography and vegetation on local microclimate are greater during periods of high variation in temperature. When there is little temporal variation in temperature, variation is primarily explained by elevation (Anderson et al. 2007; Fig. 2). This indicates that the roles of complex vegetation and topography in microclimatic buffering may be more important during relatively extreme conditions. We found that predictors of temperature patterns were largely consistent despite substantial differences in overall temperature regimes between the two years (Fig. 9). Temperature metrics representing variability were less consistent between years than metrics such as cumulative degree days and mean monthly temperatures. General consistency in our microclimate results with other studies (Chen et al. 1993, Vanwalleghe and Meentemeyer 2009, Ewers and Banks-Leite 2013) suggests that our findings may be broadly relevant in other systems. However, an important caution, since many organisms experience temperature at heights other than those monitored by our 1.5-m height sensors, is that it is possible that additional microclimatic variability exists either above or below our sensors (Bernardo 2014).

Finally, our results demonstrate that BRTs offer a powerful new approach to examining microclimate drivers. BRTs allowed comparisons of large numbers of independent variables and

models predicted independent data extremely well. Interactions among variables were common (Fig. 5) and would not have been detectable using traditional regression approaches. This machine learning approach (Elith et al. 2008) thus represents a promising option for distinguishing relative importance of complex climate drivers and generating detailed spatial climate predictions.

2.5.1 Management implications

We showed that vegetation metrics associated with older forest such as dense canopy structures, tall canopies, and high vertical complexity (Fig. 8) provided cooler microclimates than simpler forest stands. Management practices that open forest canopies or create even-aged stands such as plantations (Franklin et al. 2002, Odion and Sarr 2007) are likely to reduce the buffering capacity of forest sites, thereby limiting access to favorable microclimates. Climate warming is expected to lead to widespread loss of cool-adapted species from communities (De Frenne et al. 2013). Conserving old-growth forest and avoiding shifts to simpler forest types such as plantations is likely to help sustain favorable microclimates. Recent work shows that the understory microclimate differences we document here could be highly relevant to biodiversity conservation. De Frenne et al. (2013) found that widespread loss of cool-adapted understory plant species was attenuated in sites with dense forest canopies. This was hypothesized to be due to such stands maintaining cooler and more favorable microclimates within regions that had warmed over the long term. Also, germination rates for heat-sensitive plant species are typically higher under dense canopies (von Arx et al. 2013). Amphibians, lizards and insects are all shown to take advantage of microclimate conditions when regional climate moves beyond the range of thermal preferences (Scheffers et al. 2013, Sunday et al. 2014). Even large mammals such as elk appear to use favorable microclimates to maintain higher body condition (Long et al. 2014). However, since older seral stages provide the highest levels of buffering, management options may be limited for species inhabiting early successional forest, unless they are able to take advantage of the microclimatic buffering of older forests or cooler microclimates near old forest (Baker et al. 2014). Since the vegetation structure within 250m was important in microclimatic buffering, limiting forest fragmentation by sustaining large forest patches and minimizing edges may be an important conservation consideration.

2.5.2 Conclusions

Although elevation was a major predictor of fine-scale air temperatures on the Andrews Forest landscape, vegetation and topography played critical roles in microclimate patterns. Older forest stands with taller overstories and more complex vertical structure provided an insulating effect against temperature changes. The large influence of vegetation structure on microclimate presents the opportunity to manage for conditions that favor persistence of biodiversity in mountainous systems (Oliver et al. 2010). By preserving conditions that potentially buffer organisms from the impacts of regional warming, or at least slow the rate at which organisms have to adapt to a changing climate, it may be possible to ameliorate some the negative effects of regional warming in mountains.

TABLE 2.1. Generalized linear regression model results for the relationship between temperature metrics and the first component (PC1) of a principle component analysis representing a gradient in vegetation structure. Lower PC1 values indicate forest plantations and higher values old-growth forests (Fig. 9). Elevation (Elv) was included to control for elevation differences while examining effects of vegetation. Change in temperature metrics shows the difference in temperature (°C) or degree days (dd) across the range of PC1 values. ** indicates statistically significant effect of PC1 on temperature metrics at $P < 0.05$.

Variable	Intercept		PC1			Elv			Change in temperature metrics ~ PC1			
	Est	SE	Est	SE	<i>P</i>	Est	SE	<i>P</i>	Units	Change	LCL	UCL
2012												
CDD >0°C Jan-Mar	162.162	3.223	-0.903	3.456	0.794	-23.404	3.456	<0.0001	dd	-3.77	-35.02	12.61
CDD >0°C Apr-Jun	754.445	3.469	-11.169	3.720	0.003 **	-122.116	3.720	<0.0001	dd	-46.73	-80.35	-13.11
CDD >10°C Apr-Jun	115.065	1.613	-6.351	1.730	0.000 **	-33.660	1.730	<0.0001	dd	-26.57	-42.21	-10.94
SD wkly T Jan-Mar	1.619	0.020	0.022	0.022	0.298	0.292	0.022	<0.0001	°C	0.09	0.29	-0.07
SD wkly T Apr-Jun	3.779	0.010	-0.017	0.011	0.105	0.096	0.011	<0.0001	°C	-0.07	-0.17	0.02
Mn mo MEAN T Apr-Jun	8.249	0.038	-0.120	0.041	0.004 **	-1.383	0.041	<0.0001	°C	-0.50	-0.87	-0.13
Mn mo MAX T Apr-Jun	12.852	0.081	-0.612	0.087	0.000 **	-1.802	0.087	<0.0001	°C	-2.56	-3.34	-1.78
Mn mo MIN T Apr-Jun	4.645	0.036	0.149	0.039	0.000 **	-0.986	0.039	<0.0001	°C	0.62	0.97	0.27
MAX T warmest mo	25.221	0.141	-0.680	0.151	0.000 **	-1.054	0.151	<0.0001	°C	-2.84	-4.21	-1.48
MIN T coldest mo	-1.137	0.025	0.143	0.027	0.000 **	-0.992	0.027	<0.0001	°C	0.60	0.85	0.35
2013												
CDD >0°C Jan-Mar	195.162	4.293	-0.033	4.603	0.994	-22.708	4.603	<0.0001	dd	-0.14	-42.81	16.94
CDD >0°C Apr-Jun	886.101	3.130	-9.333	3.356	0.006 **	-121.308	3.356	<0.0001	dd	-39.05	-69.38	-8.72
CDD >10°C Apr-Jun	188.422	1.803	-6.616	1.933	0.001 **	-42.095	1.933	<0.0001	dd	-27.68	-45.16	-10.20
SD wkly T Jan-Mar	2.598	0.027	-0.026	0.029	0.363	-0.204	0.029	<0.0001	°C	-0.11	-0.37	0.09
SD wkly T Apr-Jun	4.864	0.009	-0.002	0.009	0.850	0.241	0.009	<0.0001	°C	-0.007	-0.09	0.03
Mn mo MEAN T Apr-Jun	9.718	0.034	-0.101	0.037	0.007 **	-1.357	0.037	<0.0001	°C	-0.42	-0.76	-0.09
Mn mo MAX T Apr-Jun	14.508	0.083	-0.562	0.089	<0.0001 **	-1.756	0.089	<0.0001	°C	-2.35	-3.15	-1.55
Mn mo MIN T Apr-Jun	5.934	0.041	0.181	0.043	<0.0001 **	-0.846	0.043	<0.0001	°C	0.75	1.15	0.36

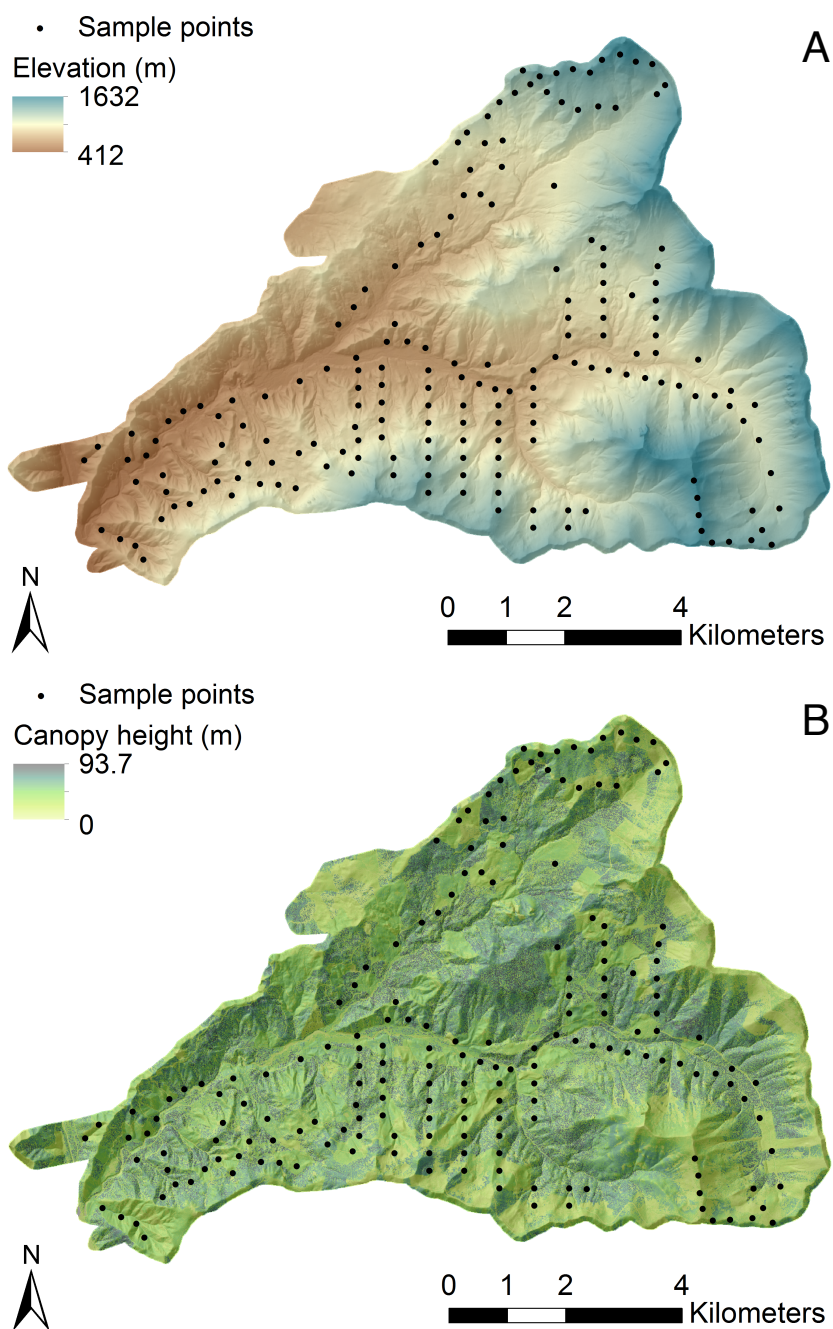


FIGURE 2.1. Maps showing A) the elevational gradient (meters) and microtopography, and B) Canopy height (meters) based on LiDAR from 2008 at the H. J. Andrews forest, Oregon, USA (Watershed Sciences 2008). Black dots show the 183 temperature sampling locations.

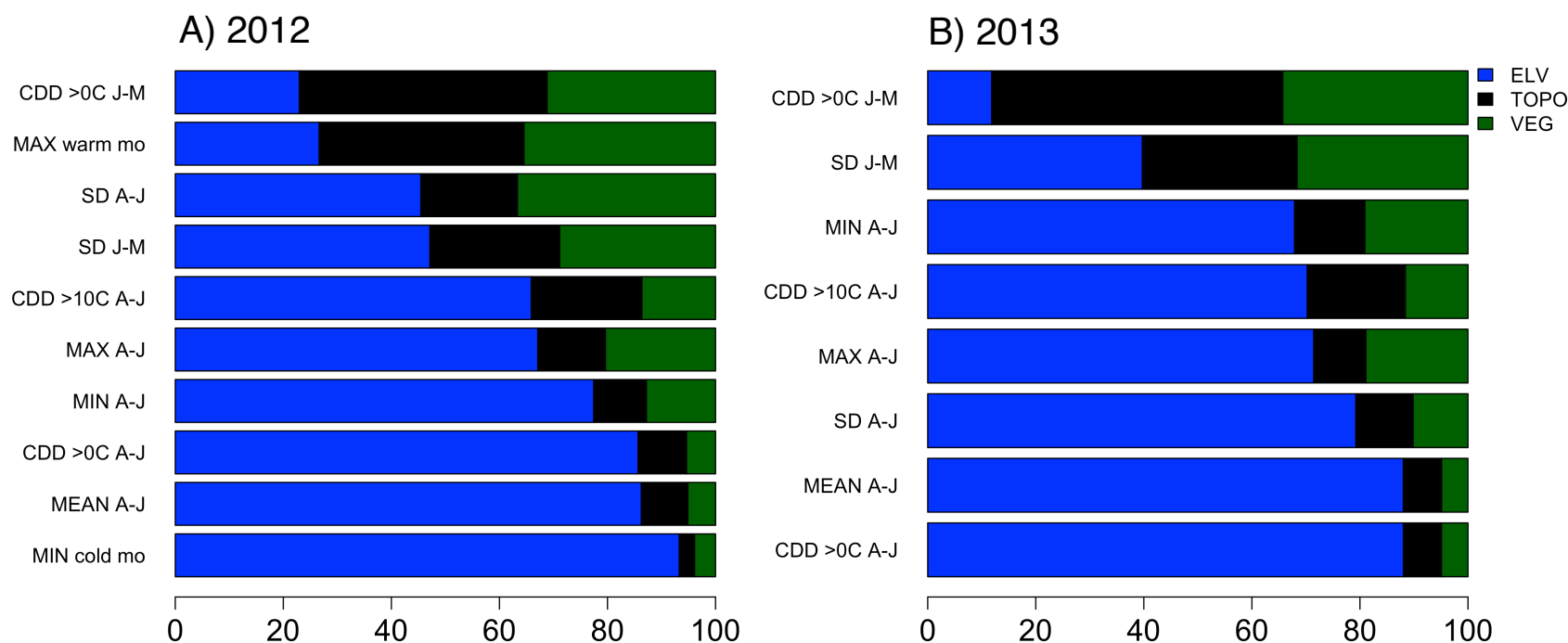


FIGURE 2.2. Relative importance of variables describing elevation, microtopography and vegetation for each temperature metric in both years A) 2012, B) 2013. Relative importance values were derived from the number of times each variable was selected in the process of model building using BRTs.

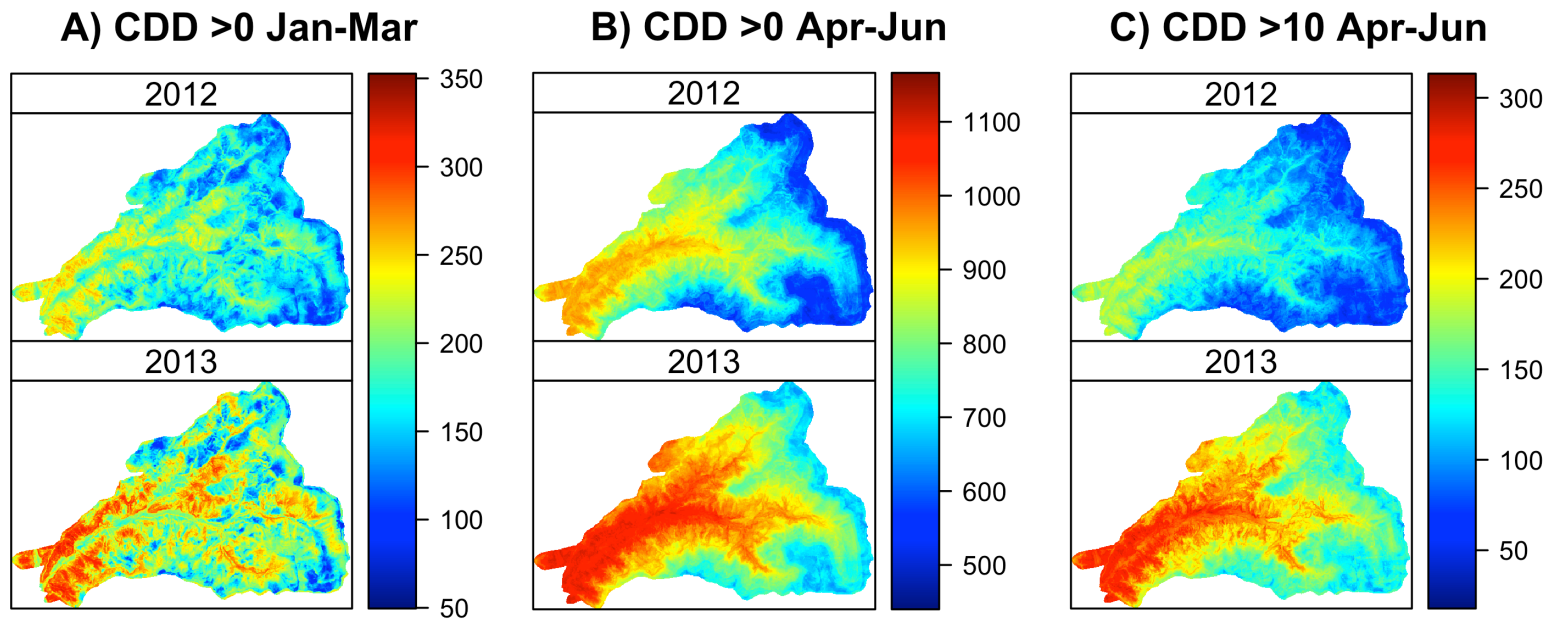


FIGURE 2.3. Spatially predicted temperature metrics of cumulative degree days at the H. J. Andrews Experimental Forest based on BRT models. Response variables are: (A) Cumulative degree days >0°C January-March (CDD0JM), (B) CDD >0°C April-June (CDD0AJ), and (C). CDD >10°C April-June (CDD0AJ). Vegetation and microtopography had a high relative influence on degree days in January-March (A), but degree days in April-June were primarily a function of elevation.

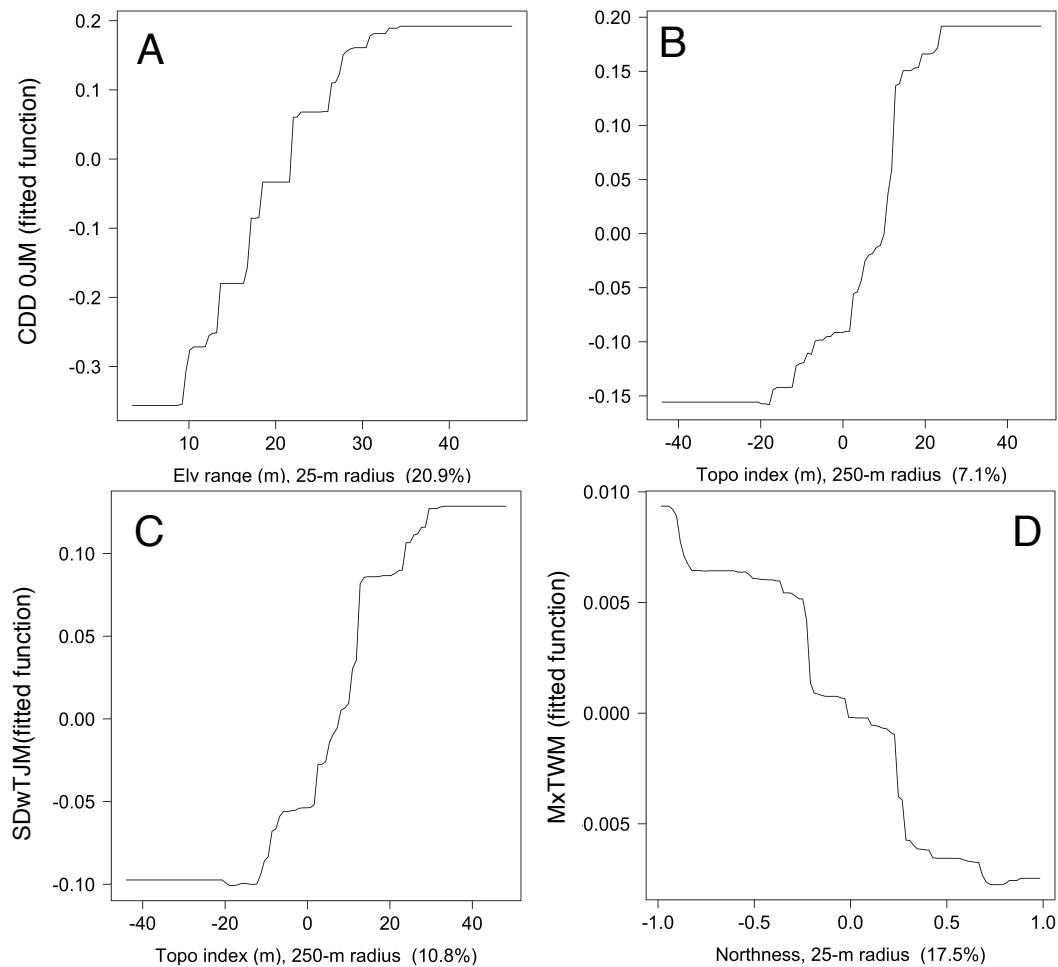


FIGURE 2.4. Partial dependence plots of key microtopographic (TOPO) variables. The fitted functions generated using boosted regression show the effect of the variable on the response after accounting for all other variables in the model. (A) Sites with a larger range in elevation within 25m (i.e., steep slopes) and (B) more exposure accumulate more degree days January-March (CDD0JM 2013). (C) Sites located in exposed areas also are more variable in temperature during this period (SDwTJM 2013). (D) Aspect played a large role in determining the maximum temperature of sites with north-facing slopes being coolest (MxTWM 2012). Relative variable importance is indicated in parentheses (RI%).

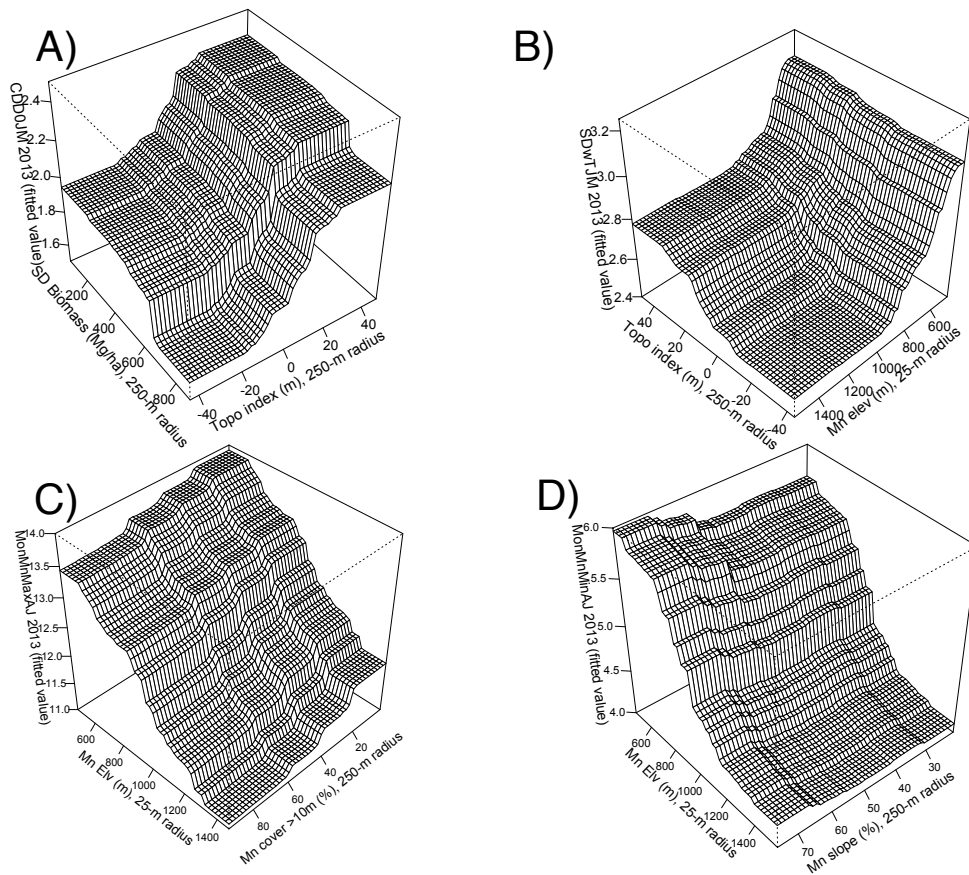


FIGURE 2.5. Key interactions identified from BRT models testing the effects of elevation, microtopography, and vegetation structure on microclimate. A) Exposed sites with low variability in biomass (e.g., plantation stands) accumulated the most degree days $>0^{\circ}\text{C}$ from January-March (CDD0JM 2013). B) Higher elevations (above $\sim 1000\text{m}$) were less variable in January-March (SDwTJM 2013), particularly if they had low topographic exposure. C) Mean monthly maximum temperature from April-June (MonMnMaxAJ 2013) was lowest at high elevations in high amounts of canopy cover in the surrounding landscape. D) An interaction between elevation and microtopography indicated that high elevation sites in areas of gentle slopes had the lowest minimum temperatures in April-June (MonMnMinAJ 2013).

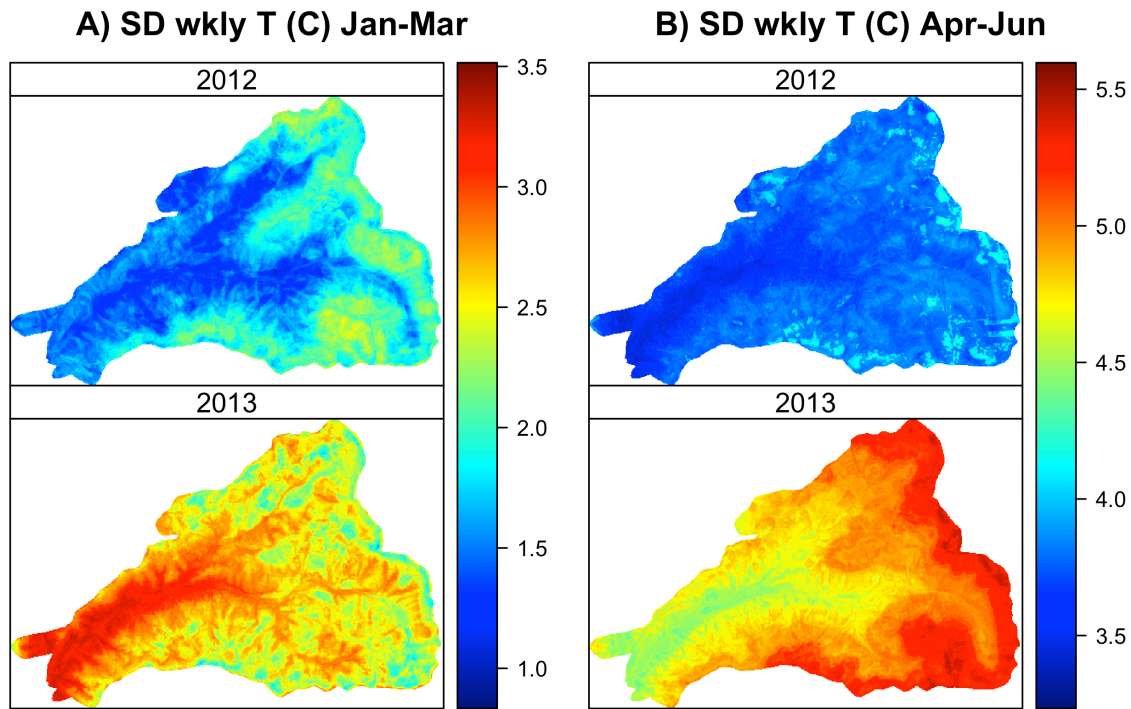


FIGURE 2.6. Spatially predicted variability in weekly temperature at the H. J. Andrews Experimental Forest based on BRT models. Response variables are: (A) Standard deviation (SD) of weekly temperature January-March (SDwTJM), and (B) SD of weekly temperature April-June (SDwTAJ). Elevation, vegetation and microtopography all had large relative influences on variability in weekly temperature in 2012 (A). In 2013 variability in January-March had a high component of vegetation and microtopography, but variation in April-June was primarily a function of elevation (B).

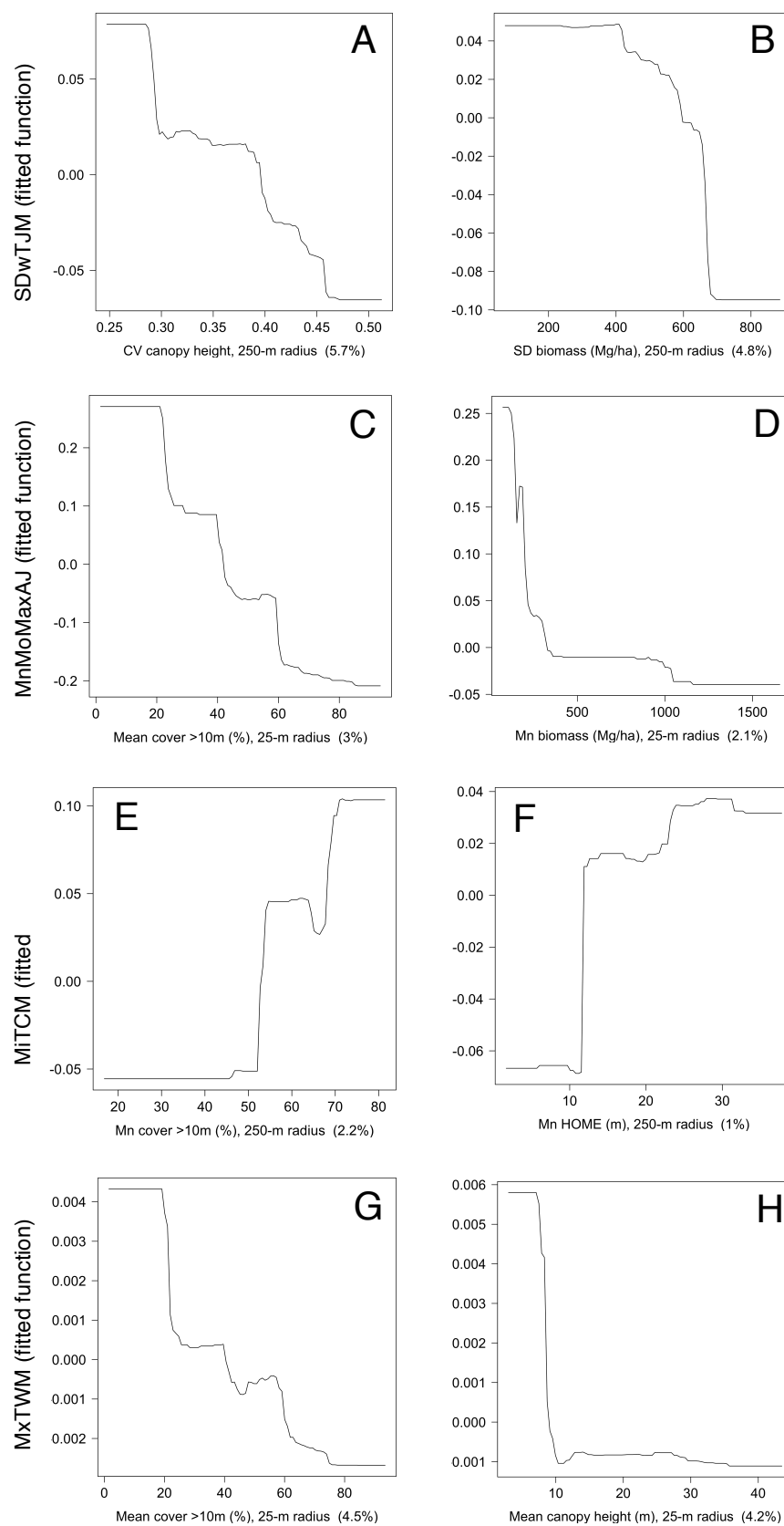


FIGURE 2.7. Partial dependence plots of key vegetation (VEG) variables. (A) Sites with a higher coefficient of variation in canopy height and (B) more variable biomass showed less variability in January-March (SDwTJM 2013). Proportion of canopy >10m (C) and increasing biomass (D) both reduce monthly maximum temperatures. Sites with a higher proportion of the canopy over 10m in height (E) and higher values of median return (HOME) (F) had the highest minimum temperatures (MiTCM 2012). Sites with a high proportion of the canopy >10m (G) and taller canopies (H) reduced the variability in temperature April-June (SDwTAJ 2013). Relative variable importance is indicated in parentheses (RI%).

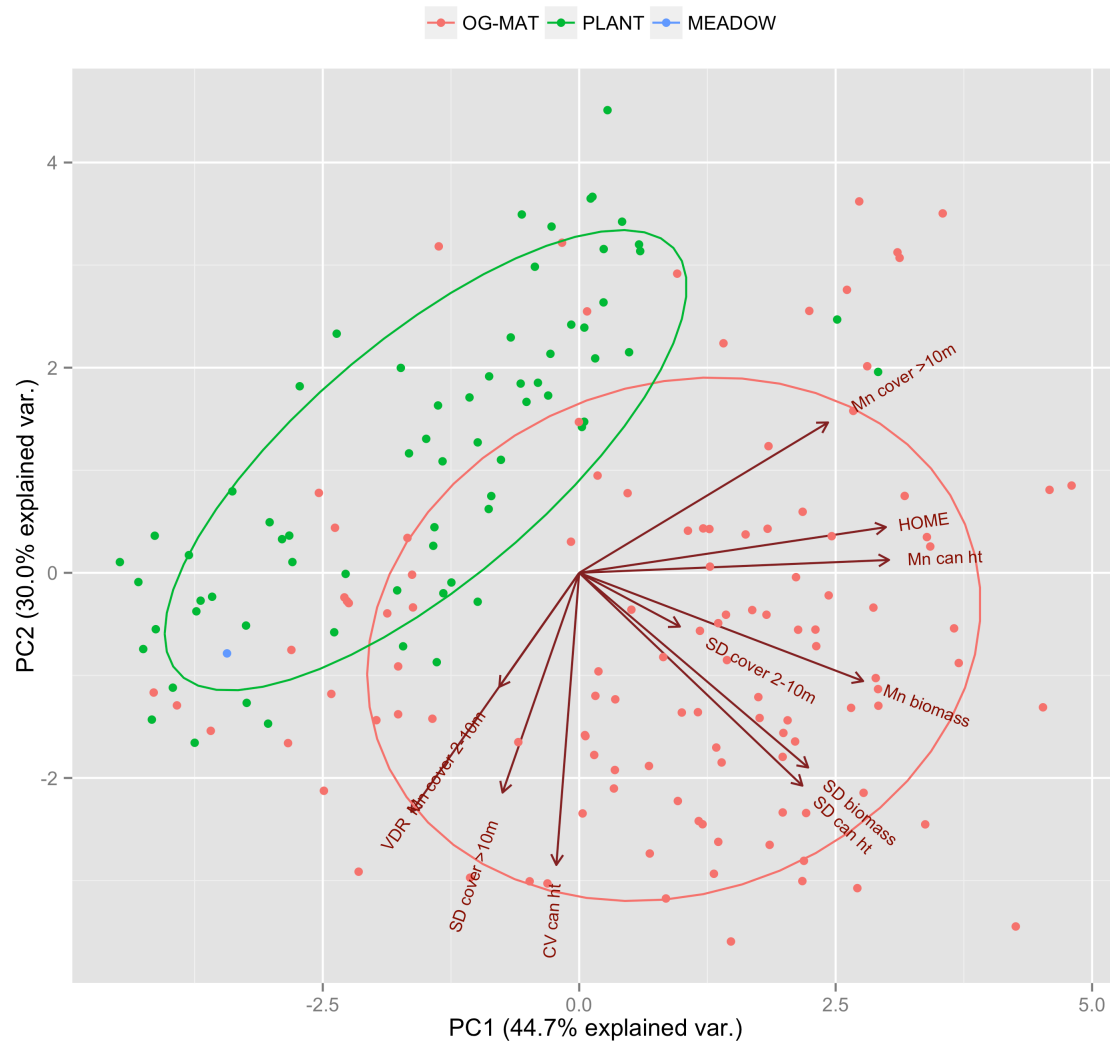


FIGURE 2.8. Principal component analysis showing how vegetation structure metrics differ between old-growth/mature forest sites (OG-MAT) and plantations (PLANT). See Appendix 3 for vegetation structure predictor variable definition

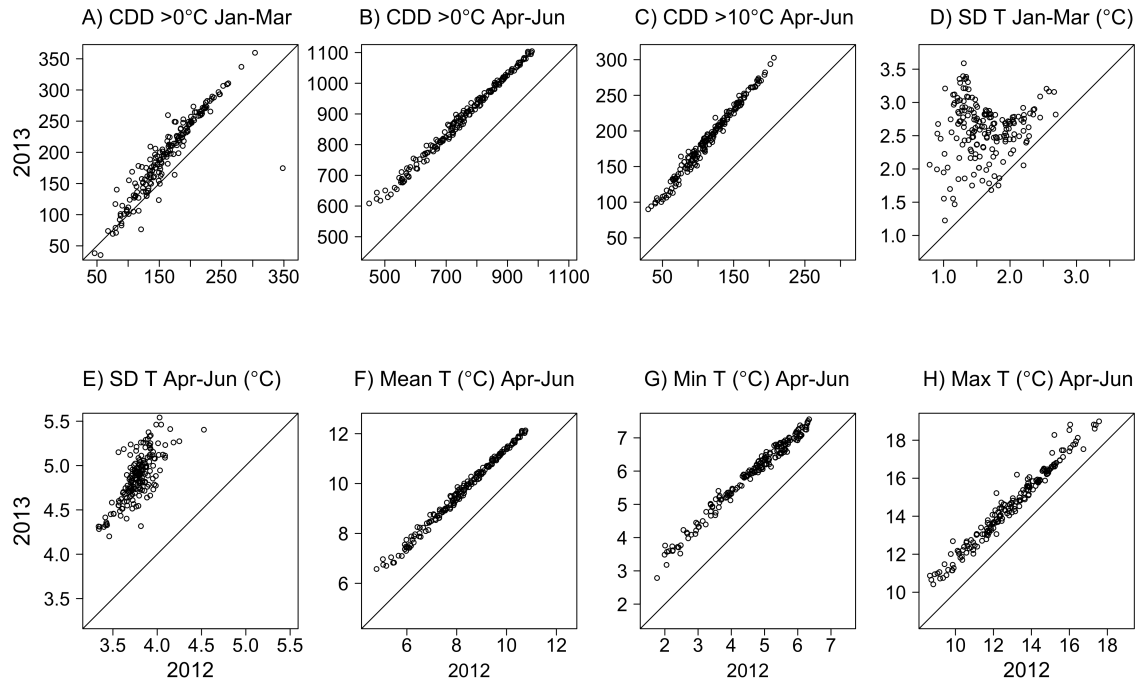


FIGURE 2.9. Comparison of temperature metrics measured in both 2012 and 2013. The majority of temperature metrics (A, B, C, F, G, H) showed extremely consistent temperature patterns in the two years despite warmer overall temperatures in 2013. Temperature variability (D, E) showed less consistency. Maximum temperature of the warmest month and minimum temperature of the coldest month were omitted from this figure because they were only calculated for 2012 due to a complete year of data.

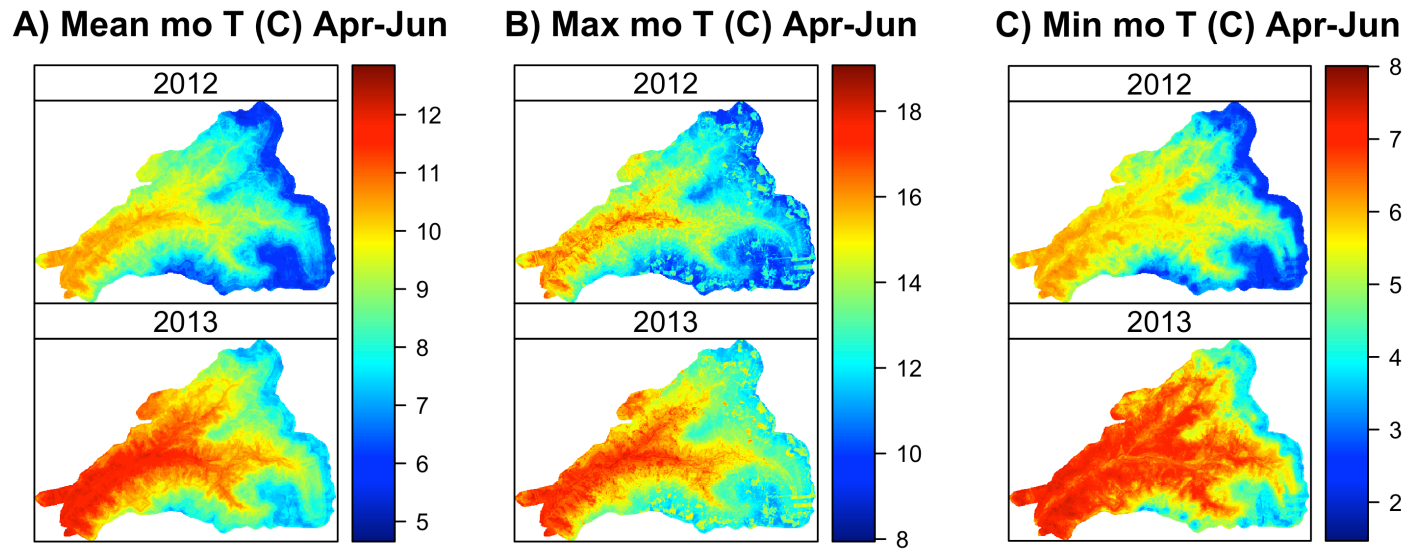


FIGURE 2.10. Spatially predicted temperature metrics showing monthly temperature at the H. J. Andrews Experimental Forest based on BRT models. Response variables are: (A) Mean monthly mean temperature April-June (MnMoMeanAJ), (B) Mean monthly maximum temperature April-June (MnMoMaxAJ), (C) Mean monthly minimum temperature April-June (MnMoMinAJ). Mean monthly temperatures were primarily a function of elevation (A), but maximum (B) and minimum temperatures (C) also had substantial relative influences of vegetation and microtopography.

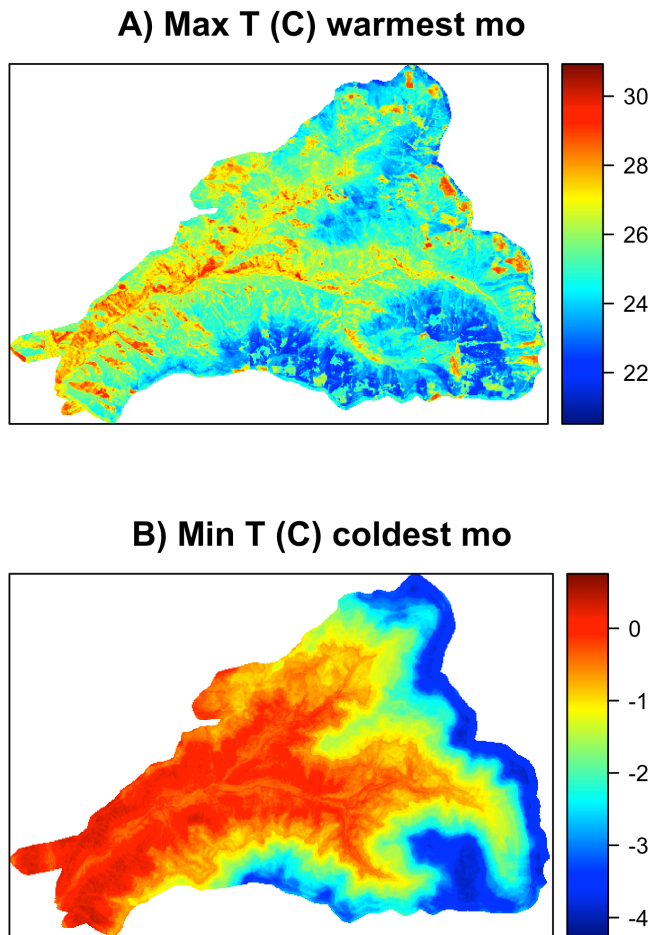


FIGURE 2.11. Spatially predicted temperature metrics showing temperature extremes at the H. J. Andrews Experimental Forest based on BRT models. Response variables are: (A) Maximum temperature of the warmest month (MxTWM), and (B) Minimum temperature of the coldest month (MiTCM). Maximum temperatures were primarily a function of vegetation and topography (A), but minimum temperatures were primarily influenced by elevation.

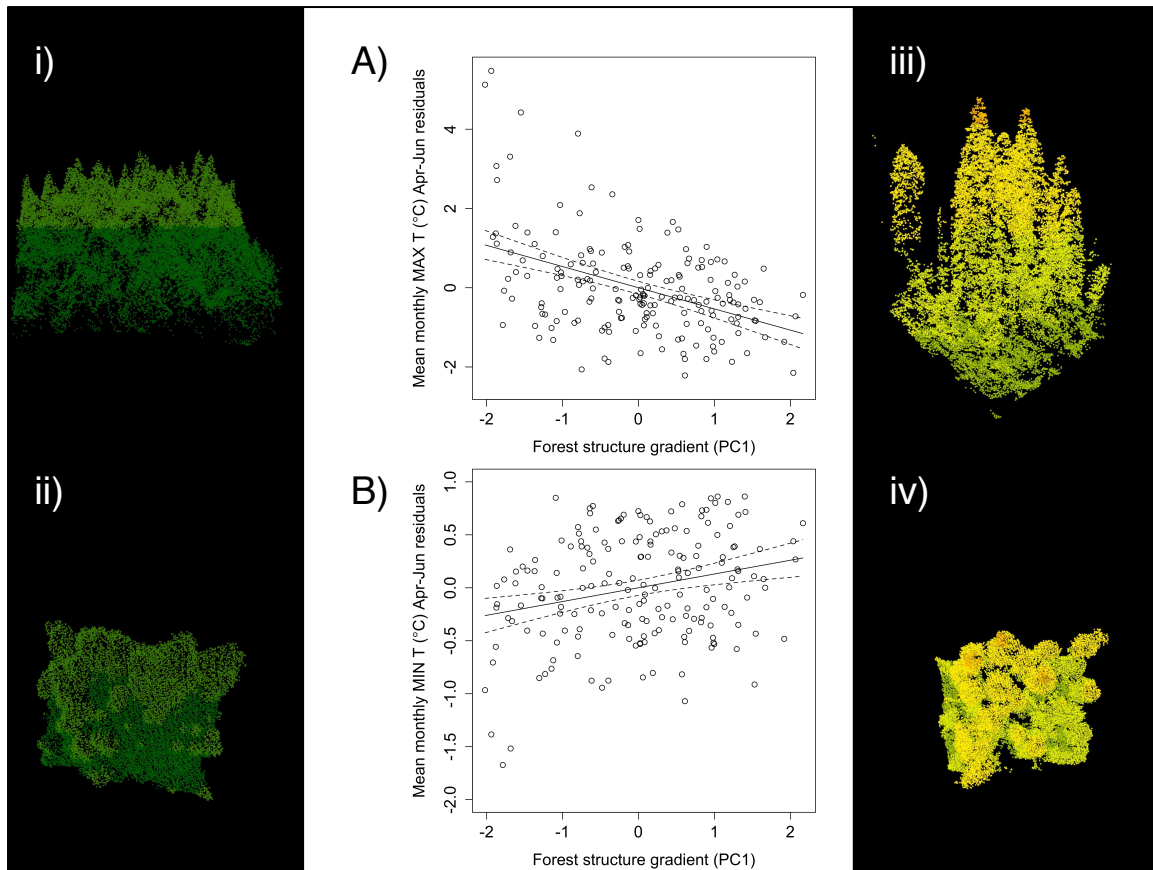


FIGURE 2.12. Results from generalized linear regression models testing the effect forest structure (PC1) on A) MonMnMaxAJ and B) MiTCM after accounting for the effect of elevation. A) and B) show the modeled relationship between forest structure (PC1) and the residuals from an elevation-only model of MonMnMaxAJ (A) and MiTCM (B). Maximum monthly temperatures observed in old-growth sites were 2.6°C (95% CI: 1.8 – 3.3°C) cooler than plantation sites during the spring-summer transition (A) and minimum temperatures during winter months were 0.6°C (95% CI: 0.4 – 0.8°C) warmer in old-growth stands (B). Three-dimensional LiDAR-generated images of old-growth forest (i = side, ii = top) and plantation forest (iii = side, iv = top) at H. J. Andrews Experimental Forest.

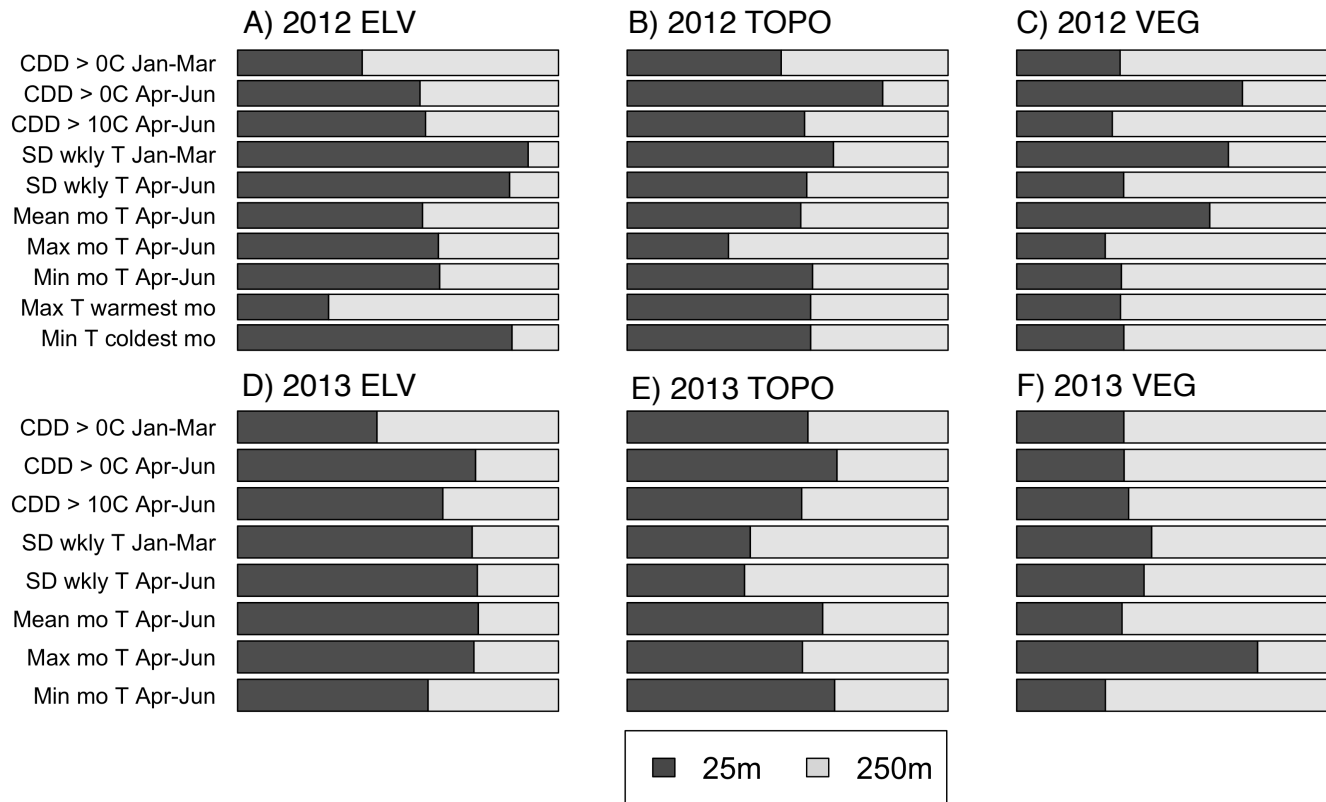


FIGURE 2.13. Relative importance of variables measured at 25m and 250m scales for each temperature metric in both years. Relative importance values are derived from the number of times each variable is selected in the process of model building using BRT

MICROCLIMATE PREDICTS WITHIN-SEASON DISTRIBUTION DYNAMICS OF
MONTANE FOREST BIRDS

Sarah J. K. Frey, Adam S. Hadley, Matthew G. Betts

3 MICROCLIMATE PREDICTS WITHIN-SEASON DISTRIBUTION DYNAMICS OF MONTANE FOREST BIRDS

3.1 ABSTRACT

Climate changes are anticipated to have pervasive negative effects on biodiversity and are expected to necessitate widespread range shifts or contractions. However, such projections are based upon the assumptions that (a) species respond primarily to broad-scale climatic regimes, and (b) that little variation in climate exists at finer spatial scales. We used dynamic occupancy models to test the degree to which microclimate influences distribution patterns of forest birds in a heterogeneous mountain environment. We hypothesized that high vagility of most forest bird species combined with the heterogeneous thermal regime of mountain landscapes would enable within-season shifts toward sites exhibiting moderated temperatures. In all models, we statistically accounted for vegetation structure, vegetation composition, and potential biases due to imperfect detection of birds. Fine-scale temperature metrics were strong predictors of bird distributions and movements; effects of temperature on within-season occupancy dynamics were as large or larger (1 to 1.7 times) than vegetation effects. Most species (86.7%) exhibited apparent within-season occupancy dynamics. However, species were almost as likely to be warm-associated (i.e., settle at warmer sites and/or vacate cooler sites; 53.3% of species) as cool-associated (i.e., settle at cooler sites and/or vacate warmer sites; 46.7% of species), suggesting that microclimate preferences are species-specific. Our results emphasize that high-resolution temperature data increase the quality of predictions about avian distribution dynamics in montane forest environments and should be included in efforts to project future distributions. We hypothesize that microclimate-associated distribution shifts may reflect species' potential for behavioral buffering from climate change in complex terrain.

3.2 INTRODUCTION

Climate change is already exerting a strong influence on species range shifts and population trends (Parmesan and Yohe 2003, Thomas et al. 2004, Both et al. 2006, Hitch and Leberg 2007, Devictor et al. 2008, Gutiérrez Illán et al. 2014). Climate change has also been

implicated in inconsistent phenological changes across taxa resulting in the decoupling of trophic interactions (Both and Visser 2005). Given that climate change is expected to amplify over the coming century (IPCC 2014), a key question is the degree to which such trends will continue, and whether biodiversity will decline as a result (Thomas et al. 2004).

Making reliable predictions about species responses to climate change has been challenging because species responses have not been monolithic; empirical studies using historical datasets have revealed high among-species variation in the degree to which populations and species distributions respond over time (Tingley et al. 2012, Gutiérrez Illán et al. 2014). Though some species demonstrate range shifting in response to climate change (Tingley and Beissinger 2009, Araújo and Peterson 2012, Virkkala et al. 2014) many species have not extended their ranges to occupy the geographic extent of apparently ‘suitable’ climates, either historically (Araújo and Pearson 2005, Moritz and Agudo 2013) or during recent rapid climate change (Thomas et al. 2004, Thuiller et al. 2004b). Though some of this variation in species responses is associated with life-history traits (Sheldon et al. 2011), much variation remains to be explained.

One hypothesis for this mismatch between climate envelope predictions and observed responses to change is that the climate data used to define suitable envelopes are based on data collected at resolutions much coarser than those perceived and used by organisms in habitat selection (Pearson and Dawson 2003, Logan et al. 2013, Bernardo 2014, Storlie et al. 2014). Most temperature data are collected at scales 10^4 -fold larger than the territory sizes of organisms of interest (Potter et al. 2013a, Bernardo 2014) and there is high potential for microclimate variation within broader regional patterns (Scherrer and Körner 2011, Franklin et al. 2013). Climate is assumed to be mainly a driver of distribution patterns at broad spatial scales (Thuiller et al. 2004a, Thomas 2010, Boucher-Lalonde et al. 2014) although habitat characteristics such as vegetation structure and composition are thought to trump the importance of climate at finer spatial scales (Brown 1995, Luoto et al. 2007). Therefore, this hidden microclimatic variation and its potential to affect distribution dynamics are often overlooked (Huey et al. 2012). Additionally, lack of high-resolution climate data, particularly under-canopy temperatures (Scherrer et al. 2011), has prohibited effective testing of the role of microclimate in fine-scale distribution dynamics.

Heterogeneous landscapes such as complex mountainous environments have been shown to promote more stable population dynamics (Oliver et al. 2010) and longer-term persistence (Vegas-Vilarrubia et al. 2012). Environmental heterogeneity offers a range of resources and microclimates that can provide options for ‘microrefugia’ where an organism can persist in the face of regional warming (Patsiou et al. 2013). In addition, microclimate variability at fine spatial scales could provide options for short-distance, adaptive movements and resource tracking within a season (Dobrowski 2010). Animals may adjust their use of local habitat in ways that allow them to persist in the face of climate change without necessitating broad-scale range shifts (Dolby and Grubb 1999, Kearney et al. 2009b). Landscapes with little variability provide fewer possibilities for new behavior (Bonebrake et al. 2014) such as shifts in habitat or diet.

An unstated assumption of most occupancy studies is one of closure between sampling periods within a breeding season (Rota et al. 2009), inferring that once territories are established in a breeding season, birds are assumed to be unlikely to shift their territory locations. However, work has recently demonstrated that within-season movements by birds may actually be relatively common (Whittaker and Marzluff 2009, McClure and Hill 2012, Gow and Stutchbury 2013) which violates the assumptions of commonly used species’ occupancy models (Rota et al. 2009) and necessitates the application of dynamic models. Observed within-season movements appear to reflect shifts to higher quality sites (Betts et al. 2008, Gilroy et al. 2010) and often represent shifts upwards along elevation gradients (Brambilla and Rubolini 2009). Given that site quality may change over the breeding season as temperatures warm (Vatka et al. 2011), being sufficiently flexible to take advantage of new favorable microclimates should be adaptive. However, the lack of detailed under-canopy microclimate data has left the role of temperature in these movements unknown since generally climate stations are widely spaced and located in open areas with great distances between stations (Scherrer et al. 2011).

Direct tracking of individual behavior to examine within-season movements (e.g., Gow and Stutchbury 2013) is logistically challenging, particularly when considering more than a single species. However, dynamic occupancy modeling offers a viable alternative for quantifying within-season movements (MacKenzie et al. 2003). These models allow changes in colonization and extinction processes across a season and have been shown to outperform static occupancy

models for many species (McClure and Hill 2012). Using this technique, the hypothesized drivers of settlement (colonization) and vacancy (extinction) processes can be examined to assess ‘apparent movement’ of individuals across a landscape (Betts et al. 2008).

In both 2012 and 2013, we sampled a forest bird community six times during the breeding season at 183 point count sites in complex mountainous terrain. We collected temperature data with sensors located at each of the count sites and calculated a suite of microclimate metrics expected to be of biological relevance (e.g., mean, minimum, and maximum temperatures and cumulative degree days). We used dynamic occupancy modeling to test the relative roles of local-scale temperatures and vegetation characteristics in apparent within-season movements while accounting for imperfect detection. We asked the following two questions: 1) Are forest bird species exhibiting apparent within-season movement? 2) To what extent are occupancy dynamics of birds predictable as a function of microclimate in relation to more traditional vegetation-based measures of habitat? We hypothesized that high vagility of most forest bird species combined with the heterogeneous thermal regime of mountain landscapes would enable within-season shifts toward sites exhibiting moderated temperatures.

3.3 METHODS

3.3.1 Study site

We collected bird occurrence data at 183 sample locations within the H. J. Andrews Experimental Forest (HJAEF) watershed. The 6400-ha HJAEF spans an elevational gradient from 410-1630 m.a.s.l. and is located in the Western Cascades of Oregon, USA (44°12' N, 122°15' W, Appendix 1). It is a forest mosaic comprised of a mix of old-growth forest, mature forests, ~60-yr old Douglas-fir (*Pseudotsuga menziesii*) plantations, alpine meadows, sitka alder (*Alnus viridis*) or vine maple (*Acer circinatum*) shrub fields, and landslides.

3.3.2 Site selection

We established our sample points so that they spanned gradients in elevation, climate, and forest vegetation structure. Specifically, we used a stratified, systematic, random design to select sample locations. We stratified across elevation, distance to road, and habitat type (plantation or mature/old-growth forest). Distance between all sampling points was $\geq 300\text{m}$.

Sample points were categorized as transect, trail, or road (the latter two categories were to facilitate site access thereby increasing sample size). Transect points were selected by placing a random grid of points across a portion of the watershed using GIS (ESRI 2011). We separated each transect by 600m and points within a transect were 300m apart. We placed trail points randomly along existing and abandoned trails (<1m wide) at 300-m intervals using GIS. Selection of road points was a two-step process. First, we placed points randomly along maintained and abandoned gravel roads at 600-m intervals using Hawth's tools (Beyer 2004) in GIS (ESRI 2011). Lastly, we chose a random direction and distance from the road (0, 50, or 100m) for the final point placement. Our final dataset was comprised of 60 transect points, 68 road points, and 55 trail points.

3.3.3 Point counts

We conducted point counts on six separate occasions from May – July in both 2012 and 2013, which corresponded to spring arrival and subsequent breeding period for the majority of the bird species at HJAEF. Point counts were conducted during favorable weather conditions by trained observers. We switched the order in which points were visited and which observer conducted the survey for each sampling session to reduce potential bias. The mean (standard deviation [SD]) length of sample occasions was 5 (1.17) days and 6 (1.22) days in 2012 and 2013, respectively. Mean (SD) break length between point count rounds was 4 (1.91) days in 2012 and 5 (1.90) days in 2013.

Point counts occurred between 05:15h and 10:30h corresponding to the period of peak singing activity. Each site visit consisted of a 10-min point count where we recorded all of the birds seen or heard within a 100-m radius. Each 10-minute point count was divided into three 3-min 20-sec sub-counts where the point count was reinitiated (*sensu* Betts et al. 2008). The sub-count during which an individual was first detected was recorded as a new record. We monitored the location of the individual birds in order to reduce the possibility of double-counting individuals. Multiple individuals were counted only when simultaneous singing or calling could be confirmed.

We detected a total of 41 species during May – July 2012 and 2013. We calculated the mean prevalence for all species in each year by calculating the proportion of sites with at least one detection over the six sampling occasions out of all sample sites (N=183). We used a 0.2

prevalence cut-off to select our final set of species. Models for species with mean prevalence less than 0.2 often failed to converge due to a low detection/non-detection ratio. After applying this prevalence threshold, 15 species remained; we used these species to model within-season occupancy dynamics (Table 1).

3.3.4 Environmental covariates

Air temperature data – In order to measure the local microclimate, we placed HOBO data loggers (Onset HOBO Pendant Temperature/Light Data Logger 64K, model UA-002-64 [n=167] and Onset HOBO Water Temperature Pro v2 Data Logger, model U22-001 [n=16]) that recorded temperature every 20 minutes at each sample point. We summarized temperature measurements from data loggers between Jan 2012 and July 2013 (See methods and Appendices 1 and 2 from Chap. 2 for details on loggers, their placement and data processing). We used five temperature metrics that we expected to influence forest birds during the breeding season and/or alter timing of important phenological events upon which birds depend. These metrics included cumulative degree days $>0^{\circ}\text{C}$ January – March and $>10^{\circ}\text{C}$ April – June, both of which are expected to be important drivers of bud break and insect abundance (Fu et al. 2012), bird phenology (Both et al. 2005), and bird distributions (Araújo et al. 2005). We included mean monthly temperatures (monthly mean, maximum, and minimum) from April – June. Mean maximum and mean minimum monthly temperatures capture temperature extremes and have been used to describe avian distributional boundaries (Root 1988) and predict abundance trends (Gutiérrez Illán et al. 2014). Mean monthly temperature describes the general temperature conditions at a site and is a common metric in species-climate studies (Virkkala et al. 2008, Stralberg et al. 2009). We chose the months of April, May and June since this is the period when we expected the majority of within-breeding season dynamics to take place.

3.3.5 Vegetation structure and composition

To quantify the gradient in forest structure, we used the first two principal components (PC) from a Principal Components Analysis (PCA) of all our LiDAR-derived vegetation variables at the 25-m scale (19 variables, see Chap. 2 Appendix 3). PC1 and 2 explained 75% of the variation present in the forest structure metrics and appeared to effectively differentiate between plantations and older forests (Chap. 2 Fig. 6). PC1 explained 45% of variance in

vegetation structure and increasing values were associated with old-growth forest characteristics (Chap. 2 Fig. 6 and Appendix 5). PC2 explained 30% of variation in vegetation structure and higher values tended to be more associated with forest plantations. We quantified forest composition by measuring the proportion of deciduous basal area at a site using variable radius prism plots and counting deciduous trees and large shrubs >2cm DBH (big-leaf maple [*Acer macrophyllum*], vine maple, red alder [*Alnus rubra*], Sitka alder, Pacific dogwood [*Cornus nuttalli*], beaked hazelnut [*Corylus cornuta*], cascara [*Rhamnus purshiana*], black cottonwood [*Populus trichocarpa*], bitter cherry [*Prunus emarginata*], Oregon white oak [*Quercus garryana*]). We chose to quantify the deciduous vegetation as our composition variable since amount of deciduous vegetation is often associated with abundance of leaf-gleaning forest birds and deciduous plant species are typically thought support higher abundances of insects (Hagar 2007, Ellis and Betts 2011).

3.3.6 Occupancy models

Apparent movement – We did not directly examine movements of individuals; rather we used patterns in settlement and vacancy from dynamic occupancy models to provide an index of within-season shifts. We therefore refer to changes in these parameters over the breeding season as ‘apparent movement’ (Betts et al. 2008, McClure and Hill 2012). Two potential biases have been identified with this approach to estimate within-season movements. Observed settlement and vacancy rates could partly result from temporary emigration and immigration in and out of the point count circle due to the combination of (a) variation in territory density and (b) territories not always falling completely within the point count radius (Chandler et al. 2011). For example, species with larger home ranges may be more likely to move out of a count circle while remaining within their original home ranges. In these cases, within-territory/home range movements could cause the appearance that a site has become vacant when the bird is actually still within its initial home range (i.e., site counted as vacant when it is not). Similarly, in areas of high density, multiple territories could overlap the count circle and the likelihood of detecting at least one individual within the count circle is higher, purely because more individuals are present.

We addressed these potential biases in estimates of apparent movement in two ways. First we used information about the home range size for each species (Table 1, Poole 2005) to test whether species with larger home ranges show higher levels of within-season dynamics, which

would suggest artificially high apparent settlement and vacancy rates (Betts et al. 2008).

Secondly, we used detections within a 100-m radius to increase the likelihood that entire territories were included within the boundaries of the sample plot. The majority of the species (12/15) we included in our study have territory sizes that are smaller than our sample plot (area of 100-m radius point count circle = 3.14 ha).

We used dynamic occupancy models (MacKenzie et al. 2003) to estimate within-season movement dynamics as a function of microclimate conditions in the HJAEF. These models use detection histories from multiple surveys (i.e., our three sub-counts) over multiple seasons (i.e., the six site visits) to estimate four parameters: 1) detection probability (p), 2) initial site occupancy (ψ), 3) site colonization (γ), and 4) local site extinction (ϵ). Occupancy models are hierarchical in that they model the observation process (detection) independent from the ecological processes of interest (site occupancy, colonization, and extinction). We adapted the multi-season framework of dynamic occupancy models to estimate apparent movement within a breeding season. For our within-season application of dynamic occupancy models we refer to colonization as site ‘settlement’ (γ) and extinction as site ‘vacancy’ (ϵ).

Dynamic occupancy models assume that populations are closed between j sub-counts and movement is explicitly modeled between t sampling occasions by the dynamic parameters (γ and ϵ). This is a Markovian process in that occupancy in time t is dependent on occupancy in time $t - 1$. A site can go from unoccupied in time $t - 1$ to occupied in time t (settlement event) or from occupied in time $t - 1$ to unoccupied in time t (vacancy event). The model structure is as follows:

$$Z_{i1} \sim \text{Bernoulli}(\psi) \text{ for } i = 1, 2, \dots, M$$

$$Z_{it} \sim \text{Bernoulli}(Z_{i,t-1}(1 - \epsilon_{it}) + (1 - Z_{i,t-1})\gamma_{it}) \text{ for } t = 2, 3, \dots, T$$

$$Y_{ijt}|Z_{it} \sim \text{Bernoulli}(Z_{it}p) \text{ for } j = 1, 2, \dots, J_i$$

where Z_{i1} is the occupancy state (1 or 0) of site i during the first sampling occasion ($t = 1$, ‘season 1’), Z_{it} is the occupancy state in subsequent sampling occasions ($t = 2, 3, \dots, T$), and Y_{ijt} is the observed occurrence status (1 or 0) at site i in sub-count j during sampling occasion t . M is the total number of sample sites, T is the total number of sampling occasions, and J is the total number of sub-counts. We conducted three sub-counts ($J = 3 \times 3$ -min 20-sec sub-counts) during

each sampling occasion ($T = 6$) at each sample site ($M = 183$ total sites). If site i is not occupied at time $t - 1$ ($Z_{i,t-1} = 0$), and the success probability of the Bernoulli is $0 * (1 - \varepsilon_{it}) + (1 - 0) * \gamma_{it}$, so the site is occupied (i.e., settled) in sampling occasion t with probability γ_{it} . Conversely, if site i is occupied in time $t - 1$ ($Z_{i,t-1} = 1$) and the success probability of the Bernoulli is given by $1 * (1 - \varepsilon_{it}) + (1 - 1) * \gamma_{it}$, the site remains occupied (i.e., does not become vacant) in sampling occasion t with probability $1 - \varepsilon_{it}$. It is important to note that colonization and extinction are not absolute; they are relative to the number of occupied and unoccupied sites in the previous sampling occasion. For example, if 20 of 100 sites were occupied in time $t - 1$ (20% occupied), with a vacancy rate of 30% and a settlement rate of 20%, 16 sites (20% of 80 unoccupied sites) would get settled, 6 sites (30% of 20 occupied sites) would be vacated, resulting in 30 sites being occupied in time t ($20 * [1 - 0.3] + [100 - 20] * 0.2 = 30$).

We estimated the four parameters (p , ψ , γ , and ε) using maximum likelihood techniques based on site detection histories (Y_{ijt}) with the following likelihood equation (MacKenzie et al. 2003, Fiske and Chandler 2011):

$$L(\psi_1, \varepsilon, \gamma, p | \{Y_{ijt}\}) = \prod_{i=1}^M \Pr(Y_{ijt})$$

Here, ψ_1 refers to the initial occupancy in the first sampling occasion, where thereafter ε and γ determine site occupancy in the following sampling occasions ('seasons'). p is the probability of detection given that site is occupied. Parameters can be modeled as a function of site- and survey-level covariates on the logit scale.

3.3.7 Model selection

In order to reduce our model set, we used a manual forward stepwise approach to select the variables that best explained detection probability and the site occupancy parameters (Olson et al. 2005, Chandler and King 2011). We selected survey- and site-level covariates we considered to be important in our system *a priori* (see temperature and vegetation metrics above). All continuous predictor variables were standardized (z-score = $[x - \text{mean}]/\text{SD}$, where x is a single covariate value for a site or survey) so that we could directly compare effect sizes. We compared support for models containing the different covariates using AIC model selection (Burnham and Anderson 2002).

Our model selection steps were as follows: 1) We first ranked univariate models for each of the covariates using AIC. 2) Then we constructed additive models including covariates based on and in order of their AIC ranking (highest to lowest). We added variables on order of support until additional covariates resulted in the model being more than 2 Δ AIC points below the top model. 3) Finally, we selected the most parameterized model (the one with the highest number of covariates) within 2 AIC points of the top model. This was almost always the top ranked model.

The top temperature and vegetation metrics were combined in additive models. However, we never combined multiple temperature metrics in any additive models due to the high inter-variable correlation we observed (Appendix 2). We did combine vegetation variables in additive models because they did not suffer from the same correlation issues (PC1 and 2 are orthogonal and our vegetation composition metric was not strongly correlated with either structural variable, Appendix 2). We also combined multiple survey-level covariates in additive models for detection.

Detection & initial occupancy – First we selected top model for detection while holding all other parameters constant. We tested for differences in detection rates based on our eight temperature and vegetation variables (see above) in addition to six survey-level variables (i.e., survey time, number of days since May 1 [day of year], observer, stream noise, weather conditions [cloud cover and wind], and a temporal autocovariate). We included a temporal autocovariate because sub-counts were not independent temporally (initial detection of a species might enhance the likelihood that an observer detects the species in a subsequent interval). This autocovariate indicated whether an individual was detected in the previous sub-count. We used the top-ranked covariates for each species for detection in the remainder of the model selection steps. To determine the baseline occurrence patterns (i.e., initial occupancy) for each species in the first site visit (mid-May) we selected the top temperature metric while accounting for vegetation structure and composition (following the model selection steps listed above). During variable selection for both detection and occupancy, we held settlement and vacancy constant.

Settlement & Vacancy – Our main focus was to understand how microclimates affect settlement and vacancy patterns during the breeding season while statistically accounting for variability in forest structure and composition. We first estimated mean settlement and vacancy rates to determine the degree to which species exhibited apparent within-season movement. We

considered species with mean vacancy or settlement probability less than 0.1 to be relatively static during the breeding season. Even though these rates are relative to the number of occupied sites in the previous time period, if estimated values approach zero it is an indication that occupancy patterns are more likely static. For both settlement and vacancy, we compared univariate models of our microclimate and vegetation metrics while holding the other dynamic parameter constant (e.g., vacancy was held constant while examining settlement and vice versa). We then combined the top variables for both settlement and vacancy into the same model to obtain the final model. All analyses were conducted in R version 3.1.1 (R Development Core Team 2011) using the ‘unmarked’ package (Fiske and Chandler 2011).

3.3.8 Relative importance of microclimate and vegetation on occupancy dynamics

Once we had identified the top models for each of the 15 species in each year, we assessed the relative importance of the temperature and vegetation metrics. We used the effect sizes and corresponding standard errors as a measure of their importance. In order to account for differences in precision of estimates, we divided all effect sizes by their corresponding standard errors (Ritchie et al. 2009). We then directly compared the absolute values to each other (as effects could be negative or positive) and deemed the variable with a larger absolute value as the more important metric. When more than one vegetation metric was in the top model, we used the one with the largest effect size. In the rare instance where none of the metrics were useful in explaining variability in the occupancy parameters we considered the effect size to be zero. We did this for initial occupancy, settlement, and vacancy.

3.3.9 Model fit

MacKenzie and Bailey (2004) proposed a method for assessing model fit for single-season occupancy models in which fit statistics are applied to combined detection histories. However this method performs poorly when the number of survey occasions and sub-counts ($J \times T$) are large and continuous variables are used (Kery and Chandler 2012). Goodness-of-fit tests for dynamic occupancy models are still considered exploratory (Kery and Chandler 2012). Adapting R code from Kery and Chandler (2012), we used parametric bootstrapping to evaluate the goodness-of-fit of the best model for each species in each year. For each species, we simulated 250 datasets from its top model in a given year, each time we refitted the model to

these simulated data and computed a fit statistic (here sum of squares error [SSE]). The simulation resulted in a reference distribution of the fit statistic from which we computed a P -value indicating the proportion of the reference distribution that was greater than the observed value. We used χ^2 to compare observed and expected fit statistics because it has been shown to perform well at evaluating goodness-of-fit for logistic regression models (Hosmer et al. 1997, MacKenzie and Bailey 2004, Kery and Chandler 2012). Models with fit statistics that are higher than the mean fit statistic (SSE) from the simulated distribution are indicative of overdispersion in the data, meaning that there is still unexplained variability. Conversely, an observed fit statistic that is lower than the mean simulated statistic indicates underdispersion, meaning that the data are less variable than one would expect based on the underlying distribution used in the model.

3.4 RESULTS

3.4.1 Detection & initial occupancy

In general, the temperature and vegetation metrics were good predictors of initial distributions of the HJAEF bird species (Fig. 1, Appendix 3). Temperature was the most important predictor (largest effect size) for 80% and 47% of species in 2012 and 2013, respectively. Of the species with temperature as a significant ($P < 0.05$) predictor in the top model (Fig. 1), roughly equal numbers were associated with warm sites (53%) versus cooler sites (47%) during initial occupancy on average across both years (Appendix 3). Vegetation (structure and/or composition) was a significant predictor of initial occupancy patterns for a substantial proportion of species in both years (2012: 33%, 2013: 47% of species, Fig. 1, Appendix 3) and was more important than temperature for 20% and 53% of species in 2012 and 2013, respectively.

Temporal autocorrelation in sub-counts was an important predictor for detection probability for all species in both years (Appendix 4). Detection probability was always higher when an individual was detected in the previous sub-count. Detection probability decreased later in the morning (8 species), later in the breeding season (7 species), with higher levels of stream noise (8 species), and with increased cloud cover (6 species). For three species in 2012 and seven in 2013, we detected differences in detection probability by observer (Appendix 4). In addition to

influences of survey-related variables on detection, we observed significant ($P < 0.05$) effects of temperature (80% of species) and vegetation (73% of species) on detection probability in at least one year (Appendix 4).

3.4.2 Apparent movement

In both years, the majority of species showed mean settlement and vacancy rates >0.1 throughout the breeding season indicating that overall occupancy patterns were dynamic (Appendix 5; settlement – 80.0% of species in both years; vacancy – 2012: 86.7%, 2013: 93.3%; overall: 86.7%). On average for all species, mean vacancy probability (Mean [SD] – 2012: 0.39 [0.20], 2013: 0.38 [0.21], Appendix 5) tended to be higher than settlement probability (2012: 0.22 [0.14], 2013: 0.22 [0.13], Appendix 5). The mean settlement and vacancy rates are interpreted as the change in occupancy that occurred between each sampling occasion (i.e., between 1 and 2, 2 and 3, 3 and 4, etc.) on average across all sites (not including any covariate effects). To reiterate, these rates are relative to the number of sites occupied in the previous sample session.

Site-level temperature metrics were strong predictors of the apparent movement we observed and temperature was equally or more effective (1 to 1.7 times) as vegetation at predicting local site occupancy dynamics in both years (Fig. 1, Tables 2 & 3, Appendix 6). Temperature metrics were the most important predictors (larger effect sizes) for at least one dynamic parameter for 73.3% and 66.7% of species in 2012 and 2013, respectively (see Tables 2 & 3 for effect sizes and standard errors [SE] from top models, see Appendix 6 for comparison of SE-adjusted effect sizes). Overall, species were almost as likely to be warm-associated (i.e., settle at warmer sites and/or vacate cooler sites; 53.3% of species) as cool-associated (i.e., settle at cooler sites and/or vacate warmer sites; 46.7% of species). We identified brown creeper (*Certhia americana*), chestnut-backed chickadee (*Poecile rufescens*), Hammond's flycatcher (*Empidonax hammondi*), Pacific wren (*Troglodytes pacificus*), Pacific-slope flycatcher (*Empidonax difficilis*), Steller's jay (*Cyanocitta stelleri*), Swainson's thrush (*Catharus ustulatus*), and western tanager (*Piranga ludoviciana*) as warm-associated species based on their overall occupancy patterns (Appendix 7). The cool-associated species (Appendix 8) were golden-crowned kinglet (*Regulus satrapa*), hermit thrush (*Catharus guttatus*), hermit warbler (*Setophaga occidentalis*), Oregon junco (*Junco hyemalis*), red-breasted nuthatch (*Sitta*

canadensis), varied thrush (*Ixoreus naevius*), and Wilson's warbler (*Cardellina pusilla*).

Preference for cool versus warm sites never switched for a species for any of the ecological parameters (Tables 2 & 3, Appendices 3 & 6). However, whether temperature alone, vegetation alone or the combined effect of vegetation and temperature were most important for a given parameter did vary within species between years (Tables 3 & 4). Species whose settlement patterns were largely temperature driven (larger effect size), 71.4% (2012) and 62.5% (2013) showed preference for sites with cooler microclimates (Table 2, Appendix 6). For species whose vacancy patterns were driven primarily by temperature, 77.8% (2012) and 55.6% (2013) were those that vacated warmer sites (Table 3, Appendix 6).

Hermit warbler (Figs. 2 & 4) is an example of a cool-associated species where site-level dynamics were largely driven by temperature, and vegetation structure to a lesser extent. Hermit warblers were both less likely to settle sites (Fig. 2A) and more likely to vacate sites (Fig. 2C) that were warmer. Predicted distribution maps (Fig. 4) show that hermit warblers shift away from warmer sites and towards cooler sites. In contrast, Pacific wren, a warm-associated species, is an example of a species where both temperature and vegetation were important for within-season dynamics (Figs. 3 & 5). Pacific wrens were more likely to settle warmer sites (Fig. 3A) and vacate cooler sites (Fig. 3E). Pacific wrens were also more likely to settle sites with old-growth characteristics (Fig. 3B) and a higher deciduous composition (Fig. 3C). Finally, Pacific wrens were more likely to vacate even-aged vegetation stands such as plantations (Fig. 3D). The predicted distribution maps for this species (Fig. 5) highlight the strong vegetation component of apparent movement in addition to temperature.

We found no relationship between home range size and probability of settlement (neither in 2012 nor 2013) or with vacancy in 2013. However, in 2012 we did find a positive relationship between home range size and mean vacancy probability ($\hat{\beta} \pm \text{SE} = 0.005 \pm 0.002$, $P = 0.052$, $r^2 = 0.204$) supporting the hypothesis that large home ranges might result in biases to dynamic occupancy estimates. This pattern was driven by the species with the largest home ranges (Steller's jay: 80ha; varied thrush: 7ha; and brown creeper: 4.2 ha). Mean home range size of the 12 remaining species was 1.2 ha [range = 0.3 – 2.8ha], Table 1). When these three outliers were removed from the sample, the relationship disappeared ($\hat{\beta} \pm \text{SE} = 0.022 \pm 0.015$, $P = 0.16$, $r^2 =$

0.11) suggesting that this problem might exist only for species with home ranges much larger than the count circle (3.14ha).

3.4.3 Model fit

Our goodness-of-fit tests indicated no or minimal lack of fit due to overdispersion in our models (Appendix 9). Goodness-of-fit tests for Steller's jay in 2012 and hermit thrush in 2013 suggested slight overdispersion ($P = 0.33$ and 0.11 , respectively). Three species (only in 2012) showed little to no difference between the observed and mean expected fit statistic ($0.25 < P < 0.75$). We did find evidence for underdispersion in our data; the majority of species had fit statistics that were lower than the distribution of bootstrapped values ($P > 0.75$). Underdispersion is generally not considered a problem as it results in inflated standard errors, leading to more conservative estimates of covariate effects (Hosmer et al. 2013). The minimal evidence of overdispersion in our data indicated that spatial autocorrelation was unlikely (Haining et al. 2009). However, spatial autocorrelation, a common property of ecological data, could potentially be problematic due to violation of sample independence assumptions (Legendre 1993). Therefore, we tested for spatial autocorrelation in our data by calculating Moran's I for the residuals from the top model for each species (see Appendix 10 for results). Moran's I values can range from 0 to 1 and values > 0.3 are considered relatively large (Lichstein et al. 2002). We found no evidence for spatial autocorrelation in the residuals (mean [SD] Moran's I for all species 2012 = -0.002 [0.014], 2013 = 0.001 [0.007]; mean [SD], P -values 2012 = 0.230 [0.046], 2013 = 0.237 [0.031]) indicating that spatial autocorrelation was not an issue in our study (Appendix 10).

3.4.4 Annual temperature consistency

We examine year-to-year consistency in temperature metrics to determine if potential for microrefugia could be predictable. Temperature metrics within sites were highly consistent between years, despite 2013 being warmer overall during the breeding season months (Fig. 6). Sites were very similar from one year to the other with respect to cumulative degree days (Fig. 6A-B, CDD >0 JM: Pearson's correlation coefficient [r] = 0.92 , $P = < 0.0001$, CDD >10 AJ: $r = 0.99$, $P = < 0.0001$). Mean, maximum and minimum monthly temperatures from April – June were also consistent across years (Fig. 6C-E, mean: $r = 0.99$, $P = < 0.0001$, max: $r = 0.98$, $P = < 0.0001$, min: $r = 0.99$, $P = < 0.0001$). Mean monthly mean and minimum from April – June were

the most common significant temperature predictors for dynamic occupancy parameters (Tables 2 & 3, 2012: mean [33.3%] and min [40%], 2013: mean and min both [26.7%]). See Appendix 11 for all model selection tables.

3.5 DISCUSSION

We present the first evidence that occupancy dynamics of forest birds can be explained by local temperature conditions. Climate is widely accepted to be a major driver of species distributions at broad spatial extents (Thuiller et al. 2004a, Thomas 2010, Boucher-Lalonde et al. 2014), but here we demonstrate that temperature is a strong predictor of within-season distribution dynamics even at very fine spatial scales.

Local habitat selection in birds has often been shown to depend on vegetation characteristics (Hildén 1965) such as structure (MacArthur et al. 1962, Seavy et al. 2009) and composition (Ellis and Betts 2011). However, local-scale temperature appears to be equal or of greater importance than vegetation for site occupancy by forest birds in our system. Clearly our findings do not downplay the important role of vegetation in species distributions; rather they highlight the need to account for microclimate variability when considering distribution changes. Occupancy dynamics for many species we examined depended on both microclimate and vegetation metrics. To the best of our knowledge, no other bird-occupancy studies have yet compared the role of local-scale temperature and vegetation in a forest system. However, there is some previous evidence that the combined effects of vegetation and temperature influence avian occurrence patterns in other systems. For example, in an exurban environment, Lumpkin and Pearson (2013) found that both temperature and habitat characteristics (building density and forest cover) affected bird occurrence patterns. Further, previous work conducted at broad spatial scales has shown a strong influence of both vegetation and temperature on bird distributions (Cumming et al. 2014).

Microclimate is known to be important for ectotherms due to thermoregulation requirements (Suggitt et al. 2012, Scheffers et al. 2014), but has only been recently considered for endotherms (Boyles et al. 2011, Bernardo 2014, Long et al. 2014). The influence of climate on endothermic species distributions has been almost exclusively explored at large spatial scales (Peterson et al. 2002, Mitikka et al. 2008, Stralberg et al. 2009, Thomas 2010), 10^4 -fold larger

than the scale at which organisms generally make habitat selection decisions (Potter et al. 2013a). An important advance in our study was that we directly measured air temperature at the same sites where we counted birds; we did not use elevation as a proxy for temperature (Klemp 2003, Maggini et al. 2011) or interpolate temperature from widely spaced meteorological stations placed in open areas (Scherrer et al. 2011). The combination of dynamic occupancy modeling and high-resolution temperature data allowed us to elucidate clear changes in intra-season distributional patterns for multiple species along a microclimate gradient.

We also found that most species of forest birds examined exhibited apparent within-season movements. Our results add to growing evidence that within-season site occupancy is less static than traditionally assumed (Betts et al. 2008, McClure and Hill 2012). For example, McClure and Hill (2012) also found dynamic occupancy models outperformed static occupancy models in a southeastern U.S. forest bird community, suggesting birds were shifting sites within a breeding season. Radio tracking (Klemp 2003, Gow and Stutchbury 2013), territory mapping (Brambilla and Rubolini 2009), and mark-recapture studies (Gilroy et al. 2010) have also demonstrated within-season movements and site shifts in birds.

Within-season shifts can be the result of three main processes: 1) habitat upgrading, 2) thermoregulation, and 3) resource tracking. Shifts are often thought to follow failed breeding attempts (Switzer 1997, Hoover 2003) or to represent upgrading along gradients in habitat quality (Betts et al. 2008). Models of habitat selection typically assume that when animals select a breeding site they possess the necessary ('ideal') information about site quality and dispersal capabilities to make the best choice (Fretwell and Lucas 1969, Pulliam and Danielson 1991). In reality, it may not be possible to obtain dependable site quality information quickly (Stamps 2006) and it may take time for individuals to gain personal information (Doligez et al. 2002, Hoover 2003). This could result in a delay between when birds initially arrive at a location and settle at a final breeding site. Alternatively, some species could still be migrating and their presence at the HJAEF might be as transients on a stopover for refuel and rest (Moore 2000) rather than a first attempt at breeding. We started our sampling in mid-May when some late arrivers could still be making their way north or to higher elevations to their final breeding grounds.

Secondly, it is likely that some portion of the shifting distribution dynamics could be due to behavioral thermoregulation (Bernardo 2014). Mammals (Long et al. 2014) and birds (Dolby and Grubb 1999) have both been shown to alter their behavior in response to temperature conditions. Other studies have documented upward shifts along elevational gradients (e.g., Klemp 2003) which are suggested to indicate shifts toward climatically suitable sites amid seasonal warming.

Finally, within season movement may enable birds to capitalize on ephemeral resources available in spatially distinct locations (Diggs et al. 2011). Within-season shifting could represent upgrading along ecological gradients in habitat quality to track changes in resources. For example, Betts et al (2008) found that as the breeding season progressed, black-throated blue warblers (*Setophaga caerulescens*) moved towards sites with characteristics known to increase reproductive success (Rodenhuse et al. 2003) such as higher elevations and sites with higher shrub densities. Hence, motivation behind settlement and vacancy decisions could potentially be linked to temperature-sensitive food resources – particularly arthropod abundance (Lack 1954, Martin 1987, Rodenhuse et al. 2003, Both et al. 2006). Temperature and degree days in late winter and spring are known to be strongly associated with important phenological events such as bud break (Yu et al. 2010, Fu et al. 2012), insect emergence (Both et al. 2009b), and insect abundance (Kingsolver et al. 2011).

An important caveat of our work is that we did not measure movement directly through methods such as telemetry (e.g., Gow and Stutchbury 2013). In particular, we were only able to quantify ‘apparent movement’ within a season based on modeled settlement and vacancy rates (MacKenzie et al. 2006, McClure and Hill 2012). Despite the fact that our models were designed to account for imperfect detection, within-territory movements of birds into and outside of our count circle between sampling sessions could appear as settlement and vacancy (Betts et al. 2008). However, based on simulation studies performed by Chandler et al. (2011), temporary emigration from a sample location is only likely to bias parameters estimates when it is not random. If patterns in temporary emigration are related to the environmental gradients of interest, then it could be erroneously identified as apparent movement. Viewed from the most conservative standpoint, our results still represent clear site occurrence patterns based on microclimate if ‘apparent movement’ is a function of higher abundances at preferred sites.

3.5.1 Implications

The primary assumption of most standard occupancy modeling techniques is one of closure between sampling occasions within a season (MacKenzie et al. 2002). We added to the mounting evidence suggesting that this assumption may be frequently violated (Rota et al. 2009). Despite our sampling occasions occurring over relative short time intervals (on average 4 – 5 days between sample occasions), we documented substantial changes in site occupancy over the breeding season for most species. This indicates that habitat selection is a dynamic process in heterogeneous mountain environments.

We have provided evidence that high-resolution temperature data is useful for species distribution modeling. Though the logistics of obtaining such high resolution temperature data may be challenging (Bennie et al. 2014), we argue that failing to incorporate local microclimate variability masks important occupancy patterns. The discrepancy in the assumed importance of climate versus vegetation on site selection processes at regional versus local scales could stem from the fact that we measure climate well at broad spatial scales and vegetation well at small spatial scales. Our results indicate that lack of fine-scale temperature data may be concealing the relative role of temperature and could lead to the appearance of vegetation as the key driver of distributions at fine scales (Luoto et al. 2007).

While most species showed apparent site shifts in response to local temperature conditions, the direction of these responses varied by species (roughly equal numbers of species were cool- and warm-associated). Moritz and Agudo (2013) found that many species had highly variable responses to climate. Many range-shift studies have reported high variability in both the degree and direction of shifts (Lenoir et al. 2010, Chen et al. 2011). Microclimate heterogeneity and species-specific responses to local-scale temperature could explain some of the inconsistencies between predicted and observed responses to climate change (Lenoir et al. 2010, Buckley and Kingsolver 2012).

Our results showing within-season movements for most species we examined suggest that forest bird species have the behavioral flexibility to track suitable microclimates within a breeding season (Boyles et al. 2011, Tuomainen and Candolin 2011). In montane landscapes, complex terrain could create buffered ‘microrefugia’ (Dobrowski 2010). This indicates that microclimate heterogeneity may be an important factor in providing options for behavioral

adaptation (Bonebrake et al. 2014) in the face of regional climate changes. Stable populations in heterogeneous landscapes could stem from increased options for tracking microclimate (Oliver et al. 2010). We detected weak evidence for population declines in species we identified as being ‘cool-associated (mean trend [95% CIs] = -1.06 % change/year [-1.96 – -0.16]; Fig. 7) at the regional scale (Breeding Bird Survey 2002-2012 trends from the Northern Pacific Rainforest region [OR, WA, CA], Sauer et al. 2014) relative to their warm-associated counterparts (-0.16 % change/year [-0.99 – 0.68]). This suggests that at least regionally, buffering capacity may be insufficient to sustain stable populations for cool-associated species in the face of climate change (CIs for trends of cool-associated species do not include 0, where trends for warm-associated species do; Fig. 7).

3.5.2 Conclusions

We demonstrated that local-scale occupancy patterns of forest birds are strongly associated with fine-scale thermal regimes in mountainous landscapes. Further, we found considerable evidence that temperature is an important factor in determining within-season distribution dynamics. The correlative relationship between occupancy dynamics and fine-scale temperature patterns, even after accounting for the influence of vegetation and imperfect detection, suggests that birds are shifting towards potentially more suitable microclimates and away from less favorable ones. This behavioral flexibility to adapt to changes within a breeding season appears widespread as it was demonstrated by almost all members of the forest bird community we examined. Future efforts should explore the degree to which such vagility and apparent flexibility in site occupancy might propagate to buffer such species against the impact of long-term regional climate change.

TABLE 3.1. Species list for the 15 bird species we examined at the H. J. Andrews Experimental Forest. Prevalence (Prev.) is the number of points for which a species was detected at least once throughout the breeding season out of the total points (183) for each year. Home range values were obtained from the online Birds of North America accounts (Poole [Editor] 2005).

Species common name	Species scientific name	Species code	Prev. 2012	Prev. 2013	Home range (ha)
Brown creeper	<i>Certhia americana</i>	BRCR	0.435	0.495	4.2
Chestnut-backed chickadee	<i>Poecile rufescens</i>	CBCH	0.913	0.826	1.3
Golden-crowned kinglet	<i>Regulus satrapa</i>	GCKI	0.674	0.647	1.6
Hammond's flycatcher	<i>Empidonax hammondii</i>	HAFL	0.386	0.446	1
Hermit thrush	<i>Catharus guttatus</i>	HETH	0.462	0.527	0.7
Hermit warbler	<i>Setophaga occidentalis</i>	HEWA	0.875	0.951	0.35
Oregon junco	<i>Junco hyemalis</i>	ORJU	0.620	0.663	0.38
Pacific Wren	<i>Troglodytes pacificus</i>	PAWR	0.821	0.793	1.38
Pacific-slope flycatcher	<i>Empidonax difficilis</i>	PSFL	0.761	0.853	2.5
Red-breasted nuthatch	<i>Sitta canadensis</i>	RBNU	0.511	0.783	1.2
Steller's jay	<i>Cyanocitta stelleri</i>	STJA	0.630	0.625	80
Swainson's thrush	<i>Catharus ustulatus</i>	SWTH	0.674	0.723	1
Varied thrush	<i>Ixoreus naevius</i>	VATH	0.609	0.565	7
Western tanager	<i>Piranga ludoviciana</i>	WETA	0.277	0.342	2.8
Wilson's warbler	<i>Cardellina pusilla</i>	WIWA	0.299	0.266	0.3

TABLE 3.2. Coefficients and standard errors for apparent settlement (γ) by species and year for top models. ** = significant at $P \leq 0.05$, * = significant at $P \leq 0.1$. See Table 1 for species code definitions. See Appendix 8 for all model selection tables.

Species	Intercept		Vegetation						Temperature										
			Veg structure 1		Veg structure 2		Veg composition		CDD >0 Jan-Mar		CDD >10 Apr-Jun		MAX Apr-Jun		MIN Apr-Jun		MEAN Apr-Jun		
	Est	SE	Est	SE	Est	SE	Est	SE	Est	SE	Est	SE	Est	SE	Est	SE	Est	SE	
2012																			
BRCR	-1.902	0.174	0.686	0.173	**	-0.193	0.133												
CBCH	0.187	0.185	0.194	0.183		-0.566	0.188	**							0.356	0.167	**		
GCKI	-1.126	0.109					-0.151	0.128									-0.556	0.112	**
HAFL	-2.670	0.287					0.397	0.189	**	-0.428	0.339								
HETH	-1.308	0.207	-0.445	0.170	**										0.165	0.186			
HEWA	-0.387	0.154	-0.182	0.158													-0.532	0.156	**
ORJU	-1.079	0.168	-0.391	0.164	**												-0.544	0.190	**
PAWR	-0.433	0.118	0.641	0.138	**		0.574	0.160	**						0.494	0.134	**		
PSFL	-0.930	0.114	0.551	0.126	**										0.258	0.125	**		
RBNU	-1.741	0.271													-0.332	0.286			
STJA	-1.068	0.204	-0.266	0.159	*												0.317	0.142	**
SWTH	-0.929	0.150	-0.268	0.138	**								0.232	0.128	*				
VATH	-1.432	0.140				-0.308	0.120	**									-0.532	0.132	**
WETA	-2.851	0.256				0.540	0.187	**			0.898	0.203	**						
WIWA	-2.953	0.188	-0.504	0.182	**						-0.384	0.171	**						
2013																			
BRCR	-1.680	0.181	0.459	0.178	**	-0.233	0.138	*	-0.343	0.224				-0.267	0.171				
CBCH	-0.635	0.135	0.320	0.150	**	-0.373	0.132	**							0.276	0.160	*		
GCKI	-1.292	0.115				-0.126	0.121										-0.915	0.135	**
HAFL	-2.186	0.179	0.468	0.161	**												0.217	0.195	
HETH	-1.856	0.119	-0.472	0.120	**	-0.255	0.124	**									-0.320	0.115	**
HEWA	-0.026	0.153	-0.429	0.171	**				-0.377	0.165	**						-0.642	0.164	**
ORJU	-1.083	0.129	-0.498	0.141	**										-0.567	0.158	**		
PAWR	-0.943	0.119	0.562	0.136	**										0.550	0.143	**		
PSFL	-0.477	0.112	0.435	0.126	**										0.439	0.127	**		
RBNU	-0.116	0.258				-0.484	0.239	**	-0.458	0.232	**		-0.538	0.242	**				
STJA	-3.269	1.643									1.327	0.920							
SWTH	-1.133	0.116					0.194	0.109	*					0.357	0.105	**			
VATH	-1.522	0.130				-0.209	0.122	*			-0.429	0.124	**						
WETA	-2.004	0.248	-0.640	0.164	**									0.208	0.150				
WIWA	-3.107	0.302				-0.645	0.259	**						-0.420	0.258	**			

TABLE 3.3. Coefficients and standard errors for apparent vacancy (ε) by species and year for top models.** = significant at $P \leq 0.05$, * = significant at $P \leq 0.1$. See Table 1 for species code definitions. See Appendix 8 for all model selection tables.

Species	Intercept		Vegetation						Temperature									
			Veg structure 1		Veg structure 2		Veg composition		CDD >0 Jan-Mar		CDD >10 Apr-Jun		MAX Apr-Jun		MIN Apr-Jun		MEAN Apr-Jun	
	Est	SE	Est	SE	Est	SE	Est	SE	Est	SE	Est	SE	Est	SE	Est	SE	Est	SE
2012																		
BRCR	1.127	0.466					0.281	0.277	1.217	0.864								
CBCH	-0.536	0.141	-0.236	0.127	*		0.147	0.121			-0.218	0.129	*					
GCKI	0.354	0.179					0.103	0.156									0.334	0.164
HAFL	-0.523	0.393	-0.711	0.412	*									-0.607	0.257	**		
HETH	0.638	0.299		0.108	0.262												0.692	0.289
HEWA	-1.012	0.158		0.177	0.134												0.539	0.209
ORJU	0.384	0.255							0.190	0.213							1.320	0.279
PAWR	-0.501	0.133	-0.306	0.136	**												-0.697	0.159
PSFL	-0.394	0.162	-0.261	0.164			0.287	0.128	**								-0.238	0.189
RBNU	-1.223	0.488	0.282	0.360														0.688
STJA	1.045	0.306							-0.271	0.244	-0.229	0.252						0.461
SWTH	-0.274	0.228	0.205	0.191														
VATH	0.952	0.281	-0.031	0.213										0.650	0.249	**		
WETA	0.814	0.465	-0.275	0.357	*												-0.275	0.357
WIWA	0.904	0.401	0.262	0.280									1.689	0.484	**			
2013																		
BRCR	0.302	0.241					0.359	0.213	*				-0.359	0.239				
CBCH	-0.568	0.209								-0.633	0.290	**					-0.319	0.184
GCKI	0.229	0.187								0.324	0.171	*					0.551	0.169
HAFL	-0.340	0.324					-0.419	0.202	**								-0.351	0.253
HETH	0.641	0.212	0.342	0.184	*												0.153	0.197
HEWA	-0.815	0.099	-0.059	0.100													0.428	0.107
ORJU	-0.096	0.202	0.017	0.198														
PAWR	-0.686	0.132					0.381	0.118	**								0.293	0.178
PSFL	-0.615	0.145	-0.328	0.144	**												-0.522	0.159
RBNU	-1.051	0.174					0.143	0.149		0.194	0.181						-0.409	0.171
STJA	-2.679	0.635	1.001	0.411	**													**
SWTH	-0.073	0.186					-0.358	0.163	**	-0.167	0.157			-0.141	0.183		0.693	0.543
VATH	1.045	0.260								-0.396	0.309	*					0.386	0.217
WETA	1.462	0.439															0.286	0.396
WIWA	-4.657	1.777					-1.128	0.457	**	-4.615	2.339	**						-1.149

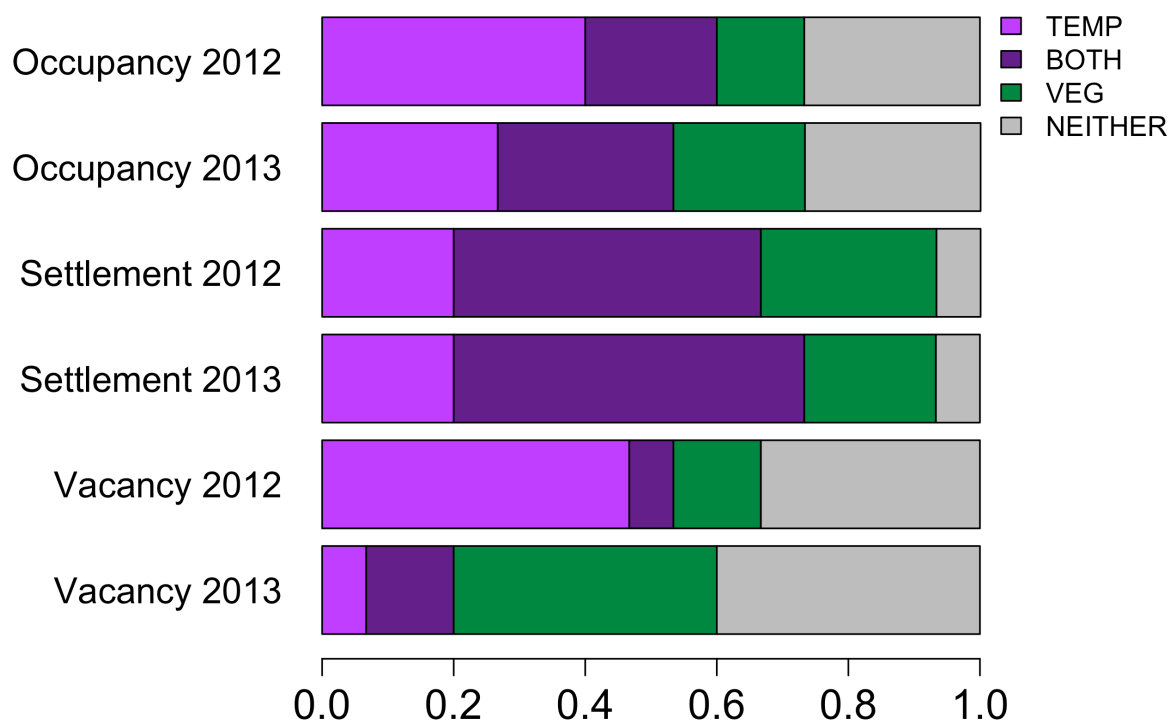


FIGURE 3.1. The proportion of species in each year for each of the ecological parameters where the effect of 1) temperature alone (TEMP), 2) both vegetation and temperature (BOTH), or 3) vegetation alone (VEG) were significant (at $P < 0.05$) in the top model, or whether 4) neither vegetation nor temperature (NEITHER) were significant in the top model. Initial occupancy described the distribution in the first sample session (mid-May). Settlement and vacancy described patterns in ‘apparent movement’ between the second and sixth sample sessions (late-May until early-July).

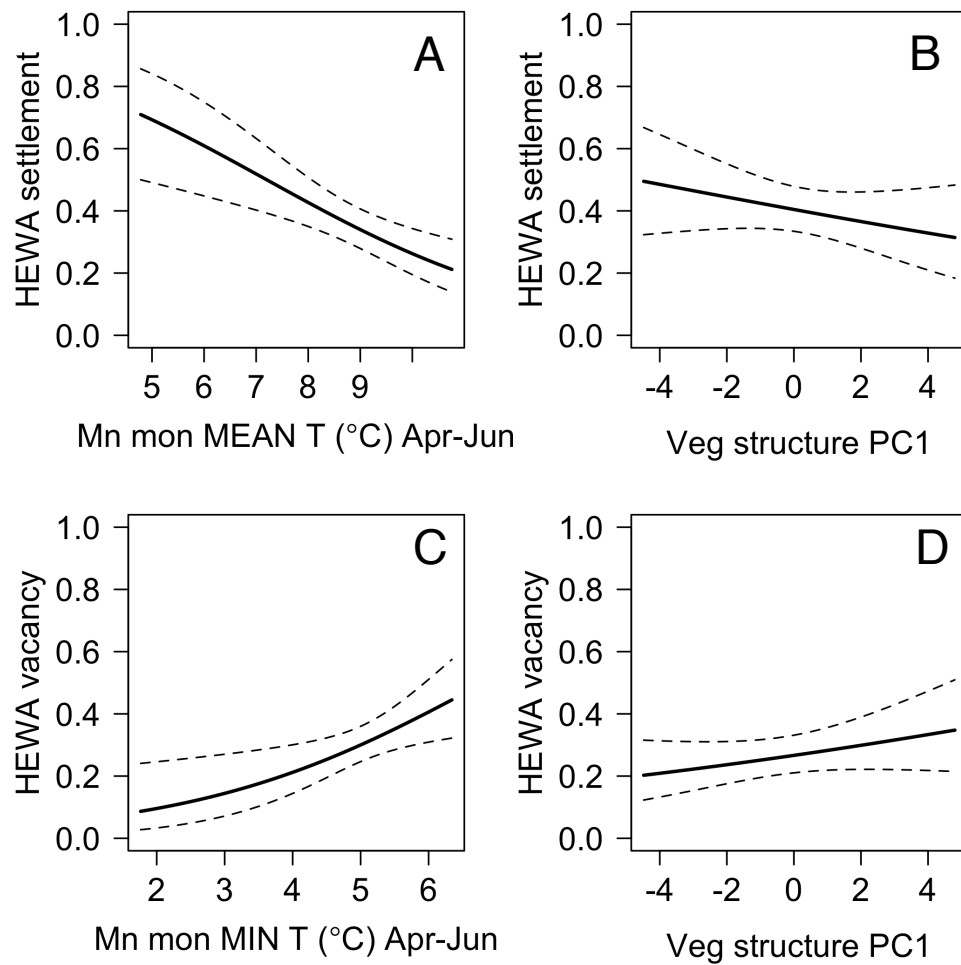


FIGURE 3.2. Hermit warbler (HEWA, *Setophaga occidentalis*) is an example of a species where local site-scale dynamics are largely driven by temperature and vegetation structure to a lesser extent. Hermit warblers were both less likely to settle sites (A) and more likely to vacate sites (C) that were warmer. Vegetation structure was not a significant predictor of either vacancy (B) or settlement (D).

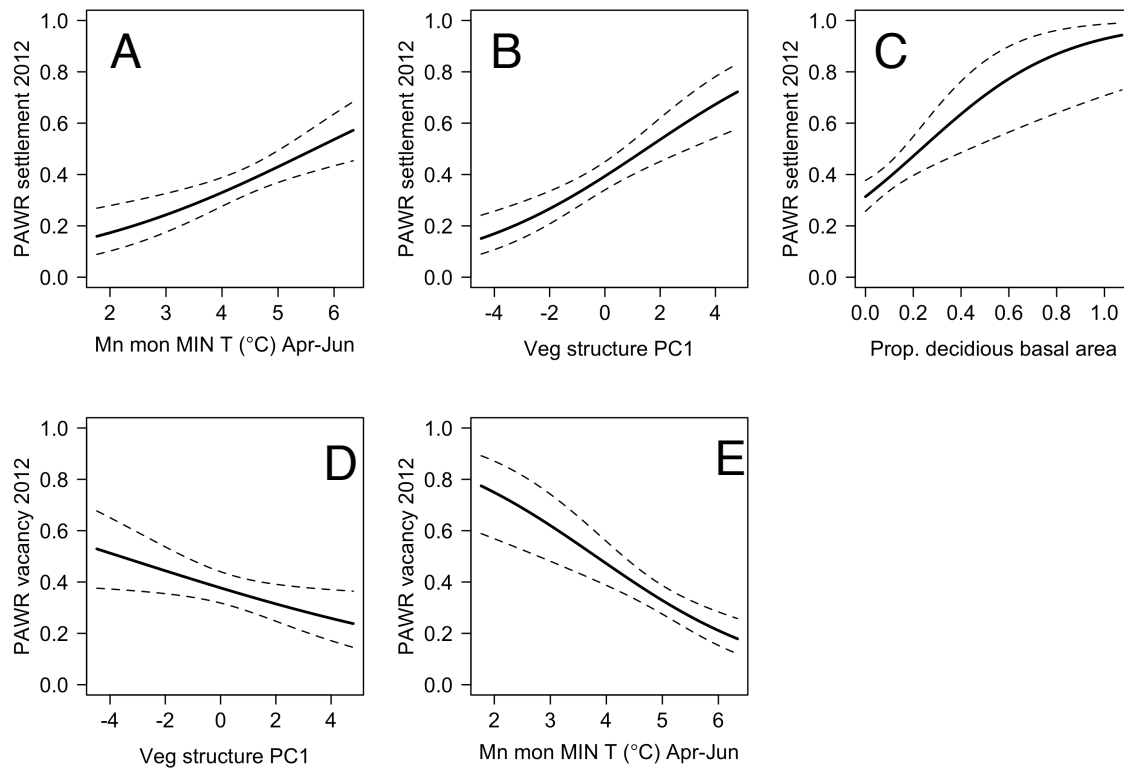


FIGURE 3.3. Pacific wren (PAWR, *Troglodytes pacificus*) is an example of a species where both temperature and vegetation were important in within season dynamics. Pacific wrens were more likely to settle warmer sites (A) and vacate cooler sites (E). Pacific wrens were more likely to settle sites with old-growth characteristics (B) and higher deciduous composition (C). Wrens were more likely to vacate even-aged vegetation stands such as plantations (D).

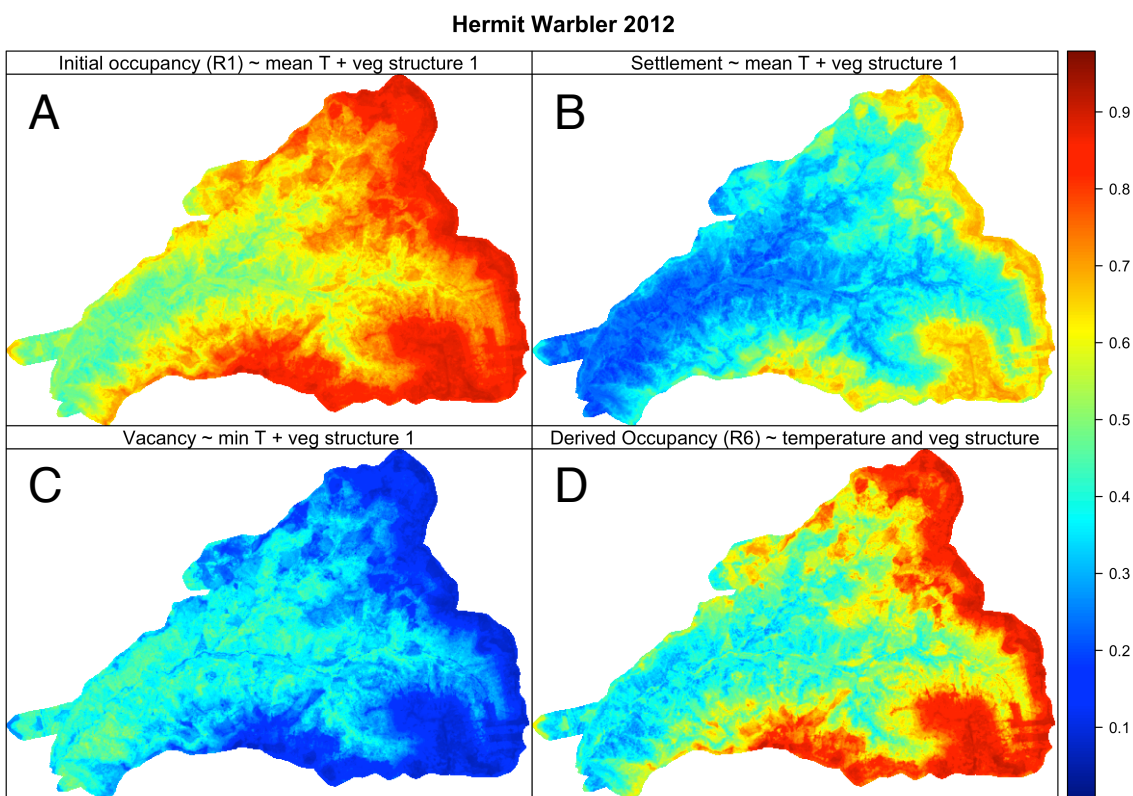


FIGURE 3.4. Predicted maps for hermit warbler (A) initial occupancy, (B) settlement, (C) vacancy and (D) final occupancy patterns at the end of the sampling period. By the end of the season (D) hermit warblers have shifted away from warmer sites towards cooler sites.

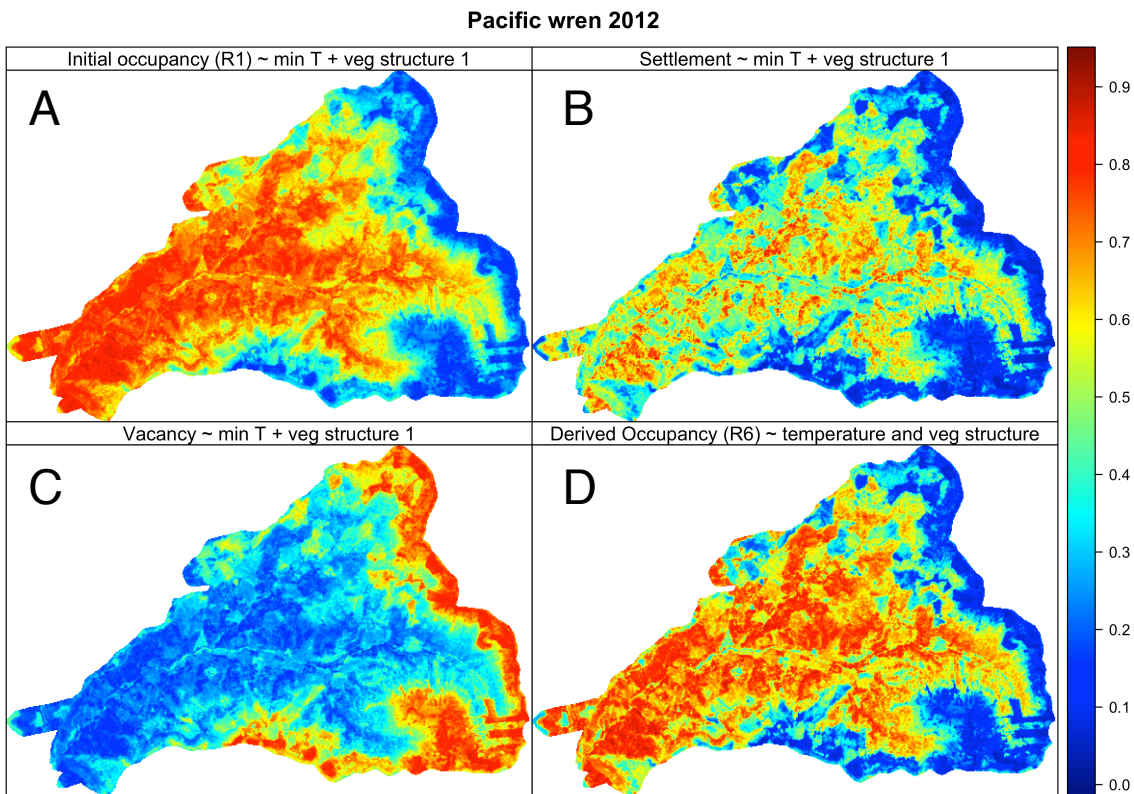


FIGURE 3.5. Predicted maps for Pacific wren (A) initial occupancy, (B) settlement, (C) vacancy and (D) final occupancy patterns at the end of the sampling period. By the end of the season (D) hermit warblers have shifted away from plantation sites towards older forest sites. Predicted maps do not include proportion of deciduous basal area since it is a local-site vegetation variable.

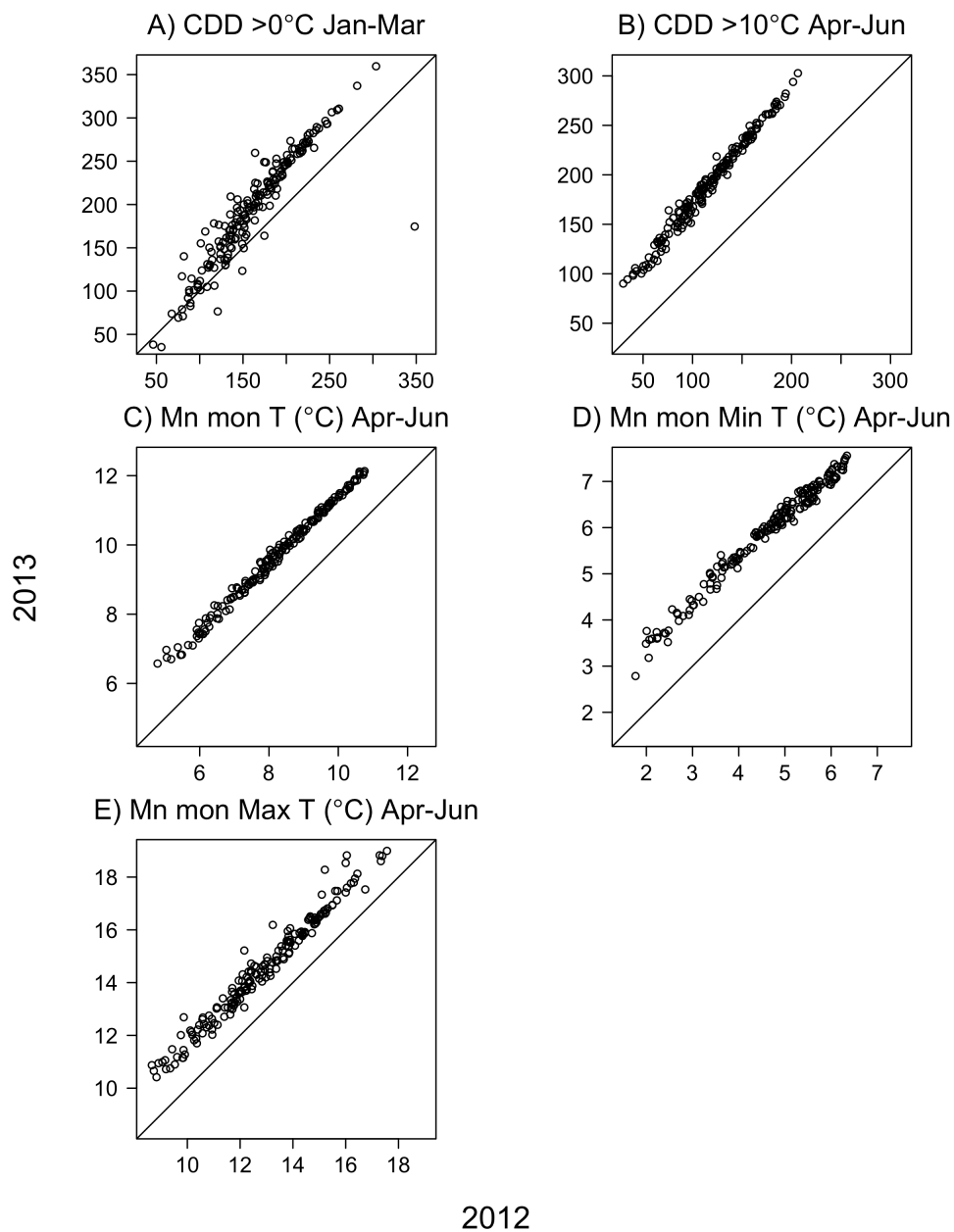


FIGURE 3.6. Year to year correlations in fine-scale temperature metrics. Temperature patterns were highly consistent between the years despite 2013 being warmer.

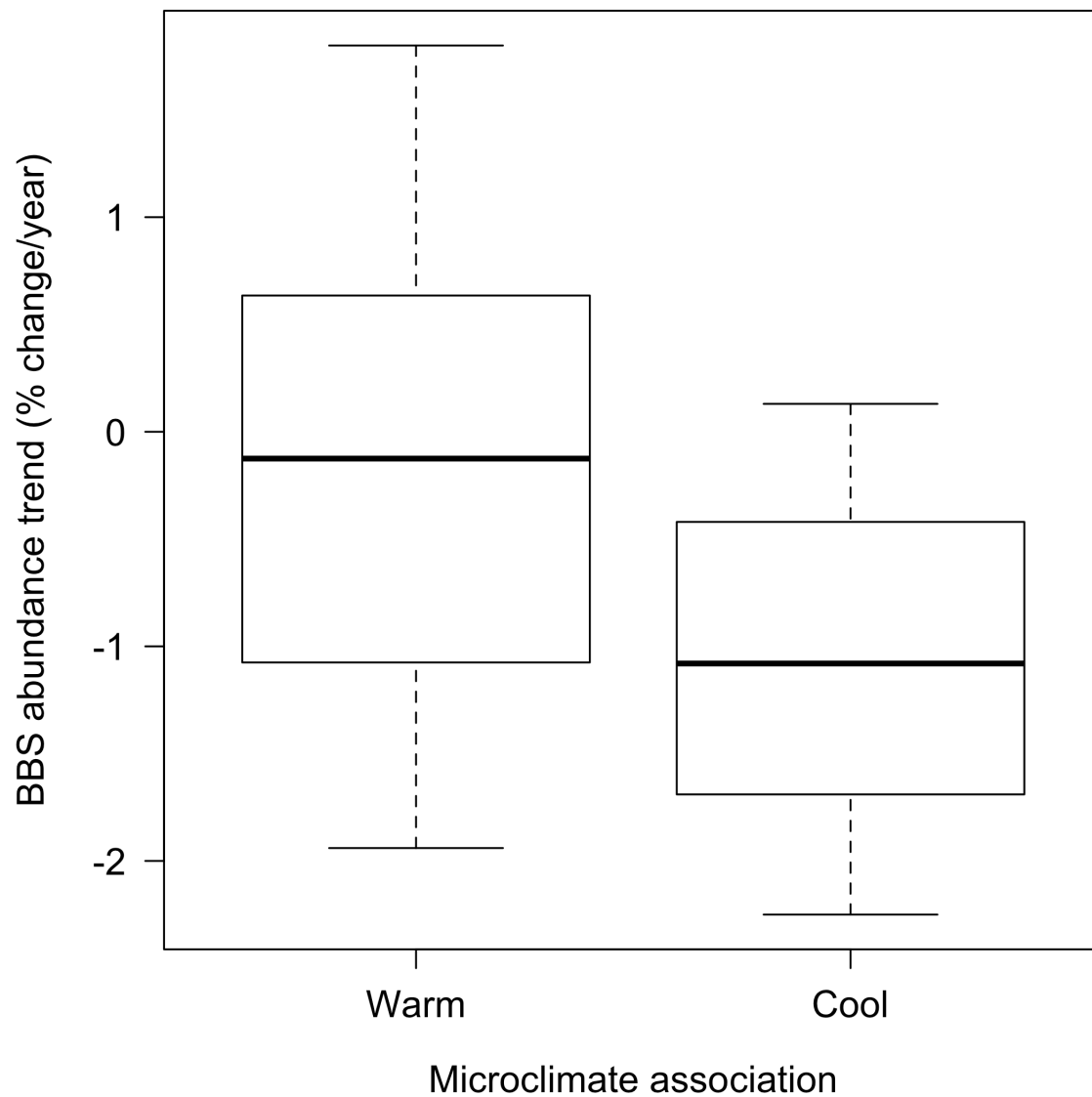


FIGURE 3.7. Mean population trend estimates from BBS data grouped by species that showed cool vs warm associations in the H. J. Andrews dataset. We detected weak evidence for population declines in species we identified as being ‘cool-associated (mean trend [95% CIs] = -1.06 %/year [-1.96 – -0.16]) at the regional scale (BBS) relative to their warm-associated counterparts (-0.16 %/year [-0.99 – 0.68]). CIs for trends of cool-associated species did not include 0, where trends for warm-associated species did. Breeding Bird Survey 2002-2012 trends from the Northern Pacific Rainforest region (OR, WA, CA; (Sauer et al. 2014).

THE IMPORTANCE OF SAMPLING SCALE AND IMPERFECT DETECTION IN
ESTIMATING LONG-TERM AVIAN ABUNDANCE TRENDS

Sarah J. K. Frey, Nick L. Rodenhouse, Adam S. Hadley, T. Scott Sillett, Richard T. Holmes,
Matthew G. Betts

ABSTRACT

Bird population trends are often used as measures of ecosystem health and in conservation planning. However, drawing firm conclusions from such trends can be complicated due to potential for trend variability across spatial scales and biases caused by imperfect detection. We estimated bird population trends from 1999-2012 for 38 species at regional, landscape and local scales to address three questions: (1) Are trends consistent across scales? (2) Can life history and ecological traits explain these population trends? (3) Does imperfect detection have the potential to mask long-term trends? We derived regional trends from the Breeding Bird Survey, landscape-scale trends from a valley-wide survey in the Hubbard Brook Experimental Forest (HBEF), New Hampshire, and local trends from surveys on a 10-ha plot in the same valley. Abundance trends of most (68.5%) forest bird species at HBEF were relatively stable over the time period observed and were correlated with regional-scale trends ($r = 0.40$, $P = 0.013$). However, more than double the number of species showed significant declines at the regional scale ($N = 16$, 42.1%) than in the undisturbed HBEF ($N = 7$, 18.4%). Life history and ecological traits did not explain any of the variability in HBEF trends. Regionally species that occur at higher elevations were more likely to be declining and species associated with older forests were more likely to be increasing. We attribute these differences to: (1) elevated rates of land-use change in the broader region and (2) that regional-scale models do not account for imperfect detection. Population trends calculated using traditional linear regression models, though correlated with detection models ($r = 0.43$), were prone to both under- and over-estimating bird population trends. Using only raw abundance data we would have missed significant population trends in 13% of species and falsely identified trends for almost 20% of species. Our results highlight the importance of accounting for imperfect detection and sampling at appropriate spatial scales in generating reliable population trend estimates. Further, relatively stable breeding-ground habitat in the HBEF appears to translate into mostly stable bird populations over the 14 years observed.

Bird population trends are used frequently as an indicator of ecosystem health from local to global scales (Canterbury et al. 2000, Betts et al. 2010, Butchart et al. 2010). However, the reliability of such trends is frequently called into question for two primary reasons. First, trends in abundance may differ depending on the spatial scale investigated (Bohning-Gaese et al. 1994). Species distributions at large spatial scales are considered primarily climate-driven (Thuiller et al. 2004a, Thomas 2010) and at finer scales, factors such as land cover and species interactions are hypothesized to play a larger role (Brown et al. 1995). Due to stochasticity in food resources, and variability in habitat change, abundance patterns at local scales may reflect very different processes than those acting at regional scales. Many studies are conducted at fine spatial scales yet aim to transfer these local patterns to the larger landscape (Urban 2005). However, the degree to which population trends are consistent across these spatial scales has rarely been examined (but see Holmes and Sherry 1988). Second, sampling techniques often introduce biases that can make inferences about populations problematic. Raw counts arise from a combination of two interrelated processes, the ecological (state) process and the observation process (Kéry 2011). Not accounting for such biases through study design and analysis can lead to biased estimates or a lack of power to detect important demographic patterns (Tyre et al. 2003, Guillera-Arroita et al. 2010). By not accounting for detection probability in estimating abundance trends, researchers risk missing trends (type I error) or identifying trends that are not real and due to changes in detection over time rather than abundance (type II error).

The Hubbard Brook Experimental Forest (HBEF), located in the White Mountains of New Hampshire, USA (43°56' N, 71°45' W; 222 – 1015 m.a.s.l.), encompasses a 3160-ha, forested valley and an 800-m elevational gradient. The HBEF has had no major anthropogenic disturbance since 1915 (Holmes 2011). We used HBEF valley-wide (landscape scale) bird surveys that have been conducted since 1999 and hierarchical models to estimate detection-corrected abundance trends for 38 species over the last decade and a half (38,521 total detections). To determine the effects of imperfect detection on trends, we estimated abundance change for forest birds in the HBEF over 14 years (1999-2012) both with, and without the use of hierarchical models that incorporate bird detection probability (Kery et al. 2009). To test the

effects of scale on avian trends, we compared landscape-scale trend estimates to both regional ⁷⁵ (New Hampshire Breeding Bird Survey [BBS]) and local (10 ha-plot) scale population trends nested within the broader HBEF. Earlier work conducted in the same area indicated that most forest bird species were declining both locally (HBEF) and statewide from 1969-1986 (Holmes and Sherry 1988) and 50% of the most common species showed significant declines from 1969-1998 in HBEF (Holmes and Sherry 2001).

To elucidate possible mechanisms for population trends at HBEF and regionally, we investigated the role of species' life history and ecological traits (Hansen and Urban 1992, Clark and Martin 2007). Life history characteristics govern a species' capability to cope with environmental change therefore influencing the direction of population trends (Bennett and Owens 2002, Angert et al. 2011). We predicted that in New England, where succession over the past century has resulted in afforestation of agricultural fields and an increase in the amount of older forest (Thompson and DeGraaf 2001, Trani et al. 2001), species associated with mature forests should be increasing and early-seral specialists declining due to loss of habitat (King and Schlossberg 2014). Further, if climate change (e.g., warming temperatures) has influenced abundance trends at any scale, then we should observe decreasing trends in species that occur primarily at high elevations (Jiguet et al. 2007, Sekercioglu et al. 2008). Migratory and resident species may be responding to different climate signals (Moller et al. 2008) and their ability to adjust to changes in phenology have been shown to vary (Fraser et al. 2013, Townsend et al. 2013). We therefore examined the influence of habitat specialization, elevational distribution, and migratory status on trends. We also included reproductive output, survival, and body mass, as they are traits that influence demography and subsequently population trends. Species with 'slower' life histories, that is those with lower reproductive output, higher survival and generally larger body sizes, should be expected to take longer to respond to changes in the environment in comparison to species that are smaller, have larger broods, and have shorter life spans (Bennett and Owens 2002, Angert et al. 2011).

4.2.1 Study site

HBEF Watershed – We used bird occurrence data collected throughout the HBEF valley. The forest is primarily contiguous second-growth (~90 yrs. old) and transitions from hardwood tree species at lower elevations to coniferous, montane species at high elevations (Fig. 1; see Schwarz et al. (2003) and Holmes (2011) for detailed study site descriptions). The extensive valley-wide dataset on forest bird populations consists of 371 sample points. Sample points were placed across the entire watershed using a systematic grid spaced 500 m (east-west) and 100- and 200-m (north-south; Schwarz et al. 2003, Doran and Holmes 2005). Sample points therefore span large gradients in elevation, climate, and forest vegetation structure and composition.

4.2.2 Watershed-Scale Avian Surveys

Point counts were conducted between one and three times from 1999–2012 (no surveys conducted in 2003-04), during the breeding period (May – July). Point counts were carried out by trained observers under favorable weather conditions (no rain, low winds). Weather conditions describing cloud cover, precipitation, and wind were recorded for each survey. Birds were classified as either singing or calling and, when possible, we determined the sex of individual birds based on behavior (singing) and/or plumage differences through visual identification. We used only singing males to maximize the probability that the individual was occupying a territory at a particular site. For non-singing species, we used both auditory and visual detections. A total of 71 species were detected at HBEF over the period of the study.

We classified locations of individual birds in two distance classes: 1) within 50 m and 2) 50-100 m. The final dataset included only observations made within 50 m of the sample point to reduce the chances of double counting individuals. To reduce observer and temporal bias, the order of counts and observers were rotated across points over the course of the three visits. Four to seven days were required to visit all points once and visits were spaced by a break of 2 – 10 days.

We chose the *a priori* 1999-2012 average HBEF prevalence cutoff of 0.01 (sensu Cumming et al. 2014), because below this threshold there were not enough data points to estimate parameters. The cut-off resulted in retaining 38 of the 71 species (Appendix 1). We used binomial mixture models for open populations (Kery et al. 2009, Kery and Royle 2010) to estimate population trends for 38 species at HBEF. This is a hierarchical model in that it explicitly estimates both the observation and ecological processes. Spatially and temporally replicated counts are conducted at i sites over j surveys. Between surveys (j) populations are assumed to be closed (no emigration or immigration). In the multi-season extension of this model, which we use here, the population closure assumption is relaxed between years (k). Counts c_{ijk} are a function of the population size at each site (N_{ik}) and are modeled as a result of a binomial process with index parameter N_{ik} and success parameter p_{ij} . The population size at each site arises from a Poisson distribution with rate parameter λ_{ik} . To estimate the population size in subsequent years and the trend in abundance, we estimate $\log(\lambda_{ik})$ as a log-linear Poisson regression where the intercept α_i is the estimate of the abundance in the first year and is added to the effect of the rate parameter r_i which reflects the annual rate of population growth. Both the detection and abundance parameters can be modeled as a function of covariates.

The model structure is as follows where i = site and j = replicate:

Ecological process:

$$N_i \mid \lambda_i \sim \text{Poi}(\lambda_i)$$

Observation process:

$$c_{ij} \mid N_i \sim \text{Bin}(N_i, p_{ij})$$

The model extended to multiple years and to include covariate effects where k = year, w = covariate:

Ecological process:

$$N_{ik} \sim \text{Poi}(\lambda_{ik})$$

$$\log(\lambda_{ik}) = \alpha_i + r_i \times (k - 1) + \beta_w \times x_{ikw}$$

Observation process:

$$c_{ijk} \mid N_{ik} \sim \text{Bin}(N_{ik}, p_{ijk})$$

$$\text{Logit}(p_{ijk}) = \alpha_{ijk} + \beta_w \times x_{ijkw}$$

We fit our models in a Bayesian framework using modified code from Kery et al. (2009) and Kery and Royle (2010). We used the ‘rjags’ package in program R (R Development Core Team 2011) in conjunction with JAGS version 3.3.0 (Plummer 2003). In a Bayesian mode of inference, Markov chain Monte Carlo (MCMC) simulations are used to estimate model parameters. In the simulations, repeated draws are made from the posterior distribution to estimate model parameters and associated error. We used three consecutive chains consisting of 500,000 iterations each with a ‘burn-in’ period of 250,000 iterations and thinned by 150 draws. This combination gave us a total of 3333 draws. Following Kery and Royle (2010), we used conventional uninformative priors for all parameters to indicate no previous knowledge of their potential values (see Appendix A for more details).

4.2.4 Linear regression with raw counts

We compared N-mixture models that account for imperfection detection with traditional methods for estimating abundance trends that assume perfect detection. Using the HBEF data, we calculated a single abundance value for each species in each year. We used the mean count at each site when there were multiple visits. We then averaged this mean count from all of the sites in that year. We used these values (mean abundance across all sites) and estimated the trend using linear regression in program R (R Development Core Team 2011). We used the same method to calculate the local 10-ha plot abundance trends based on the raw counts of the individuals.

4.2.5 Comparison of trends by spatial scale

Hubbard Brook Long-term Research in Environmental Biology (LTREB) plot – Since 1969, detailed data were collected on a gridded 10-ha plot located between 300-400 m.a.s.l. at HBEF. We used abundance data from the same time period as the HBEF valley-wide dataset (1999-2012) to estimate local-scale trends in the LTREB 10-ha plot. Imperfect detection was unlikely in this dataset because the survey protocol entailed two observers conducting synchronized, 5-minute counts every 50m along parallel, 500m line transects. The two transects were 100m apart, and over the hour-long surveys, observers mapped the locations and movements of all individuals encountered within a 100m strip centered on the transect line. One observer (RTH) typically mapped all birds on the 10ha plot for an additional 1-3 hours per week. See Holmes and Sturges (1975) and Holmes and Sherry (2001) for further detail. These data were collected weekly from late May through early July each year. Bird counts and territory maps were combined to generate abundance estimates for each species encountered.

Regional (New Hampshire) BBS – We used the BBS data from the state of New Hampshire, which included 25 routes. Routes were located across multiple vegetation types (forest, edge, fields, successional) and distributed widely across the state. Each route was visited by a volunteer observer in between late May and early July to conduct 3-min point counts along the 50 points that make up the route (each point is 0.8 km apart); see Sauer et al. (2014). Trend estimates were calculated using hierarchical models that account for differences in observers, years, and stratum directly in the model framework. BBS trends are modeled using Poisson regression for overdispersed data, implemented in a Bayesian framework. While this method does not explicitly account for imperfect detection, it includes parameters that describe variation in the observation process (Link and Sauer 2002, Sauer and Link 2011). For all trend estimates we evaluated significance at $\alpha = 0.10$ and considered trends to be statistically significant if the 90% confidence intervals did not overlap zero (Peterjohn and Sauer 1994).

4.2.4 Life history traits

For the 38 species included in the abundance trend analysis (based on the 0.01 prevalence cutoff), we compiled information on the following ecological and life history traits from Birds of

North America (BNA) online accounts (Poole 2005): 1) migratory status (resident, short-distance migrant, or long-distance migrant), 2) survival, 3) reproductive output, and 4) body mass. We used the HBEF data to calculate additional traits including: 5) habitat specialization (See SSI below), 6) altitude at peak abundance (See details below), 7) forest age at peak abundance (measured with basal area and canopy height). We calculated a species specialization index (SSI) following Julliard et al. (2006). We used the average maximum abundance value for each year in each site and then related these values to vegetation classes at HBEF (hardwood, softwood, mixed – hardwood dominant, mixed – softwood dominant) by calculating the mean and standard deviation of the abundance values that fell into each of these four cover types. We then calculated the coefficient of variation (standard deviation/mean) for each species. This value was used to describe the degree to which a species is generalized in its use of available habitats. SSI values ranged from 1.77 (representing highly specialized) to 0.14 (reflecting high generalism). To calculate elevation and forest age at peak abundance, we used yearly mean maximum abundance for each sample plot then calculated the elevation, mean canopy height (LiDAR derived; Goetz et al. 2010), and basal area (DBH>10cm, 25-m radius from on-the-ground vegetation surveys; Schwarz et al. 2003) at which maximum abundance occurred. Information regarding migratory status, survival, and reproductive output were obtained from species' Birds of North America (BNA) accounts online (Poole 2005). Body mass was derived from Sibley (Sibley 2000) for consistency since the BNA accounts almost always contained a body mass measurement for each species; however they were often only for one sex, or in only one part of the species range. We used linear mixed effects models (lme package in R; Bates 2012) to model trends as a function of life history and ecological traits. We accounted for lack of independence within phylogenetic groups by including family as a random effect (Sol et al. 2005, Amiel et al. 2011).

4.3.1 Effects of spatial scale

The trends observed at HBEF were significantly and positively correlated with statewide BBS trends ($r = 0.40$, $P = 0.013$; Fig. 2). While generally the trends corresponded at the two scales, some large differences existed. The majority (68.5%) of the HBEF species showed no significant trend in abundance over the 14-year period (Fig. 2A). Twenty-two species declined; however only seven (18.4%) of them significantly (90% credible intervals [CRIs] did not overlap zero, Fig. 2A). Fifteen species increased, five of which were significant (13.1%, Fig. 2A). In contrast, BBS trends for NH indicated that most species either declined or increased, rather than remaining stable (Fig. 2B). More than half of the species (52.6%) exhibited a significant trend (90% CRIs did not overlap zero). Across the state of New Hampshire, 16 species significantly declined (42.1%) and only four species significantly increased (10.5%).

The trend estimates for the LTREB plot and HBEF were not significantly correlated ($r = 0.12$, $P = 0.57$; Fig. 3). However, this appeared to be largely a result of trend estimate differences for white-breasted nuthatch (*Sitta canadensis*), which showed opposite significant trends between the two datasets. Removing this species resulted in a significant and positive correlation between the HBEF landscape-scale and local trends ($r = 0.66$, $P = 0.0009$). On the LTREB plot, only a subset of the species in the HBEF and BBS datasets were sampled (23 of the 38 species; Fig. 3A). Four species significantly declined (17.4%) and 10 significantly increased (43.5%), and the remainder showed no significant trend (39.1%).

We found no evidence that life history and ecological traits explained bird population trends in the HBEF; all 95% confidence intervals overlapped zero (Fig. 4A). Conversely, The BBS trends indicated that high-elevation species were more likely to be declining than species more commonly found at middle and lower elevations (effect size \pm SE [95% CIs]: $\hat{\beta} = -0.81 \pm 0.40$ [-1.614, -0.001]). Additionally, variability in BBS trends were explained by a species' mean canopy height and mean basal area as well as migratory status (Fig. 4B). Species that were more abundant in forest stands with taller canopies ($\hat{\beta} = 1.22 \pm 0.35$ [0.51, 1.92]) and larger basal area ($\hat{\beta} = 0.98 \pm 0.37$ [0.23, 1.72]) were also more likely to have increasing trends. Long-distance

migrants were more likely to be declining in abundance across NH ($\hat{\beta} = -1.48 \pm 0.67$ [-2.83, - 0.13]). 82

4.3.2 Effects of imperfect detection on population trends

Population trend estimates from the hierarchical model, which accounted for imperfect detection, were correlated with the estimates from the linear regression using the raw counts from HBEF (Pearson's correlation coefficient (r) = 0.43, P = 0.007; Fig. 5). However, we found substantial differences in individual species' trend estimates between the two methods. First, hierarchical model trends estimates indicated that changes in abundance over time were larger than estimates from traditional linear regression models – particularly for species found to be significantly declining or increasing. Models ignoring imperfect detection also missed statistically significant trends for five species (two decreasing, three increasing). Further, using traditional regression models we identified seven significant trends (five decreasing, two increasing) that were not present in the trend results from the hierarchical models. Finally, hierarchical models showed much lower variability in the error around parameter estimates among species. This was possibly a result of sparse data for species that were difficult to detect.

4.4 DISCUSSION

Landscape-scale, avian population trends at HBEF were correlated with both BBS regional trends and local-scale LTREB plot trends. These correlations indicate some consistency in mechanisms driving trends across the spatial scales. However, despite these general similarities, we observed some important differences across scales. Most species in the HBEF showed a relatively stable trend in abundance from 1999 - 2012. In contrast, the number of significantly declining species statewide was more than double that of HBEF. Several possible explanations exist for these differences. First, BBS data does not exclusively account for detection probability. Variation in detection probability may be incorrectly associated with abundance (Kéry 2011) which results in estimating trends in the observation process rather than our ecological variable of interest. As noted above, had we not corrected for detection biases

within the watershed dataset we would have had different trends for 31.6% of the species we examined. Secondly, land-use changes over the sampling period are different at regional and watershed scales. HBEF is a contiguous tract of relatively undisturbed forest that has seen no anthropogenic change during the period in which we monitored bird populations. Conversely, regional sampling is not limited to undisturbed forest habitats and is subjected to land use change from two co-occurring processes: 1) human disturbance and 2) afforestation and succession. Thus, at the regional scale there is more disturbance and forest fragmentation from roads (Ortega and Capen 1999), rural housing development (Kluza et al. 2000), and forestry practices (Kittredge Jr et al. 2003) which have all been shown to affect birds. In New England, forest cover tends to be increasing and aging, resulting in a decrease in early-seral habitats as previously cleared land succeeds into woodland (King and Schlossberg 2014). Finally, BBS data relies heavily on roadside sampling to achieve desired spatial and temporal replication. While this is often necessary due to logistical constraints, it limits the scope of inference for populations beyond road networks and may influence detection probability (Bart et al. 1995, Keller and Scallan 1999). Additionally, land use changes next to roads may not be reflective of practices at larger scales (Betts et al. 2007).

Population trends from the local-scale LTREB plot generally reflected trends from the landscape-scale. The yearly variation in abundance in the 10-ha LTREB plot was overall more variable, which was expected due to higher stochasticity at smaller spatial scales (Villard and Maurer 1996, Morrison et al. 2010). Abundance across the entire valley averages out this variability and provides a more even picture of the bird populations (Wiens 1989). Patchiness in habitat types and resources across the HBEF means that bird densities are likely not equal across the entire watershed. Sampling at fine spatial scales provides extremely high-resolution data that cannot be attained when sampling is conducted across entire landscapes; resolution is usually reduced with increases in spatial extent (Urban 2005, Betts et al. 2006). The spatial scale at which one samples will inevitably be a function of the type of information required to understand species distributions and drivers of population trends.

None of the variation in the trends observed at HBEF could be explained by life history or ecological traits. Although the forest at HBEF has not changed as a result of human

disturbance in the recent decades, it has undergone natural succession (Siccama et al. 2007). HBEF is comprised of relatively contiguous mature forest without many early-seral habitats. While life history traits were not useful for describing population trends at HBEF, we did see examples of species' trends suggesting change in abundance due to increasing forest age and changing structure. Species associated with mature forest structure (e.g., furrowed bark, tree cavities) all had increasing trends at the landscape scale (i.e., white-breasted nuthatch, pileated woodpecker [*Dryocopus pileatus*], black-and-white warbler [*Mniotilta varia*], and red-breasted nuthatch [*Sitta canadiensis*]). Beech bark disease, which results in more standing and downed dead trees (Houston 1994) may also lead to an increase in bark-feeding specialists. As the forest across HBEF aged, we expected to see declines in second-growth associates. In part this was the case; American redstart (*Setophaga ruticilla*), Canada warbler (*Cardellina canadensis*), ruffed grouse (*Bonasa umbellus*), and veery (*Catharus fuscescens*) declined in abundance at HBEF; however two other early-seral associates, Nashville warbler (*Vermivora ruficapilla*) and white-throated sparrow (*Zonotrichia albicollis*), did not. Earlier trend analyses at the local scale at HBEF (1969-1998, 10-ha plot, Holmes and Sherry 2001) did, however, find a link between species trends and changes in the forest habitat due to natural succession at the local scale, so perhaps successional effects had mostly run their course by the time of our study initiation (1999). Forest birds in the HBEF did not appear to be declining as a result of climate change; high-elevation species were no more likely to be declining than their low-elevation counterparts. High-elevation species, such as blackpoll warbler (*Setophaga striata*), magnolia warbler (*Setophaga magnolia*), and yellow-bellied flycatcher (*Empidonax flaviventris*), did not indicate any decrease in abundance over time at HBEF. This is in contrast to some recent studies that cite shifts in species distributions or population declines as a result of warming temperatures (Both et al. 2006, Parmesan 2006, Devictor et al. 2008). One possible explanation is that despite warming temperatures across the HBEF and northern New Hampshire (Groffman et al. 2012, Climate Solutions New England 2014), little warming has been observed during the period during which bird sampling took place (Townsend et al. 2013). Other explanations include the possibility that responses to warming temperatures are lagged and we did not pick up on them over this time

period or that some species could be adapting behaviorally to changes in temperature regimes⁸⁵ (Boyles et al. 2011).

In contrast, particular traits appeared to be associated with species trends from BBS data. The clear successional signal in BBS trends likely occurs because it is a sample of a larger area where more succession and afforestation is taking place. Land-cover change as a result of increasing forest cover and increasing forest age has the potential to reduce species diversity as early-seral species decline. As the forest continues to grow and mature, early-seral species continue to decline and contribute to a loss in avian biodiversity in the region (Hunt 1998, King and Schlossberg 2014). Species occurring at higher elevations were more likely to be declining at the regional scale (i.e., BBS data). Six out of the 16 species significantly declining regionally are most common at elevations > 700m (blackpoll warbler [929.04m], Canada warbler [730.8m], white-throated sparrow [770.6m], red-breasted nuthatch [770.2m], yellow-bellied flycatcher [866.6m], and slate-colored junco [809.01m]). Temperature trends in the region showed increases in temperature over the last four decades (Clark and Martin 2007) with more warming taking place in the winter months (Huntington et al. 2009). In the western US (Gutiérrez Illán et al. 2014) found that similar changes in winter temperature and precipitation were strong predictors for population trends.

Abundance trend estimates derived from raw counts were correlated with those accounting for imperfect detection – which is reassuring for long-term population estimates derived from un-corrected data (e.g., North American Bird Conservation Initiative 2013). Importantly, no trends reversed direction after accounting for imperfect detection. Congruence between these two methods suggests that studies that do not separate the observation process from the ecological process should not be dismissed. However, in our study, accounting for imperfect detection using more sophisticated sampling and analysis methods had clear advantages, namely more accurate trend detection as well as reduced error estimates. Because many of the species have low detection probabilities, abundance was severely underestimated when detection was assumed to be perfect. This is an important difference because we overlooked significant trends for five species and falsely identified trends in seven others using traditional, non-detection corrected models. Our findings are consistent with other tests; for

example, Kéry et al. (2009) did not detect a population trend for sand lizards (*Lacerta agilis*) 86 at their inland site when they used estimates from a Poisson regression that did not account for detection probability. Archaux et al. (2012) determined that even small differences in detection probability between treatments increased the chance of misidentifying a treatment effect when none existed. These other studies along with our findings highlight both type I and type II errors associated with traditional non-detection corrected methods; both errors are particularly problematic if estimates are used in the formulation of management and conservation decisions. In almost all bird population datasets, detection probabilities are less than one; therefore estimates of ecological parameters such as occupancy and abundance will be biased low and relationships with environmental covariates will be obscured (Kéry 2011). Increasing both the precision of trend estimates and the ability to detect trends greatly improves our ability to make appropriate conservation recommendations.

Conclusions

We found that landscape-scale trend estimates were correlated with both regional and local population trends although correlations were tenuous. Differences in trends across scales were sufficient to suggest that trends collected at one scale may not necessarily be reflective of those in another. When possible, the scale at which populations are sampled should be matched to the scale of conservation management. Overall our results show that failing to account for detection biases can lead to unreliable trend estimation. Therefore, techniques to account for imperfect detection should be incorporated into trend analyses when suitable data exist. New studies designed to detect population trends should collect and structure data to allow estimation of detection probability. This forethought will reduce the possibility of both type I and II errors and will improve our ability to make informed conservation efforts.

FIGURES

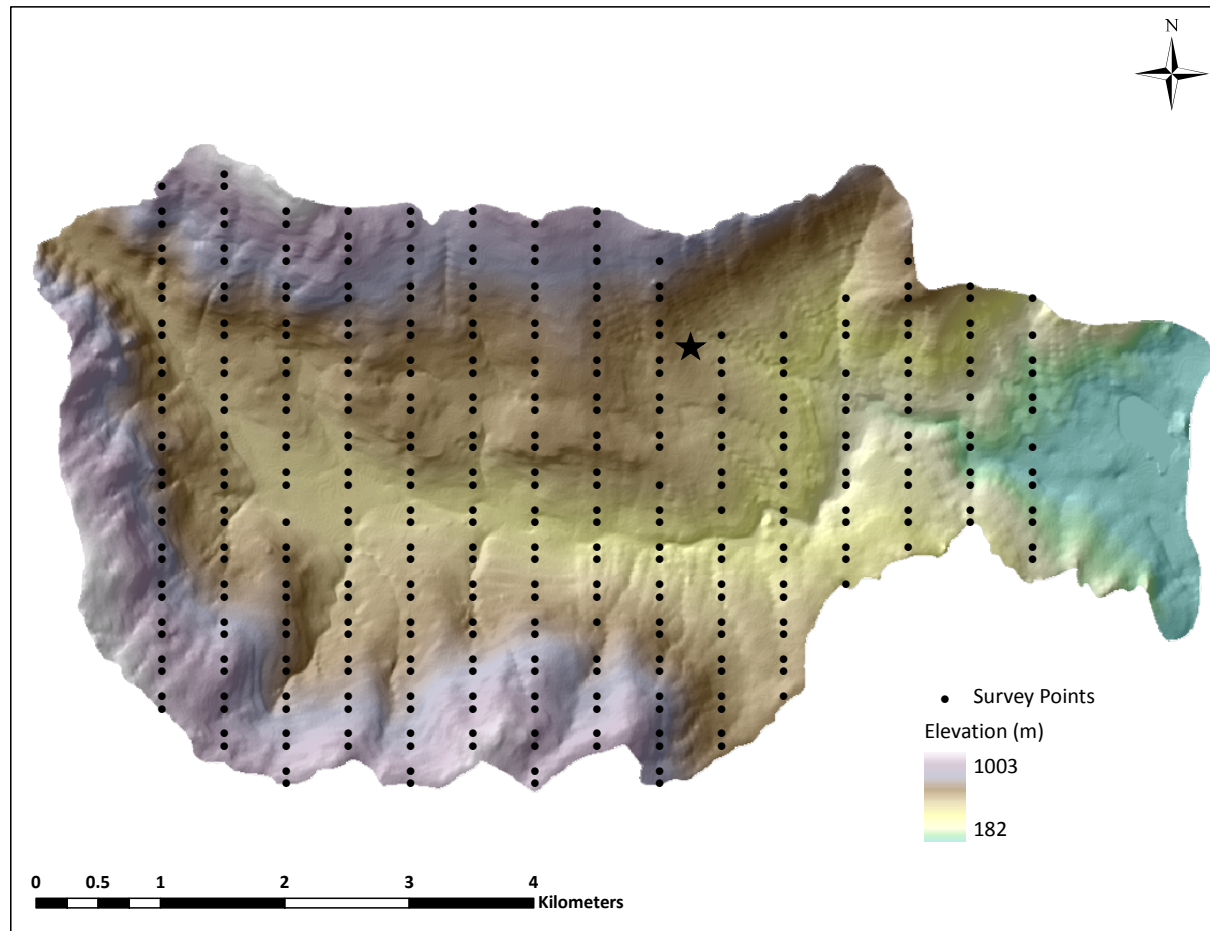
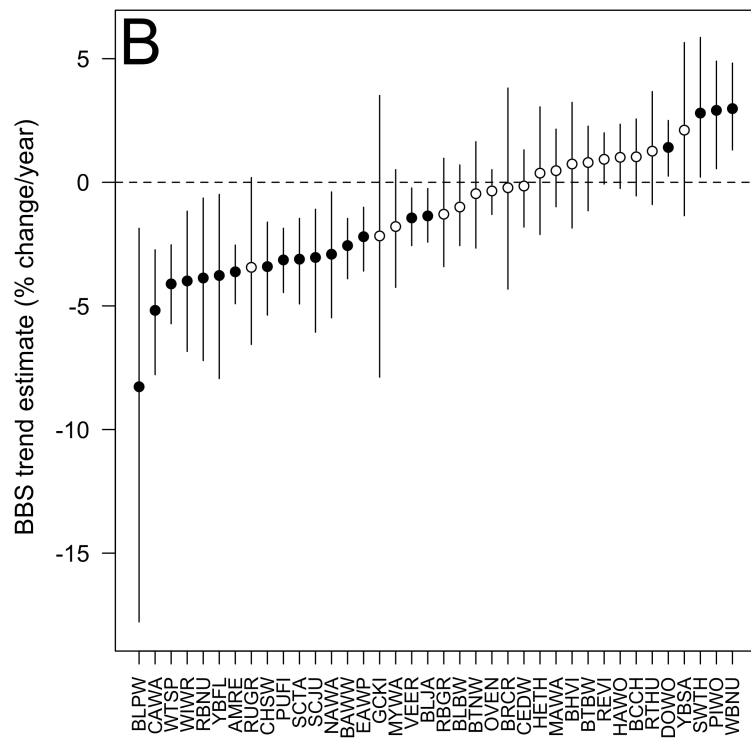
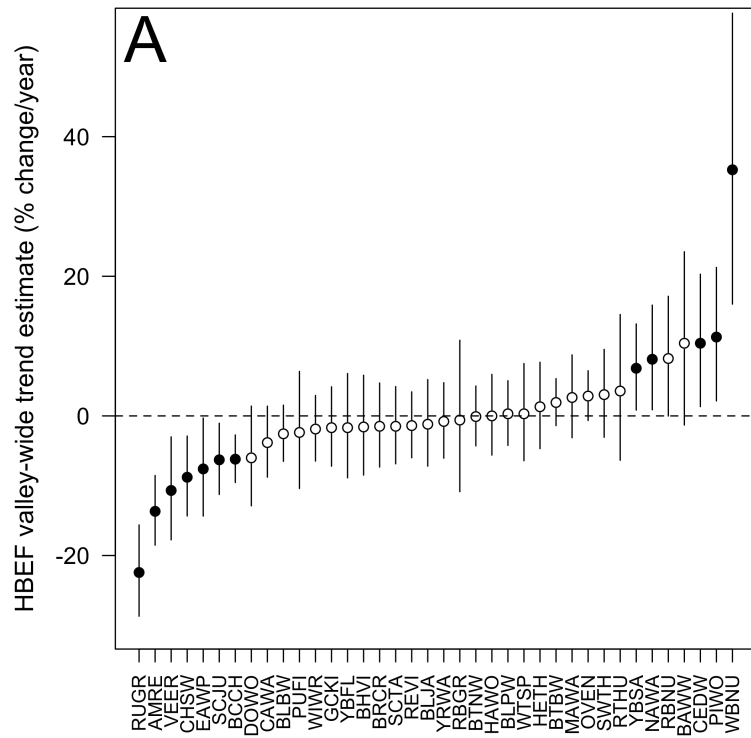


FIGURE 4.1. Map of the 3400-ha Hubbard Brook Experimental Forest study area showing valley-wide 371 sample points (black dots), LTREB plot (star), and elevational distribution (in meters).



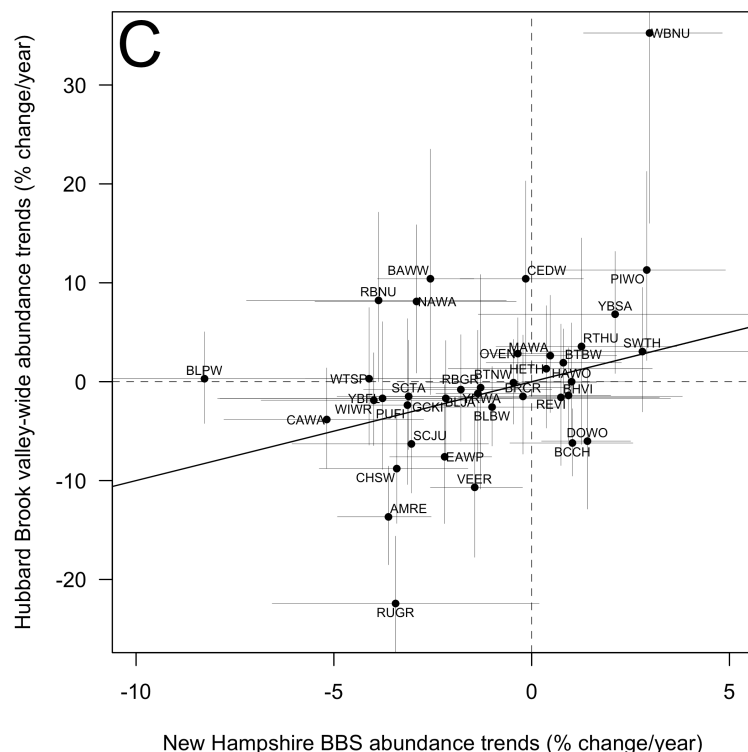


FIGURE 4.2. A) Abundance trend estimates (% change/year) for 38 bird species at Hubbard Brook Experimental Forest in the White Mountains of New Hampshire from 1999-2012. Trend estimates account for sampling error due to uneven detection rates. Error bars are 90% credible intervals. B) Breeding bird survey abundance trend estimates for 38 bird species in the state of New Hampshire, USA from 1999-2012. Error bars are 90% credible intervals. Filled circles represent significant trends (90% CIs do not overlap 0). Open circles are stable, or non-significant trends (90% CIs overlap 0). See Appendix 1 for definition of species codes. C) Direct comparison of abundance trends by species between HBEF and BBS. The solid line is 1:1 (intercept = 0, slope = 1). The dotted lines divide the plot into four quadrants: top right = both trends are positive, top left = HBEF hierarchical models predict positive trend, traditional models predict negative trend, bottom right = traditional models predict positive trend, hierarchical models predict negative trend, and bottom left = both trends are negative.

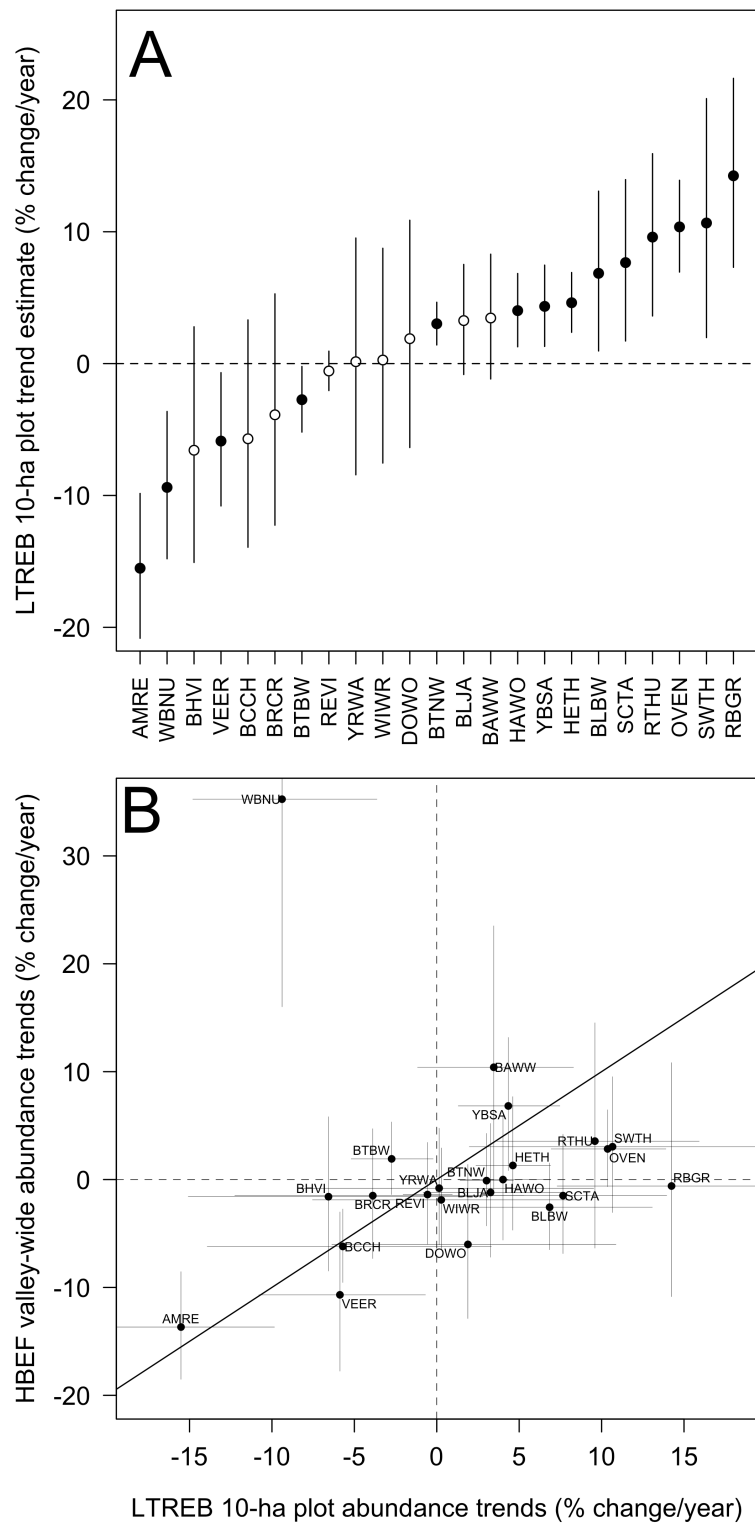


FIGURE 4.3. A) 1999-2012 abundance trends from the long-term (LTREB) 30x30m plot at Hubbard Brook. Error bars are 90% confidence intervals. Filled circles represent significant trends (90% CIs do not overlap 0). Open circles are stable, or non-significant trends (90% CIs overlap 0). See Appendix 1 for definition of species codes. B) Direct comparison of abundance trends by species between HBEF and LTREB plot. The solid line is 1:1 (intercept = 0, slope = 1). The dotted lines divide the plot into four quadrants: top right = both trends are positive, top left = HBEF hierarchical models predict positive trend, traditional models predict negative trend, bottom right = traditional models predict positive trend, hierarchical models predict negative trend, and bottom left = both trends are negative.

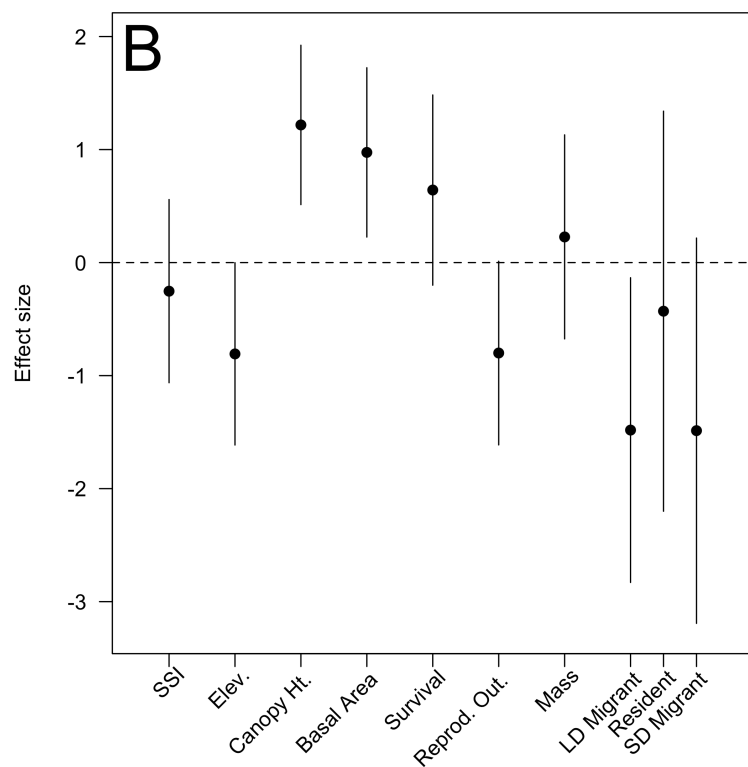
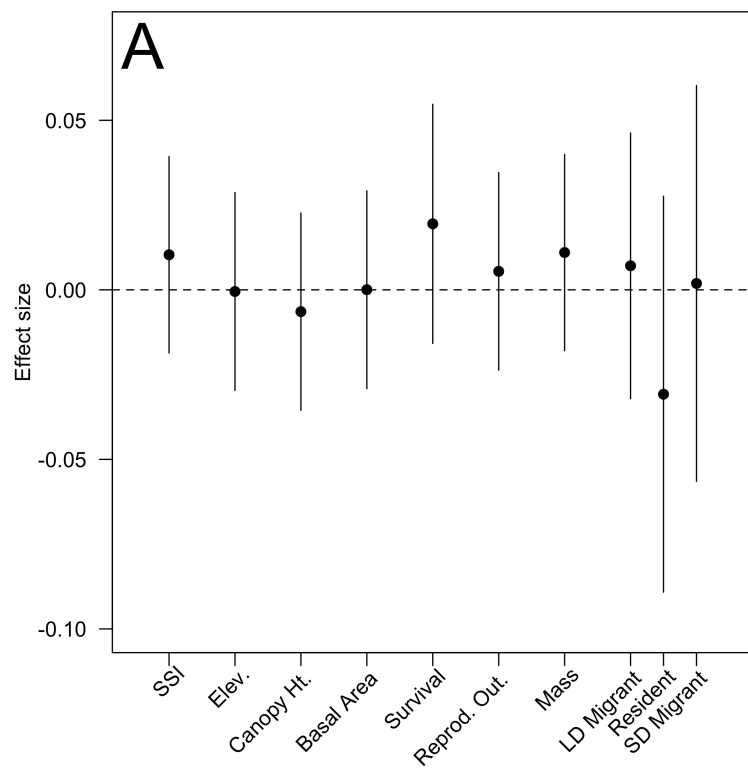


FIGURE 4.4. A) Effect size estimates for the influence of life history traits on patterns in abundance trends from Hubbard Brook Valley. Estimates are from univariate generalized mixed models with family as the random effect. Error bars are 95% confidence intervals. B) Effect size estimates for the influence of life history traits on patterns in abundance trends from the New Hampshire Breeding Bird Survey. Estimates are from univariate generalized mixed models with family as the random effect. Error bars are 95% confidence intervals. SSI = species specialization index (see methods for how this variable is calculated), low value indicates a generalist species and a high number indicates a specialist species. Elev., Canopy Ht., and Basal Area refer to the mean elevation, canopy height, and basal area at which the species is most abundant. Migration: LD = long distance, SD = short distance.

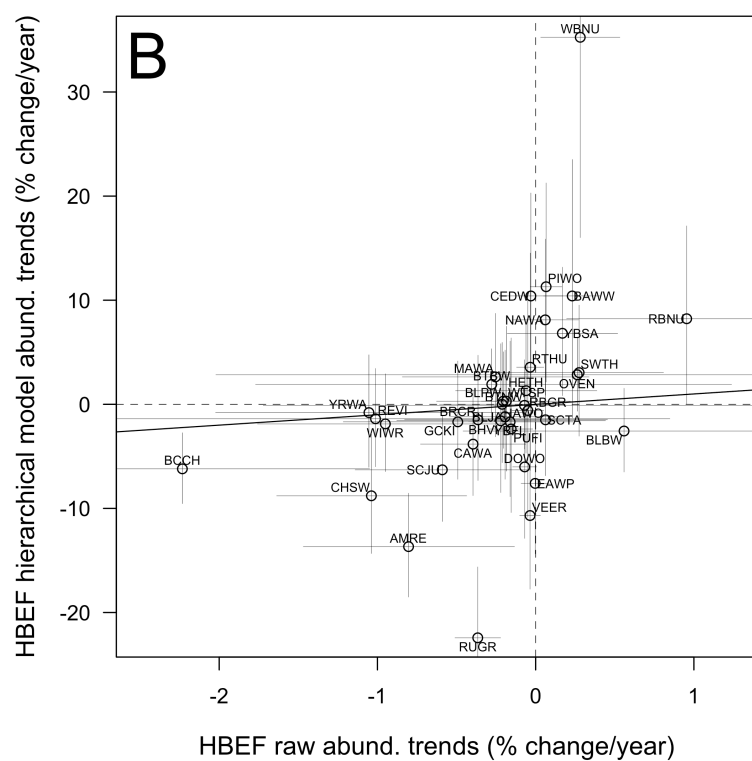
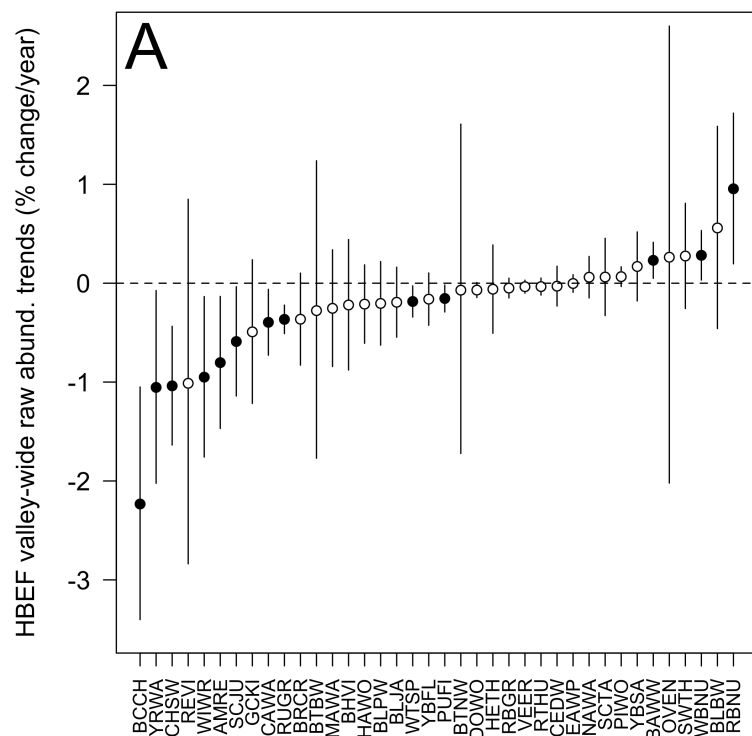


FIGURE 4.5. A) HBEF trend estimates using linear regression that assumes perfect detection of⁹⁵ all species (uses raw counts to infer ecological state of interest, in this case abundance). Filled circles represent significant trends (90% CIs do not overlap 0). Open circles are stable, or non-significant trends (90% CIs overlap 0). See Appendix 1 for definition of species codes. B) Direct comparison of abundance trends by species between HBEF hierarchical models and traditional models using raw counts. The solid line is 1:1 (intercept = 0, slope = 1). The dotted lines divide the plot into four quadrants: top right = both trends are positive, top left = HBEF hierarchical models predict positive trend, traditional models predict negative trend, bottom right = traditional models predict positive trend, hierarchical models predict negative trend, and bottom left = both trends are negative.

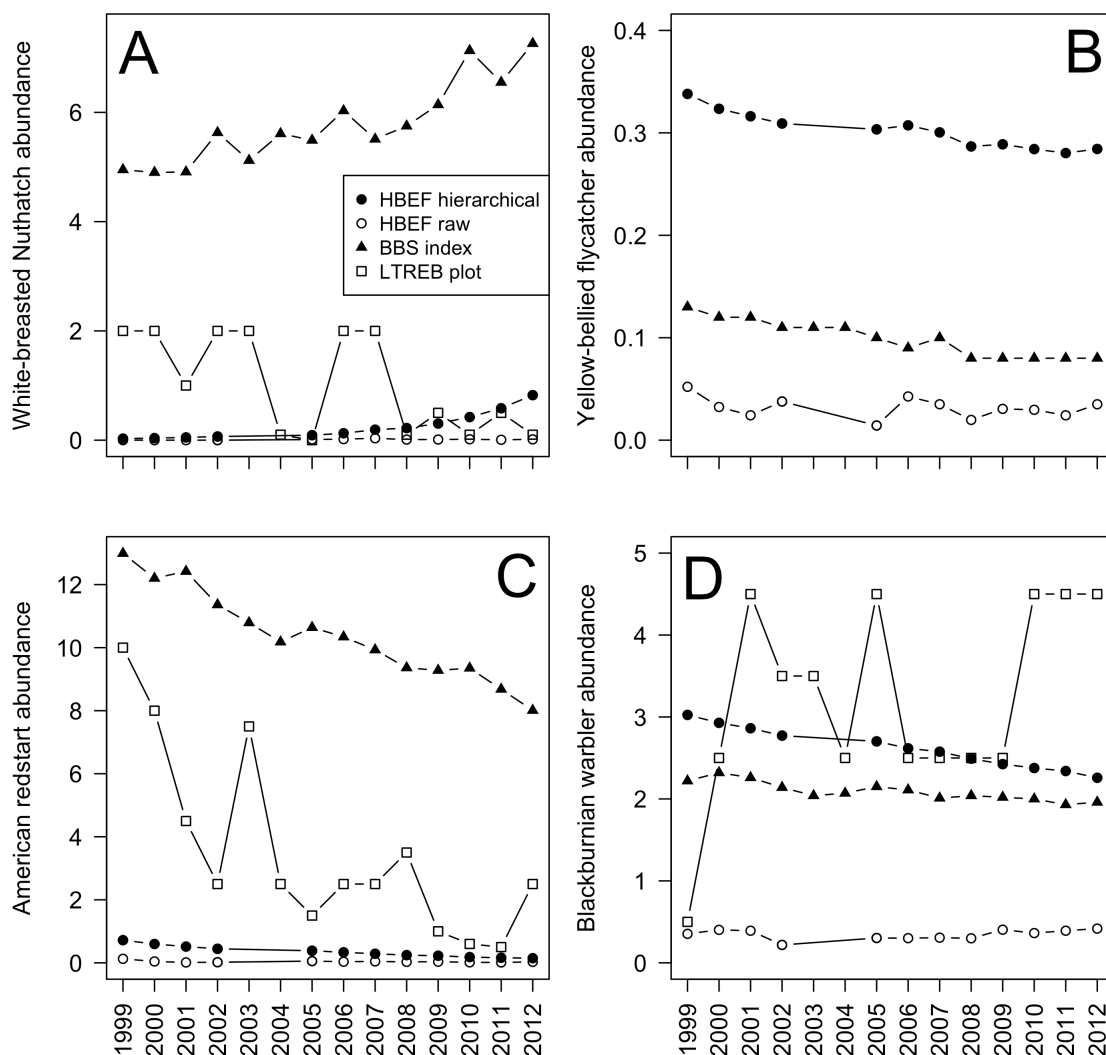


FIGURE 4.6. Comparison of abundance trends between scales and modeling methods for four species. HBEF raw abundance and estimates from the hierarchical model are number of individuals in a point count circle (50-m radius around sample point). Abundance in the LTREB plot is the number of individuals within the 10-ha plot. The BBS produces an index of relative abundance per sampling route (25 miles in length). A) White-breasted nuthatch was increasing in BBS and HBEF datasets, but decreasing in the LTREB plot. B) Yellow-bellied flycatcher was declining in both BBS and HBEF. C) American redstart, was declining in all datasets and was

almost absent from HBEF at the end of the 14-year period. D) Blackburnian warbler was relatively stable at HBEF, increasing in the LTREB and decreasing in the BBS dataset.

My dissertation research investigated fine-scale patterns in microclimate, the role of microclimate in avian occupancy dynamics, and stability of bird population trends in heterogeneous montane environments. I used a combination of novel modeling methods and sophisticated data collection approaches to explore assumptions underlying predictions of biodiversity responses to environmental changes. In this thesis I have demonstrated that scale is an important consideration in both quantifying environmental predictors and modeling avian distributions and population trends. Scale mattered for 1) understanding relative drivers of local-scale microclimate, 2) uncovering the relative roles of temperature and vegetation in site occupancy dynamics of a forest bird community, and 3) consistency of avian population trends.

I found that high microclimate variability existed at fine spatial scales (**Chapter 2**). Although elevation was the dominant driver in local-scale microclimate patterns, vegetation and microtopography also showed substantial relative contributions. Collection of high-resolution temperature data has been dismissed as being unrealistic due to the logistical difficulties involved (Bennie et al. 2014) and it has been assumed that this level of resolution will be no more relevant for biodiversity than information collected from widely-distributed meteorological stations (Xu et al. 2004). My results (**Chapter 2 & 3**) suggest that this view may be shortsighted. I showed that high-resolution temperature patterns can be accurately modeled using increasingly available remote sensing information. Elevation, microtopography, and LiDAR-derived vegetation structure metrics were able to explain the majority of variability in local microclimate and our models performed well at predicting on independent data. This suggests that efforts should be made to replicate my work in other systems to uncover general patterns that would permit widespread modeling of detailed temperature data across landscapes.

The high relative importance of elevation and microtopography in temperature patterns that I observed was not surprising (Dobrowski 2010), but the capacity of vegetation structure to play a role in microclimate was greater than expected in previous work (Lookingbill and Urban 2003). I showed that the role of vegetation structure in microclimate patterns was equivalent to that of microtopography (**Chapter 3**). Other studies are congruent with vegetation influences on

microclimate. However, most of these showed differences between dramatically different vegetation types such as forest and grassland (Suggitt et al. 2011) or forest and young plantations (Chen et al. 1993, Baker et al. 2014, Hardwick et al. 2015). Forest patch size can generate different microclimates in montane landscapes (Vanwalleghe and Meentemeyer 2009) and tropical systems (Ewers and Banks-Leite 2013). I observed mean monthly differences of several degrees when comparing >60 year old plantations with old-growth forest stands. I revealed that old growth tended to buffer sites against temperature extremes and keep sites both cooler in the summer and warmer in the winter; plantations and even-aged stands did not provide the same buffering capacity.

In my third chapter, I discovered that high-resolution temperature data such as I collected in **Chapter 2** can provide valuable insight into avian occupancy patterns. I showed that occupancy was dependent on temperature as much as or more than local vegetation characteristics. My results suggest that in addition to known influences at broad spatial scales (Thuiller et al. 2004a, Thomas 2010, Boucher-Lalonde et al. 2014), temperature may also play an important role in occupancy patterns at fine spatial scales. Previously, lack of fine-scale temperature data may have been masking the important role temperature can play in occupancy dynamics (Potter et al. 2013a).

In **Chapter 4** I tested the degree to which population trends are consistent across spatial scales. I found that landscape-scale trends were correlated with regional and local trends, but generally these correlations were tenuous. Trend differences depending on scale of data collection caution against the use of ecological data from one scale to infer to other scales (Bohning-Gaese 1997). In contrast, Holmes and Sherry (1988) found congruence between BBS (regional) and HBEF (local 10-ha plot) population trends for an earlier time period (1969-1986). This suggests that when processes underling population trends are consistent across scales parallel trends result, but population drivers are unlikely to always have equivalent rates at local, landscape and regional extents.

More species were declining at the regional scale compared to within the HBEF during the 14-year period I examined. I hypothesized that this difference stemmed from the relatively

undisturbed and contiguous nature of the forest within HBEF compared to the regional scale.¹⁰⁰ The HBEF is comprised of fairly even-aged older second-growth forests with little early-successional forest present. In contrast, the regional landscape remains dynamic and has been subject to several different processes of habitat change. First, afforestation and succession are occurring across New England resulting in decreasing amounts of early-seral habitats (King and Schlossberg 2014). The decline of early-seral species I observed at the regional scale mirrors the trend in land cover and forest age transitions. Loss of these early-successional species at the HBEF scale may have largely finished before the period we examined. There were insufficient numbers of several early-seral associates to run the trend analysis models for these species, but these species were abundant in earlier time periods (Holmes and Sherry 2001). One of the few early-successional species (Hunt 1998) with sufficient numbers to permit trend modeling was American redstart (*Setophaga ruticilla*). This species was declining during earlier studies (Holmes and Sherry 2001) and at the end of my sampling period it was almost entirely absent from HBEF. Species associated with older forests were also increasing at the regional scale, which fits with the widespread pattern of afforestation and aging forest structures. Unlike HBEF, the regional scale has experienced fragmentation and habitat loss due to rural housing developments (Kluza et al. 2000), road networks (Ortega and Capen 1999), and timber harvest (Kittredge Jr et al. 2003) – all of which have been shown to influence birds. It is possible that these processes may have contributed to declining population trends in migrants and high-elevation species at the regional scale.

Heterogeneous landscapes such as complex mountainous environments have been shown to promote more stable population dynamics (Oliver et al. 2010) and longer-term persistence (Vegas-Vilarrubia et al. 2012), implying potential for buffering biodiversity from broader-scale changes. In mountainous landscapes, vagile organisms may adjust their use of local habitat in ways that allow them to persist in the face of climate change without necessitating broad-scale range shifts (Dolby and Grubb 1999, Kearney et al. 2009a). In **Chapter 3** I showed the potential for behavioral flexibility to track local microclimate maybe widespread in forest bird species. Given that HBEF is an undisturbed montane forest landscape, the effects of regional climate

change may be reduced for avian populations due to the lack of land cover change and increased availability of diverse microclimates.

Future directions

Inferences and observations from this work lead to further questions and hypotheses to be tested in future research:

1. I hypothesized that buffered microclimates can act as microrefugia in mountainous terrain to slow avian population declines as the climate warms. I found that cool-associated species tended to be those more likely to be declining at the regional scale (BBS data; **Chapter 3**). If mountainous terrain helps to provide options for microclimate buffering (Sears et al. 2011), then dividing BBS routes into topographically heterogeneous versus topographically simple routes, we should observe stable trends in heterogeneous routes and larger declines in simple routes.

2. Are effects of temperature on avian occupancy dynamics driven by birds tracking ephemeral resources? Patterns in the diet of forest bird species could be examined across time and space. Arthropod data across sample sites could also be used to examine whether site vacancy/settlement rates are a function of prey availability.

3. Can stable land cover buffer the effects of climate change? High-elevation species and migrants were significantly declining at the regional extent, but had stable populations within HBEF (**Chapter 4**). The combined effects of climate and land use have been hypothesized to represent a “deadly cocktail” for biodiversity (Travis 2003). While their combined effects on biodiversity are not well understood (de Chazal and Rounsevell 2009), each independently have been linked to widespread declines and range contractions in birds (Jetz et al. 2007). Comparing trends from BBS routes with disturbed versus stable land use histories would provide an opportunity to test whether trends of high-elevation species and migrants differ along routes depending on land use.

Conservation and policy implications

1. Plantations and even-aged forest stands are less buffered than old-growth. My ¹⁰²

results highlight that typical forest management practices that result in even-aged stands (Franklin and Forman 1987) are substantially altering microclimate compared to old-growth stands. Plantations and even-aged stands were both warmer in the summer and cooler during the winter. Conserving remaining late-seral forests may help to buffer biodiversity from regional climate warming since these stands can be nearly 3°C cooler than managed stands. Measuring microclimate across seral stages is useful in that it can provide insight into the effects of different management techniques (Chen et al. 1999).

2. Vegetation surrounding a site also influences local-scale temperature. Vegetation within 250m of a sample site had a large relative influence on fine-scale temperature patterns. This suggests that consideration needs to be given to the land cover of the surrounding area. Narrow forest elements and small patches of forest with high edge to interior ratios may not provide the equivalent insulating capacity as larger patches of forest. Retaining old-growth forest adjacent to managed stands could potentially be used to minimize the changes in microclimate that result from conversion of forest from older to younger and less structurally diverse stands (Baker et al. 2014).

3. Birds have the behavioral flexibility to track favorable microclimates. At HJAEF, the majority of the bird species indicated some level of change in site occupancy patterns during the breeding season. I connected these dynamic occurrence patterns with local-scale vegetation and temperature conditions. While my results are correlative, they do provide substantial evidence for the importance of microclimate in determining fine-scale occupancy dynamics for bird species representing a range in life-history traits. This has far-reaching implications for the impact of climate change on biodiversity by demonstrating potential for behavioral adaptation via local distributional adjustments over relatively small temporal scales. The inherent variability in microclimate conditions found in heterogeneous montane landscapes could mitigate impacts of climate change for species with this adaptive capacity.

4. Population trends are unlikely to be transferable across scales. I documented stable trends at HBEF, but found that many species were either significantly declining or increasing at

the regional scale. My results caution against attempts to use trend data collected at one scale¹⁰³ to infer to another. Careful consideration should be taken when selecting the scale at which to measure ecological processes in order to make accurate and informative conclusions (Wiens 1989).

5. Detection needs to be accounted for to obtain accurate estimations of population trends and occurrence patterns. My test of the importance of explicitly incorporating detection probability in trend models in **Chapter 4** revealed that failing to account for differences in detection can result in alarming differences in trends. Without having accounted for imperfect detection I would have both missed trends and identified trends where none were present. Assuming perfect detection, trends in detection could be mistaken for trends in abundance or occurrence, compromising the ability to make informed conservation and management decisions (Kery et al. 2009, Kéry 2011). This same issue may also have weakened my direct comparison of HBEF and BBS trends because of differences in data collection methods. While BBS trends are calculated using sophisticated methods that take observer variability into account, they do not explicitly separate the observation from the ecological processes (Sauer and Link 2011). In **Chapter 3**, variation in detection probability was well explained by multiple survey-level and site-level characteristics, suggesting that detection is indeed quite variable across many factors. The differences in detection probability along gradients in vegetation and temperature that I observed highlight that without having taken detection into account, I may have erroneously attributed changes in detection for ones in our ecological processes of interest.

- Amiel, J. J., R. Tingley, and R. Shine. 2011. Smart moves: Effects of relative brain size on establishment success of invasive amphibians and reptiles. *PLoS One* **6**:e18277.
- Anderson, P. D., D. J. Larson, and S. S. Chan. 2007. Riparian buffer and density management influences on microclimate of young headwater forests of western Oregon. *Forest Science* **53**:254-269.
- Angert, A. L., L. G. Crozier, L. J. Rissler, S. E. Gilman, J. J. Tewksbury, and A. J. Chunco. 2011. Do species' traits predict recent shifts at expanding range edges? *Ecology Letters* **14**:677-689.
- Araújo, M. B. and R. G. Pearson. 2005. Equilibrium of species' distributions with climate. *Ecography* **28**:693-695.
- Araújo, M. B. and A. T. Peterson. 2012. Uses and misuses of bioclimatic envelope modeling. *Ecology* **93**:1527-1539.
- Araújo, M. B., W. Thuiller, P. H. Williams, and I. Reginster. 2005. Downscaling European species atlas distributions to a finer resolution: implications for conservation planning. *Global Ecology and Biogeography* **14**:17-30.
- Archaux, F., P.-Y. Henry, and O. Gimenez. 2012. When can we ignore the problem of imperfect detection in comparative studies? *Methods in Ecology and Evolution* **3**:188-194.
- Ashcroft, M. B. 2010. Identifying refugia from climate change. *Journal of Biogeography* **37**:1407-1413.
- Baker, T. P., G. J. Jordan, E. A. Steel, N. M. Fountain-Jones, T. J. Wardlaw, and S. C. Baker. 2014. Microclimate through space and time: Microclimatic variation at the edge of regeneration forests over daily, yearly and decadal time scales. *Forest Ecology and Management* **334**:174-184.
- Bart, J., M. Hofschén, and B. G. Peterjohn. 1995. Reliability of the breeding bird survey: Effects of restricting surveys to roads. *Auk* **112**:758-761.
- Bates, D. 2012. nlme: Linear and Nonlinear Mixed Effects Models. R Core team **3.1-104**.
- Bellard, C., C. Bertelsmeier, P. Leadley, W. Thuiller, and F. Courchamp. 2012. Impacts of climate change on the future of biodiversity. *Ecology Letters* **15**:365-377.
- Bennett, P. M. and I. P. F. Owens. 2002. *Evolutionary Ecology of Birds - Life histories, Mating Systems and Extinction*.
- Bennie, J., R. J. Wilson, I. M. D. Maclean, and A. J. Suggitt. 2014. Seeing the woods for the trees – when is microclimate important in species distribution models? *Global Change Biology* **20**:2699-2700.
- Bernardo, J. 2014. Biologically grounded predictions of species resistance and resilience to climate change. *Proceedings of the National Academy of Sciences* **111**:5450-5451.
- Betts, M. G., A. W. Diamond, G. J. Forbes, M. A. Villard, and J. S. Gunn. 2006. The importance of spatial autocorrelation, extent and resolution in predicting forest bird occurrence. *Ecological Modelling* **191**:197-224.
- Betts, M. G., J. C. Hagar, J. W. Rivers, J. D. Alexander, K. McGarigal, and B. C. McComb. 2010. Thresholds in forest bird occurrence as a function of the amount of early-seral broadleaf forest at landscape scales. *Ecological Applications* **20**:2116-2130.

- Betts, M. G., D. Mitchell, A. W. Dlamond, and J. Bety. 2007. Uneven rates of landscape change as a source of bias in roadside wildlife surveys. *Journal of Wildlife Management* **71**:2266-2273.
- Betts, M. G., N. L. Rodenhouse, T. S. Sillett, P. J. Doran, and R. T. Holmes. 2008. Dynamic occupancy models reveal within-breeding season movement up a habitat quality gradient by a migratory songbird. *Ecography* **31**:592-600.
- Beyer, H. L. 2004. Hawth's Analysis Tools for ArcGIS. Available at <http://www.spatial ecology.com/htools>.
- Bjornstad, O. N. 2013. ncf: spatial nonparametric covariance functions. R package version 1.1-5.
- Bohning-Gaese, K. 1997. Determinants of avian species richness at different spatial scales. *Journal of Biogeography* **24**:49-60.
- Bohning-Gaese, K., M. L. Taper, and J. H. Brown. 1994. Avian community dynamics are discordant in space and time. *Oikos* **70**:121-126.
- Bonebrake, T. C., C. L. Boggs, J. A. Stamberger, C. A. Deutsch, and P. R. Ehrlich. 2014. From global change to a butterfly flapping: biophysics and behaviour affect tropical climate change impacts. *Proceedings of the Royal Society B-Biological Sciences* **281**:20141264.
- Both, C., R. G. Bijlsma, and M. E. Visser. 2005. Climatic effects on timing of spring migration and breeding in a long-distance migrant, the pied flycatcher *Ficedula hypoleuca*. *Journal of Avian Biology* **36**:368-373.
- Both, C., S. Bouwhuis, C. M. Lessells, and M. E. Visser. 2006. Climate change and population declines in a long-distance migratory bird. *Nature* **441**:81-83.
- Both, C., M. van Asch, R. G. Bijlsma, A. B. van den Burg, and M. E. Visser. 2009a. Climate change and unequal phenological changes across four trophic levels: constraints or adaptations? *Journal of Animal Ecology* **78**:73-83.
- Both, C., C. A. M. Van Turnhout, R. G. Bijlsma, H. Siepel, A. J. Van Strien, and R. P. B. Foppen. 2009b. Avian population consequences of climate change are most severe for long-distance migrants in seasonal habitats. *Proceedings of the Royal Society of London B: Biological Sciences* **282**:20091525.
- Both, C. and M. E. Visser. 2005. The effect of climate change on the correlation between avian life-history traits. *Global Change Biology* **11**:1606-1613.
- Botkin, D. B., H. Saxe, M. B. Araujo, R. Betts, R. H. W. Bradshaw, T. Cedhagen, P. Chesson, T. P. Dawson, J. R. Etterson, D. P. Faith, S. Ferrier, A. Guisan, A. S. Hansen, D. W. Hilbert, C. Loehle, C. Margules, M. New, M. J. Sobel, and D. R. B. Stockwell. 2007. Forecasting the effects of global warming on biodiversity. *BioScience* **57**:227-236.
- Boucher-Lalonde, V., A. Morin, and D. J. Currie. 2014. A consistent occupancy-climate relationship across birds and mammals of the Americas. *Oikos* **123**:1029-1036.
- Boyles, J. G., F. Seebacher, B. Smit, and A. E. McKechnie. 2011. Adaptive thermoregulation in endotherms may alter responses to climate change. *Integrative and Comparative Biology* **51**:676-690.
- Brambilla, M. and D. Rubolini. 2009. Intra-seasonal changes in distribution and habitat associations of a multi-brooded bird species: implications for conservation planning. *Animal Conservation* **12**:71-77.
- Brown, J. H. 1995. *Macroecology*. University of Chicago Press, Chicago, IL.

- Brown, J. H., D. W. Mehlman, and G. C. Stevens. 1995. Spatial variation in abundance. *Ecology* **76**:2028-2043.
- Buckley, L. B. and J. G. Kingsolver. 2012. Functional and phylogenetic approaches to forecasting species' responses to climate change. *Annual Review of Ecology, Evolution, and Systematics* **43**:205-226.
- Burnham, K. P. and D. R. Anderson. 2002. Model selection and multimodel inference: A practical information-theoretic approach. 2nd edition. Springer-Verlag, Inc., New York, NY.
- Butchart, S. H. M., M. Walpole, B. Collen, A. van Strien, J. P. W. Scharlemann, R. E. A. Almond, J. E. M. Baillie, B. Bomhard, C. Brown, J. Bruno, K. E. Carpenter, G. M. Carr, J. Chanson, A. M. Chenery, J. Csirke, N. C. Davidson, F. Dentener, M. Foster, A. Galli, J. N. Galloway, P. Genovesi, R. D. Gregory, M. Hockings, V. Kapos, J.-F. Lamarque, F. Leverington, J. Loh, M. A. McGeoch, L. McRae, A. Minasyan, M. H. Morcillo, T. E. E. Oldfield, D. Pauly, S. Quader, C. Revenga, J. R. Sauer, B. Skolnik, D. Spear, D. Stanwell-Smith, S. N. Stuart, A. Symes, M. Tierney, T. D. Tyrrell, J.-C. Vié, and R. Watson. 2010. Global Biodiversity: Indicators of Recent Declines. *Science* **328**:1164-1168.
- Canterbury, G. E., T. E. Martin, D. R. Petit, L. J. Petit, and D. F. Bradford. 2000. Bird communities and habitat as ecological indicators of forest condition in regional monitoring. *Conservation Biology* **14**:544-558.
- Chandler, R. B. and D. I. King. 2011. Habitat quality and habitat selection of golden-winged warblers in Costa Rica: an application of hierarchical models for open populations. *Journal of Applied Ecology* **48**:1038-1047.
- Chandler, R. B., J. A. Royle, and D. I. King. 2011. Inference about density and temporary emigration in unmarked populations. *Ecology* **92**:1429-1435.
- Chen, I. C., J. K. Hill, R. Ohlemuller, D. B. Roy, and C. D. Thomas. 2011. Rapid range shifts of species associated with high levels of climate warming. *Science* **333**:1024-1026.
- Chen, J., J. F. Franklin, and T. A. Spies. 1993. Contrasting microclimates among clearcut, edge, and interior of old-growth Douglas-fir forest. *Agricultural and Forest Meteorology* **63**:219-237.
- Chen, J., S. C. Saunders, T. R. Crow, R. J. Naiman, K. D. Broszofsky, G. D. Mroz, B. L. Brookshire, and J. F. Franklin. 1999. Microclimate in forest ecosystem and landscape ecology: Variations in local climate can be used to monitor and compare the effects of different management regimes. *BioScience* **49**:288-297.
- Clark, M. E. and T. E. Martin. 2007. Modeling tradeoffs in avian life history traits and consequences for population growth. *Ecological Modelling* **209**:110-120.
- Climate Solutions New England. 2014. Climate change in northern New Hampshire: Past, present, and future. Sustainability Insititute at the University of New Hampshire, Durham, NH.
- Copeland, J. H., R. A. Pielke, and T. G. F. Kittel. 1996. Potential climatic impacts of vegetation change: A regional modeling study. *Journal of Geophysical Research: Atmospheres* **101**:7409-7418.
- Cumming, S. G., D. Stralberg, K. L. Lefevre, P. Sólymos, E. M. Bayne, S. Fang, T. Fontaine, D. Mazerolle, F. K. A. Schmiegelow, and S. J. Song. 2014. Climate and vegetation

- hierarchically structure patterns of songbird distribution in the Canadian boreal region.¹⁰⁷ *Ecography* **37**:137-151.
- Daly, C., D. R. Conklin, and M. H. Unsworth. 2010. Local atmospheric decoupling in complex topography alters climate change impacts. *International Journal of Climatology* **30**:1857-1864.
- de Chazal, J. and M. D. A. Rounsevell. 2009. Land-use and climate change within assessments of biodiversity change: A review. *Global Environmental Change-Human and Policy Dimensions* **19**:306-315.
- De Frenne, P., F. Rodríguez-Sánchez, D. A. Coomes, L. Baeten, G. Verstraeten, M. Vellend, M. Bernhardt-Römermann, C. D. Brown, J. Brunet, J. Cornelis, G. M. Decocq, H. Dierschke, O. Eriksson, F. S. Gilliam, R. Hédél, T. Heinken, M. Hermy, P. Hommel, M. A. Jenkins, D. L. Kelly, K. J. Kirby, F. J. G. Mitchell, T. Naaf, M. Newman, G. Peterken, P. Petřík, J. Schultz, G. Sonnier, H. Van Calster, D. M. Waller, G.-R. Walther, P. S. White, K. D. Woods, M. Wulf, B. J. Graae, and K. Verheyen. 2013. Microclimate moderates plant responses to macroclimate warming. *Proceedings of the National Academy of Sciences*.
- Devictor, V., R. Julliard, D. Couvet, and F. Jiguet. 2008. Birds are tracking climate warming, but not fast enough. *Proceedings of the Royal Society B-Biological Sciences* **275**:2743-2748.
- Diggs, N. E., P. P. Marra, and R. J. Cooper. 2011. Resource limitation drives patterns of habitat occupancy during the nonbreeding season for an omnivorous songbird. *Condor* **113**:646-654.
- Dobrowski, S. Z. 2010. A climatic basis for microrefugia: the influence of terrain on climate. *Global Change Biology* **17**:1022-1035.
- Dobrowski, S. Z., J. T. Abatzoglou, J. A. Greenberg, and S. G. Schladow. 2009. How much influence does landscape-scale physiography have on air temperature in a mountain environment? *Agricultural and Forest Meteorology* **149**:1751-1758.
- Dolby, A. S. and T. C. Grubb. 1999. Effects of winter weather on horizontal and vertical use of isolated forest fragments by bark-foraging birds. *Condor* **101**:408-412.
- Doligez, B., E. Danchin, and J. Clobert. 2002. Public information and breeding habitat selection in a wild bird population. *Science* **297**:1168-1170.
- Doran, P. J. and R. T. Holmes. 2005. Habitat occupancy patterns of a forest dwelling songbird: causes and consequences. *Canadian Journal of Zoology* **83**:1297-1305.
- Dunstan, P. K., F. Althaus, A. Williams, and N. J. Bax. 2012. Characterising and predicting benthic biodiversity for conservation planning in deepwater environments. *PLoS One* **7**:e36558.
- Elith, J. and J. R. Leathwick. 2014. Boosted regression trees for ecological modeling. R vignette for package 'dismo'.
- Elith, J., J. R. Leathwick, and T. Hastie. 2008. A working guide to boosted regression trees. *Journal of Animal Ecology* **77**:802-813.
- Ellis, T. M. and M. G. Betts. 2011. Bird abundance and diversity across a hardwood gradient within early seral plantation forest. *Forest Ecology and Management* **261**:1372-1381.
- ESRI. 2011. ArcGIS Desktop: Release 10. Redlands, CA: Environmental Systems Research Institute.
- Ewers, R. M. and C. Banks-Leite. 2013. Fragmentation impairs the microclimate buffering effect of tropical forests. *PLoS One* **8**:e58093.

- Fiske, I. and R. Chandler. 2011. unmarked: An R Package for Fitting Hierarchical Models of Wildlife Occurrence and Abundance. *Journal of Statistical Software* **43**:1-23.
- Franklin, J., F. W. Davis, M. Ikegami, A. D. Syphard, L. E. Flint, A. L. Flint, and L. Hannah. 2013. Modeling plant species distributions under future climates: how fine scale do climate projections need to be? *Global Change Biology* **19**:473-483.
- Franklin, J. E. and R. T. T. Forman. 1987. Creating landscape patterns by forest cutting: Ecological consequences and principles. *Landscape Ecology* **1**:5-18.
- Franklin, J. F., T. A. Spies, R. V. Pelt, A. B. Carey, D. A. Thornburgh, D. R. Berg, D. B. Lindenmayer, M. E. Harmon, W. S. Keeton, D. C. Shaw, K. Bible, and J. Chen. 2002. Disturbances and structural development of natural forest ecosystems with silvicultural implications, using Douglas-fir forests as an example. *Forest Ecology and Management* **155**:399-423.
- Fraser, K. C., C. Silverio, P. Kramer, N. Mickle, R. Aeppli, and B. J. M. Stutchbury. 2013. A trans-hemispheric migratory songbird does not advance spring schedules or increase migration rate in response to record-setting temperatures at breeding sites. *PloS One* **8**.
- Fretwell, S. D. and H. L. Lucas. 1969. On territorial behavior and other factors influencing habitat distribution in birds. *Acta Biotheoretica* **19**:16-36.
- Fridley, J. D. 2009. Downscaling climate over complex terrain: high finescale (< 1000 m) spatial variation of near-ground temperatures in a montane forested landscape (Great Smoky Mountains). *Journal of Applied Meteorology and Climatology* **48**:1033-1049.
- Fu, Y. H., M. Campioli, G. Deckmyn, and I. A. Janssens. 2012. The impact of winter and spring temperatures on temperate tree budburst dates: Results from an experimental climate manipulation. *PLoS One* **7**:e47324.
- Gilroy, J. J., G. Q. A. Anderson, P. V. Grice, J. A. Vickery, and W. J. Sutherland. 2010. Mid-season shifts in the habitat associations of Yellow Wagtails *Motacilla flava* breeding in arable farmland. *Ibis* **152**:90-104.
- Goetz, S. J., D. Steinberg, M. G. Betts, R. T. Holmes, P. J. Doran, R. Dubayah, and M. Hofton. 2010. Lidar remote sensing variables predict breeding habitat of a Neotropical migrant bird. *Ecology* **91**:1569-1576.
- Gow, E. A. and B. J. M. Stutchbury. 2013. Within-season nesting dispersal and molt dispersal are linked to habitat shifts in a Neotropical migratory songbird. *Wilson Journal of Ornithology* **125**:696-708.
- Groffman, P. M., L. E. Rustad, P. H. Templer, J. L. Campbell, L. M. Christenson, N. K. Lany, A. M. Soggi, M. A. Vadeboncoeur, P. G. Schaberg, G. F. Wilson, C. T. Driscoll, T. J. Fahey, M. C. Fisk, C. L. Goodale, M. B. Green, S. P. Hamburg, C. E. Johnson, M. J. Mitchell, J. L. Morse, L. H. Pardo, and N. L. Rodenhouse. 2012. Long-term integrated studies show complex and surprising effects of climate change in the northern hardwood forest. *Bioscience* **62**:1056-1066.
- Guillera-Aroita, G., M. S. Ridout, and B. J. T. Morgan. 2010. Design of occupancy studies with imperfect detection. *Methods in Ecology and Evolution* **1**:131-139.
- Gutiérrez Illán, J., C. D. Thomas, J. A. Jones, W.-K. Wong, S. M. Shirley, and M. G. Betts. 2014. Precipitation and winter temperature predict long-term range-scale abundance changes in Western North American birds. *Global Change Biology*:n/a-n/a.

- Hagar, J. C. 2007. Wildlife species associated with non-coniferous vegetation in Pacific Northwest conifer forests: A review. *Forest Ecology and Management* **246**:108-122.
- Haining, R., J. Law, and D. Griffith. 2009. Modelling small area counts in the presence of overdispersion and spatial autocorrelation. *Computational Statistics & Data Analysis* **53**:2923-2937.
- Hansen, A. J. and D. L. Urban. 1992. Avian response to landscape pattern: The role of species life histories. *Landscape Ecology* **7**:163-180.
- Hardwick, S. R., R. Toumi, M. Pfeifer, E. C. Turner, R. Nilus, and R. M. Ewers. 2015. The relationship between leaf area index and microclimate in tropical forest and oil palm plantation: Forest disturbance drives changes in microclimate. *Agricultural and Forest Meteorology* **201**:187-195.
- Hijmans, R. J., S. Phillips, J. Leathwick, and J. Elith. 2013. dismo: Species distribution modeling. R package version 0.8-17. <http://CRAN.R-project.org/package=dismo>.
- Hildén, O. 1965. Habitat selection in birds: A review. *Annales Zoologici Fennici* **2**:53-75.
- Hitch, A. T. and P. L. Leberg. 2007. Breeding distributions of North American bird species moving north as a result of climate change. *Conservation Biology* **21**:534-539.
- Holmes, R. T. 2011. Avian population and community processes in forest ecosystems: Long-term research in the Hubbard Brook Experimental Forest. *Forest Ecology and Management* **262**:20-32.
- Holmes, R. T. and T. W. Sherry. 1988. Assessing population trends of New Hampshire forest birds: Local vs. regional patterns. *Auk* **105**:756-768.
- Holmes, R. T. and T. W. Sherry. 2001. Thirty-year bird population trends in an unfragmented temperate deciduous forest: Importance of habitat change. *Auk* **118**:589-609.
- Hoover, J. P. 2003. Decision rules for site fidelity in a migratory bird, the prothonotary warbler. *Ecology* **84**:416-430.
- Hosmer, D. W., S. Hosmer T Fau - Le Cessie, S. Le Cessie S Fau - Lemeshow, and S. Lemeshow. 1997. A comparison of goodness-of-fit tests for the logistic regression model.
- Hosmer, J., D. W., S. Lemeshow, and R. X. Sturdivant. 2013. *Applied Logistic Regression*. 3rd edition. John Wiley & Sons, Inc., Hoboken, New Jersey.
- Houston, D. R. 1994. Major new tree disease epidemics: Beech bark disease. *Annual Review of Phytopathology* **32**:75-87.
- Huey, R. B., M. R. Kearney, A. Krockenberger, J. A. M. Holtum, M. Jess, and S. E. Williams. 2012. Predicting organismal vulnerability to climate warming: roles of behaviour, physiology and adaptation. *Philosophical Transactions of the Royal Society B-Biological Sciences* **367**:1665-1679.
- Hunt, P. D. 1998. Evidence from a landscape population model of the importance of early successional habitat to the American redstart. *Conservation Biology* **12**:1377-1389.
- Huntington, T. G., A. D. Richardson, K. J. McGuire, and K. Hayhoe. 2009. Climate and hydrological changes in the northeastern United States: recent trends and implications for forested and aquatic ecosystems. This article is one of a selection of papers from NE Forests 2100: A Synthesis of Climate Change Impacts on Forests of the Northeastern US and Eastern Canada. *Canadian Journal of Forest Research* **39**:199-212.
- IPCC. 2014. *Climate Change 2014: Impacts, Adaptation, and Vulnerability. Part A: Global and Sectoral Aspects. Contribution of Working Group II to the Fifth Assessment Report of*

- the Intergovernmental Panel on Climate Change. Cambridge University Press, Cambridge, United Kingdom and New York, NY, USA.
- Jetz, W., D. S. Wilcove, and A. P. Dobson. 2007. Projected impacts of climate and land-use change on the global diversity of birds. *PloS Biology* **5**:1211-1219.
- Jiguet, F., A.-S. Gadot, R. Julliard, S. E. Newson, and D. Couvet. 2007. Climate envelope, life history traits and the resilience of birds facing global change. *Global Change Biology* **13**:1672-1684.
- Julliard, R., J. Clavel, V. Devictor, F. Jiguet, and D. Couvet. 2006. Spatial segregation of specialists and generalists in bird communities. Pages 1237-1244. Wiley-Blackwell.
- Kearney, M., R. Shine, and W. P. Porter. 2009a. The potential for behavioral thermoregulation to buffer "cold-blooded" animals against climate warming. *Proceedings of the National Academy of Sciences of the United States of America* **106**:3835-3840.
- Kearney, M., R. Shine, and W. P. Porter. 2009b. The potential for behavioral thermoregulation to buffer "cold-blooded" animals against climate warming. *Proceedings of the National Academy of Sciences* **106**:3835-3840.
- Keller, C. M. E. and J. T. Scallan. 1999. Potential roadside biases due to habitat changes along breeding bird survey routes. *Condor* **101**:50-57.
- Kéry, M. 2011. Towards the modelling of true species distributions. *Journal of Biogeography*:no-no.
- Kery, M. and R. Chandler. 2012. unmarked vignette: Dynamic occupancy models in unmarked. Swiss Ornithological Institute and USGS Patuxent Wildlife Research Center.
- Kery, M., R. M. Dorazio, L. Soldaat, A. van Strien, A. Zuiderwijk, and J. A. Royle. 2009. Trend estimation in populations with imperfect detection. *Journal of Applied Ecology* **46**:1163-1172.
- Kery, M. and J. A. Royle. 2010. Hierarchical modelling and estimation of abundance and population trends in metapopulation designs. *Journal of Animal Ecology* **79**:453-461.
- Kéry, M., J. A. Royle, and H. Schmid. 2005. Modeling avian abundance from replicated counts using binomial mixture models. *Ecological Applications* **15**:1450-1461.
- King, D. I. and S. Schlossberg. 2014. Synthesis of the conservation value of the early-successional stage in forests of eastern North America. *Forest Ecology and Management* **324**:186-195.
- Kingsolver, J. G., H. A. Woods, L. B. Buckley, K. A. Potter, H. J. MacLean, and J. K. Higgins. 2011. Complex life cycles and the responses of insects to climate change. *Integrative and Comparative Biology* **51**:719-732.
- Kittredge Jr, D. B., A. O. Finley, and D. R. Foster. 2003. Timber harvesting as ongoing disturbance in a landscape of diverse ownership. *Forest Ecology and Management* **180**:425-442.
- Klemp, S. 2003. Altitudinal dispersal within the breeding season in the Grey Wagtail *Motacilla cinerea*. *Ibis* **145**:509-511.
- Kluza, D. A., C. R. Griffin, and R. M. Degraaf. 2000. Housing developments in rural New England: effects on forest birds. *Animal Conservation* **3**:15-26.
- Lack, D. 1954. *The Natural Regulation of Animal Numbers*. Oxford University Press.

- 111
- Lefsky, M. A., W. B. Cohen, S. A. Acker, G. G. Parker, T. A. Spies, and D. Harding. 1999. LiDAR remote sensing of the canopy structure and biophysical properties of Douglas-fir western hemlock forests. *Remote Sensing of Environment* **70**:339-361.
- Legendre, P. 1993. Spatial autocorrelation: Trouble or new paradigm. *Ecology* **74**:1659-1673.
- Lenoir, J., J. C. Gegout, A. Guisan, P. Vittoz, T. Wohlgemuth, N. E. Zimmermann, S. Dullinger, H. Pauli, W. Willner, and J. C. Svenning. 2010. Going against the flow: potential mechanisms for unexpected downslope range shifts in a warming climate. *Ecography* **33**:295-303.
- Li, H., X. Deng, D.-Y. Kim, and E. P. Smith. 2014. Modeling maximum daily temperature using a varying coefficient regression model. *Water Resources Research* **50**:3073-3087.
- Lichstein, J. W., T. R. Simons, S. A. Shriver, and K. E. Franzreb. 2002. Spatial autocorrelation and autoregressive models in ecology. *Ecological Monographs* **72**:445-463.
- Likens, G. E., F. H. Bormann, N. M. Johnson, D. W. Fisher, and R. S. Pierce. 1970. Effects of forest cutting and herbicide treatment on nutrient budgets in the Hubbard Brook watershed-ecosystem. *Ecological Monographs* **40**:23-47.
- Link, W. A. and J. R. Sauer. 2002. A hierarchical analysis of population change with application to Cerulean Warblers. *Ecology* **83**:2832-2840.
- Loarie, S. R., P. B. Duffy, H. Hamilton, G. P. Asner, C. B. Field, and D. D. Ackerly. 2009. The velocity of climate change. *Nature* **462**:1052-1055.
- Logan, M. L., R. K. Huynh, R. A. Precious, and R. G. Calsbeek. 2013. The impact of climate change measured at relevant spatial scales: new hope for tropical lizards. *Global Change Biology* **19**:3093-3102.
- Long, R. A., R. T. Bowyer, W. P. Porter, P. Mathewson, K. L. Monteith, and J. G. Kie. 2014. Behavior and nutritional condition buffer a large-bodied endotherm against direct and indirect effects of climate. *Ecological Monographs* **84**:513-532.
- Lookingbill, T. R. and D. L. Urban. 2003. Spatial estimation of air temperature differences for landscape-scale studies in montane environments. *Agricultural and Forest Meteorology* **114**:141-151.
- Lumpkin, H. A. and S. M. Pearson. 2013. Effects of exurban development and temperature on bird species in the southern Appalachians. *Conservation Biology* **27**:1069-1078.
- Luoto, M. and R. K. Heikkinen. 2008. Disregarding topographical heterogeneity biases species turnover assessments based on bioclimatic models. *Global Change Biology* **14**:483-494.
- Luoto, M., R. Virkkala, and R. K. Heikkinen. 2007. The role of land cover in bioclimatic models depends on spatial resolution. *Global Ecology and Biogeography* **16**:34-42.
- MacArthur, R. H., J. W. MacArthur, and J. Preer. 1962. On bird species diversity II: Prediction of bird census from habitat measurements. *The American Naturalist* **96**:167-174.
- MacKenzie, D., J. Nichols, J. Hines, M. Knutson, and A. Franklin. 2003. Estimating site occupancy, colonization, and local extinction when a species is detected imperfectly. *Ecology* **84**:2200-2207.
- MacKenzie, D., J. Nichols, G. Lachman, S. Droege, J. Royle, and C. Langtimm. 2002. Estimating site occupancy rates when detection probabilities are less than one. *Ecology* **83**:2248-2255.

- MacKenzie, D., J. Nichols, J. Royle, K. Pollock, L. Bailey, and J. Hines. 2006. *Occupancy estimation and modeling: Inferring patterns and dynamics of species occurrence*. Elsevier Inc., Oxford, UK.
- MacKenzie, D. I. and L. L. Bailey. 2004. Assessing the Fit of Site-Occupancy Models. *Journal of Agricultural, Biological & Environmental Statistics* **9**:300-318.
- Maggini, R., A. Lehmann, M. Kéry, H. Schmid, M. Beniston, L. Jenni, and N. Zbinden. 2011. Are Swiss birds tracking climate change?: Detecting elevational shifts using response curve shapes. *Ecological Modelling* **222**:21-32.
- Martin, T. E. 1987. Food as a limit on breeding birds - a life-history perspective. *Annual Review of Ecology and Systematics* **18**:453-487.
- McClure, C. J. W. and G. E. Hill. 2012. Dynamic versus static occupancy: How stable are habitat associations through a breeding season? *Ecosphere* **3**.
- Means, J. E., S. A. Acker, B. J. Fitt, M. Renslow, L. Emerson, and C. J. Hendrix. 2000. Predicting forest stand characteristics with airborne scanning lidar. *Photogrammetric Engineering & Remote Sensing* **66**:1367-1371.
- Mitikka, V., R. K. Heikkinen, M. Luoto, M. B. Araujo, K. Saarinen, J. Poyry, and S. Fronzek. 2008. Predicting range expansion of the map butterfly in Northern Europe using bioclimatic models. *Biodiversity and Conservation* **17**:623-641.
- Moller, A. P., D. Rubolini, and E. Lehikoinen. 2008. Populations of migratory bird species that did not show a phenological response to climate change are declining. *Proceedings of the National Academy of Sciences* **105**:16195-16200.
- Moore, F. R. 2000. Stopover ecology of nearctic-neotropical landbird migrants: habitat relations and conservation implications. *Studies in Avian Biology*:1-33.
- Moritz, C. and R. Agudo. 2013. The future of species under climate change: Resilience or decline? *Science* **341**:504-508.
- Morrison, C. A., R. A. Robinson, J. A. Clark, and J. A. Gill. 2010. Spatial and temporal variation in population trends in a long-distance migratory bird. *Diversity and Distributions* **16**:620-627.
- Myers, N., R. A. Mittermeier, C. G. Mittermeier, G. A. B. da Fonseca, and J. Kent. 2000. Biodiversity hotspots for conservation priorities. *Nature* **403**:853-858.
- North American Bird Conservation Initiative, U. S. C. 2013. *The State of the Birds 2013 Report on Private Lands*. U.S. Department of Interior, Washington, D.C.
- Odion, D. C. and D. A. Sarr. 2007. Managing disturbance regimes to maintain biological diversity in forested ecosystems of the Pacific Northwest. *Forest Ecology and Management* **246**:57-65.
- Oke, T. R., J. M. Crowther, K. G. McNaughton, J. L. Monteith, and B. Gardiner. 1989. The micrometeorology of the urban forest. *Philosophical Transactions of the Royal Society B: Biological Sciences* **324**:335-349.
- Oliver, T., D. B. Roy, J. K. Hill, T. Brereton, and C. D. Thomas. 2010. Heterogeneous landscapes promote population stability. *Ecology Letters* **13**:473-484.
- Olson, G. S., R. G. Anthony, E. D. Forsman, S. H. Ackers, P. J. Loschl, J. A. Reid, K. M. Dugger, E. M. Glenn, and W. J. Ripple. 2005. Modeling of site occupancy dynamics for Northern Spotted Owls, with emphasis on the effects of Barred Owls. *Journal of Wildlife Management* **69**:918-932.

- Ortega, Y. K. and D. E. Capen. 1999. Effects of forest roads on habitat quality for ovenbirds in a forested landscape. *Auk* **116**:937-946.
- Parmesan, C. 2006. Ecological and evolutionary responses to recent climate change. *Annual Review of Ecology, Evolution, and Systematics* **37**:637-669.
- Parmesan, C. and G. Yohe. 2003. A globally coherent fingerprint of climate change impacts across natural systems. *Nature* **421**:37-42.
- Patsiou, T. S., E. Conti, N. E. Zimmermann, S. Theodoridis, and C. F. Randin. 2013. Topo-climatic microrefugia explain the persistence of a rare endemic plant in the Alps during the last 21 millennia. *Global Change Biology* **20**:2286-2300.
- Pearson, R. G. and T. P. Dawson. 2003. Predicting the impacts of climate change on the distribution of species: are bioclimate envelope models useful? *Global Ecology & Biogeography* **12**:361-371.
- Pepin, N. and M. Losleben. 2002. Climate change in the Colorado Rocky Mountains: free air versus surface temperature trends. *International Journal of Climatology* **22**:311-329.
- Peterjohn, B. G. and J. R. Sauer. 1994. Population trends of woodland birds from the North American Breeding Bird Survey. *Wildlife Society Bulletin* **22**:155-164.
- Peterson, A. T., M. A. Ortega-Huerta, J. Bartley, V. Sanchez-Cordero, J. Soberon, R. H. Buddemeier, and D. R. B. Stockwell. 2002. Future projections for Mexican faunas under global climate change scenarios. *Nature* **416**:626-629.
- Plummer, M. 2003. JAGS: A program for analysis of Bayesian graphical models using Gibbs sampling.
- Poole, A., Editor. 2005. The Birds of North America Online: <http://bna.birds.cornell.edu/BNA/>. Cornell Laboratory of Ornithology, Ithaca, NY.
- Potter, K. A., H. Arthur Woods, and S. Pincebourde. 2013a. Microclimatic challenges in global change biology. *Global Change Biology* **19**:2932-2939.
- Potter, K. A., H. A. Woods, and S. Pincebourde. 2013b. Microclimatic challenges in global change biology. *Global Change Biology* **19**:2932-2939.
- Pulliam, H. R. and B. J. Danielson. 1991. Sources, sinks, and habitat selection: A landscape perspective on population-dynamics. *The American Naturalist* **137**:S50-S66.
- R Development Core Team. 2011. R: A Language and Environment for Statistical Computing. R Foundation for Statistical Computing, Vienna, Austria.
- Ritchie, L. E., M. G. Betts, G. Forbes, and K. Vernes. 2009. Effects of landscape composition and configuration on northern flying squirrels in a forest mosaic. *Forest Ecology and Management* **257**:1920-1929.
- Rodenhouse, N. L., T. S. Sillett, P. J. Doran, and R. T. Holmes. 2003. Multiple density-dependence mechanisms regulate a migratory bird population during the breeding season. *Proceedings of the Royal Society B-Biological Sciences* **270**:2105-2110.
- Root, T. 1988. Environmental factors associated with avian distributional boundaries. *Journal of Biogeography* **15**:489-505.
- Rota, C. T., R. J. F. Jr, R. M. Dorazio, and M. G. Betts. 2009. Occupancy estimation and the closure assumption. *Journal of Applied Ecology* **46**:1173-1181.
- Sauer, J. R., J. E. Hines, J. E. Fallon, K. L. Pardieck, J. D. J. Ziolkowski, and W. A. Link. 2014. The North American Breeding Bird Survey, Results and Analysis 1966 - 2012. Version 02.19.2014. USGS Patuxent Wildlife Research Center, Laurel, MD.

- Sauer, J. R. and W. A. Link. 2011. Analysis of the North American Breeding Bird Survey Using Hierarchical Models. *Auk* **128**:87-98.
- Scheffers, B. R., R. M. Brunner, S. D. Ramirez, L. P. Shoo, A. Diesmos, and S. E. Williams. 2013. Thermal buffering of microhabitats is a critical factor mediating warming vulnerability of frogs in the Philippine biodiversity hotspot. *Biotropica* **45**:628-635.
- Scheffers, B. R., D. P. Edwards, A. Diesmos, S. E. Williams, and T. A. Evans. 2014. Microhabitats reduce animal's exposure to climate extremes. *Global Change Biology* **20**:495-503.
- Scherrer, D. and C. Körner. 2011. Topographically controlled thermal-habitat differentiation buffers alpine plant diversity against climate warming. *Journal of Biogeography* **38**:406-416.
- Scherrer, D., S. Schmid, and C. Korner. 2011. Elevational species shifts in a warmer climate are overestimated when based on weather station data. *International Journal of Biometeorology* **55**:645-654.
- Schwarz, P. A., T. J. Fahey, and C. E. McCulloch. 2003. Factors controlling spatial variation of tree species abundance in a forested landscape. *Ecology* **84**:1862-1878.
- Sears, M. W., E. Raskin, and M. J. Angilletta. 2011. The world is not flat: Defining relevant thermal landscapes in the context of climate change. *Integrative and Comparative Biology* **51**:666-675.
- Seavy, N. E., J. H. Viers, and J. K. Wood. 2009. Riparian bird response to vegetation structure: a multiscale analysis using LiDAR measurements of canopy height. *Ecological Applications* **19**:1848-1857.
- Sekercioglu, C. H., S. H. Schneider, J. P. Fay, and S. R. Loarie. 2008. Climate change, elevational range shifts, and bird extinctions. *Conservation Biology* **22**:140-150.
- Seo, C., J. H. Thorne, L. Hannah, and W. Thuiller. 2009. Scale effects in species distribution models: implications for conservation planning under climate change. *Biology Letters* **5**:39-43.
- Sheldon, K. S., S. Yang, and J. J. Tewksbury. 2011. Climate change and community disassembly: impacts of warming on tropical and temperate montane community structure. *Ecology Letters* **14**:1191-1200.
- Sibley, D. A. 2000. *The Sibley guide to birds*. Alfred A. Knopf, New York.
- Siccama, T. G., T. J. Fahey, C. E. Johnson, T. W. Sherry, E. G. Denny, E. B. Girdler, G. E. Likens, and P. A. Schwarz. 2007. Population and biomass dynamics of trees in a northern hardwood forest at Hubbard Brook. *Canadian Journal of Forest Research* **37**:737-749.
- Sol, D., L. Lefebvre, and J. D. Rodriguez-Teijeiro. 2005. Brain size, innovative propensity and migratory behaviour in temperate Palaearctic birds. *Proceedings of the Royal Society B: Biological Sciences* **272**:1433-1441.
- Stamps, J. A. 2006. The silver spoon effect and habitat selection by natal dispersers. *Ecology Letters* **9**:1179-1185.
- Storlie, C., A. Merino-Viteri, B. Phillips, J. VanDerWal, J. Welbergen, and S. Williams. 2014. Stepping inside the niche: microclimate data are critical for accurate assessment of species' vulnerability to climate change. *Biology Letters* **10**:20140576.

- Stralberg, D., D. Jongsomjit, C. A. Howell, M. A. Snyder, J. D. Alexander, J. A. Wiens, and T. L. Root. 2009. Re-shuffling of species with climate disruption: a no-analog future for California birds? *PLoS One* **4**:e6825.
- Suggitt, A. J., P. K. Gillingham, J. K. Hill, B. Huntley, W. E. Kunin, D. B. Roy, and C. D. Thomas. 2011. Habitat microclimates drive fine-scale variation in extreme temperatures. *Oikos* **120**:1-8.
- Suggitt, A. J., C. Stefanescu, F. Paramo, T. Oliver, B. J. Anderson, J. K. Hill, D. B. Roy, T. Brereton, and C. D. Thomas. 2012. Habitat associations of species show consistent but weak responses to climate. *Biology Letters* **8**:590-593.
- Sunday, J. M., A. E. Bates, M. R. Kearney, R. K. Colwell, N. K. Dulvy, J. T. Longino, and R. B. Huey. 2014. Thermal-safety margins and the necessity of thermoregulatory behavior across latitude and elevation. *Proceedings of the National Academy of Sciences* **111**:5610-5615.
- Switzer, P. V. 1997. Factors affecting site fidelity in a territorial animal, *Perithemis tenera*. *Animal Behaviour* **53**:865-877.
- Thomas, C. D. 2010. Climate, climate change and range boundaries. *Diversity and Distributions* **16**:488-495.
- Thomas, C. D., A. Cameron, R. E. Green, M. Bakkenes, L. J. Beaumont, Y. C. Collingham, B. F. N. Erasmus, M. F. de Siqueira, A. Grainger, L. Hannah, L. Hughes, B. Huntley, A. S. van Jaarsveld, G. F. Midgley, L. Miles, M. A. Ortega-Huerta, A. Townsend Peterson, O. L. Phillips, and S. E. Williams. 2004. Extinction risk from climate change. *Nature* **427**:145-148.
- Thompson, F. R. and R. M. DeGraaf. 2001. Conservation approaches for woody, early successional communities in the eastern United States. *Wildlife Society Bulletin* **29**:483-494.
- Thuiller, W., M. B. Araujo, and S. Lavorel. 2004a. Do we need land-cover data to model species distributions in Europe? *Journal of Biogeography* **31**:353-361.
- Thuiller, W., M. B. Araujo, R. G. Pearson, R. J. Whittaker, L. Brotons, and S. Lavorel. 2004b. Biodiversity conservation: Uncertainty in predictions of extinction risk. *Nature* **430**.
- Tingley, M. W. and S. R. Beissinger. 2009. Detecting range shifts from historical species occurrences: new perspectives on old data. *Trends in Ecology & Evolution* **24**:625-633.
- Tingley, M. W., M. S. Koo, C. Moritz, A. C. Rush, and S. R. Beissinger. 2012. The push and pull of climate change causes heterogeneous shifts in avian elevational ranges. *Global Change Biology* **18**:3279-3290.
- Townsend, A. K., T. S. Sillett, N. K. Lany, S. A. Kaiser, N. L. Rodenhouse, M. S. Webster, and R. T. Holmes. 2013. Warm springs, early lay dates, and double brooding in a North American migratory songbird, the black-throated blue warbler. *PloS One* **8**.
- Trani, M. K., R. T. Brooks, T. L. Schmidt, V. A. Rudis, and C. M. Gabbard. 2001. Patterns and trends of early successional forests in the Eastern United States. *Wildlife Society Bulletin* **29**:413-424.
- Travis, J. M. J. 2003. Climate change and habitat destruction: a deadly anthropogenic cocktail. *Proceedings of the Royal Society of London Series B-Biological Sciences* **270**:467-473.
- Tuomainen, U. and U. Candolin. 2011. Behavioural responses to human-induced environmental change. *Biological Reviews* **86**:640-657.

- Tyre, A. J., B. Tenhumberg, S. A. Field, D. Niejalke, K. Parris, and H. P. Possingham. 2003. ¹¹⁶
Improving precision and reducing bias in biological surveys: Estimating false-negative error rates. *Ecological Applications* **13**:1790-1801.
- Urban, D. L. 2005. Modeling ecological processes across scales. *Ecology* **86**:1996-2006.
- Vanwalleghe, T. and R. K. Meentemeyer. 2009. Predicting forest microclimate in heterogeneous landscapes. *Ecosystems* **12**:1158-1172.
- Vatka, E., M. Orell, and S. Rytkönen. 2011. Warming climate advances breeding and improves synchrony of food demand and food availability in a boreal passerine. *Global Change Biology* **17**:3002-3009.
- Vegas-Vilarrubia, T., S. Nogué, and V. Rull. 2012. Global warming, habitat shifts and potential refugia for biodiversity conservation in the neotropical Guayana Highlands. *Biological Conservation* **152**:159-168.
- Villard, M. A. and B. A. Maurer. 1996. Geostatistics as a tool for examining hypothesized declines in migratory songbirds. *Ecology* **77**:59-68.
- Virkkala, R., R. K. Heikkinen, A. Lehtikainen, and J. Valkama. 2014. Matching trends between recent distributional changes of northern-boreal birds and species-climate model predictions. *Biological Conservation* **172**:124-127.
- Virkkala, R., R. K. Heikkinen, N. Leikola, and M. Luoto. 2008. Projected large-scale range reductions of northern-boreal land bird species due to climate change. *Biological Conservation* **141**:1343-1353.
- von Arx, G., E. Graf Pannatier, A. Thimonier, and M. Rebetez. 2013. Microclimate in forests with varying leaf area index and soil moisture: potential implications for seedling establishment in a changing climate. *Journal of Ecology* **101**:1201-1213.
- Watershed Sciences. 2008. LiDAR Remote Sensing Data Collection: HJ Andrews & Willamette National Forest. Corvallis, OR.
- Whittaker, K. A. and J. M. Marzluff. 2009. Species-specific survival and relative habitat use in an urban landscape during the postfledging period. *Auk* **126**:288-299.
- Wiens, J. A. 1989. Spatial scaling in ecology. *Functional Ecology* **3**:385-397.
- Wiens, J. A. and D. Bachelet. 2010. Matching the multiple scales of conservation with the multiple scales of climate change. *Conservation Biology* **24**:51-62.
- Xu, M., Y. Qi, J. Chen, and B. Song. 2004. Scale-dependent relationships between landscape structure and microclimate. *Plant Ecology* **173**:39-57.
- Yao, X., B. Fu, Y. Lü, F. Sun, S. Wang, and M. Liu. 2013. Comparison of four spatial interpolation methods for estimating soil moisture in a complex terrain catchment. *PLoS One* **8**:e54660.
- Yu, H., E. Luedeling, and J. Xu. 2010. Winter and spring warming result in delayed spring phenology on the Tibetan Plateau. *Proceedings of the National Academy of Sciences* **107**:22151-22156.

APPENDICES

APPENDIX 2.1. Details concerning deployment and maintenance of temperature sensors.

All HOBOs were placed 1.5m from the ground. We used a flexible fiberglass post to support the logger and to allow for bending of the entire unit under the weight of snow. For a sun shield, we used half of a 3-inch diameter schedule 40 PVC pipe, cut to 6-in in length (Fig. S1). We oriented the entire setup to face south using a compass. We set them to record temperature every 20 minutes. We offloaded data from the units twice a year (May and July) and changed the batteries once a year based on sampling frequency (generally on the second offload session of each year).



Figure S1. Photo of HOBO temperature sensor in the field. Loggers were 1.5m off ground and shaded with a white PVC hood.

APPENDIX 2.2. Details about temperature data processing (cleaning, flagging, pruning, and filling).

We first compiled offloaded files into a continuous time series by site. We used a Python script (<http://www.python.org>) to flag, clean, average, and fill datasets. Flagging identified several problems including no data, incorrect logging intervals, extreme values, jumps in values, and periods when the logger was under snow. Data for which the logger had recorded date and time but no temperature were flagged as no data. Incorrect logging intervals were not separated by the programmed interval of 15 or 20 minutes, associated with missing values. Values outside of the sensor range (-20° to 70°C) were flagged as extreme. Jumps in values were defined as a change in temperature of more than 5°C in one time interval and appeared to be related to infrequent faulty readings. Our method for flagging snow used a forward rolling window. If the variation in temperatures within a 24-hr period was less than 0.5°C and the temperatures were below 1°C , we considered that time period to indicate snow. To account for the forward rolling window, we also flagged periods in which snow was present in the past 24-hrs.

After flagging, we pruned all flagged lines with the exception of incorrect logging intervals. We used these cleaned files and averaged the data hourly, noting the number of readings which contributed to each hourly value. We saved each cleaned hourly value to use for filling. Each cleaned file was regressed using a linear regression (NumPy) against each other file. We then preferentially filled each file using cleaned (unfilled) data and the corresponding regressions from other sites based on their fit. Thus, a site with an R^2 of 0.99 was used before a site with an R^2 of 0.98. Predicted values were calculated using the regression equation and included in the filled dataset along with the corresponding regression and fit for quality control. This filling continued until all of the programmed date range was filled or until further filling was no longer possible.

APPENDIX 2.3. Predictor variables used to predict patterns in microclimate metrics. Variables were put into categories: elevation (ELV), microtopography (TOPO), and vegetation structure (VEG). All of the vegetation variables were derived from LiDAR data collected at the HJAEF in 2008 during the leaf-on period (Watershed Services 2008).

Variable name	Category	Description
Mean elevation	ELV	Mean elevation (m), bare Earth LiDAR
SD elevation	TOPO	Standard deviation of elevation (m), bare Earth LiDAR
Mean slope	TOPO	Mean slope (%), bare Earth LiDAR
Mean eastness	TOPO	Mean $\sin(\text{aspect} * \pi/180)$, values between 1 and -1
Mean northness	TOPO	Mean $\cos(\text{aspect} * \pi/180)$, values between 1 and -1
SD slope	TOPO	Standard deviation of slope (%), bare Earth LiDAR
Topo index	TOPO	Topo index is calculated by subtracting the mean elevation within a radius around the point from the elevation value at the sample point itself. Negative values are on local low spots, positive values are on local high spots (following Daly 2010).
Elevation range	TOPO	Range in elevation (maximum - minimum), bare Earth LiDAR
Mean canopy height	VEG	Mean LiDAR vegetation height (m)
Mean biomass	VEG	Mean biomass, derived from LiDAR vegetation dataset
Mean cover 0-2m	VEG	Mean canopy point density of points 0-2m off the ground (all vegetation LiDAR returns)
Mean cover 2-10m	VEG	Mean canopy point density of points 2-10m off the ground (all vegetation LiDAR returns)
Mean cover >10m	VEG	Mean canopy point density of points >10m off the ground (all vegetation LiDAR returns)
Mean coef of variation	VEG	Mean height metric from first returns only, coefficient of variation exclude points below 1 meter, vegetation LiDAR
Mean HOME	VEG	Mean height of median energy (HOME, m), HOME is the height at which 50% of energy returned
Mean VDR	VEG	Mean vertical distribution ratio (VDR, unit-less), Calculated as $(\text{canopy height} - \text{HOME})/\text{canopy height}$. VDR can be defined as “a normalized ratio between the canopy height and HOME products, which provided an index of the vertical distribution of intercepted canopy elements (Goetz et al. 2010).
SD canopy height	VEG	Standard deviation of canopy height (m), vegetation LiDAR
SD biomass	VEG	Standard deviation of biomass (Mg/ha), derived from LiDAR vegetation dataset
SD cover 0-2m	VEG	Standard deviation of canopy point density of points 0-2m off the ground (all vegetation LiDAR returns)
SD cover 2-10m	VEG	Standard deviation of canopy point density of points 2-10m off the ground (all vegetation LiDAR returns)
SD cover >10m	VEG	Standard deviation of canopy point density of points >10m off the ground (all vegetation LiDAR returns)

APPENDIX 2.4. BRT model settings (Learning rate, No. trees), performance diagnostics (Deviance, Deviance SE, CV corr, CV SE), and tests for spatial autocorrelation in the BRT model residuals (Moran's I and P). In order to reach 1000 trees for some models, we were required to reduce the learning rate below 0.01 (the suggested starting value for this parameter). The 'Units' and 'Transf' columns indicate the temperature metric units and any transformation done before modeling. SE = standard error, No. = number, CV = cross-validation, corr = correlation.

Temperature metric	Units	Transf	Deviance	Deviance SE	Learning rate	No. trees	CV corr	CV SE	Moran's <i>I</i>	<i>P</i>
2012										
CDD >0°C Jan-Mar	dd	dd/100	0.12474	0.02264	0.005	1500	0.694	0.062	-0.026	0.200
CDD >0°C Apr-Jun	dd	dd/100	0.14674	0.01593	0.01	1100	0.957	0.006	-0.014	0.175
CDD >10°C Apr-Jun	dd	dd/100	0.02971	0.00443	0.008	1300	0.898	0.016	-0.012	0.180
SD wkly T Jan-Mar	°C	NA	0.04922	0.01283	0.006	1700	0.835	0.028	-0.007	0.268
SD wkly T Apr-Jun	°C	NA	0.50022	0.06532	0.01	2200	0.807	0.026	-0.004	0.271
MEAN mo mn Apr-Jun	°C	NA	0.18916	0.02287	0.008	1350	0.952	0.008	-0.015	0.176
MAX mo mn Apr-Jun	°C	NA	0.93530	0.18974	0.006	1250	0.870	0.029	-0.006	0.267
MIN mo mn Apr-Jun	°C	NA	0.14526	0.01026	0.01	1800	0.941	0.008	-0.009	0.136
MAX T warmest mo	°C	°C/100	0.00022	0.00006	0.004	1600	0.754	0.037	-0.008	0.283
MIN T coldest mo	°C	NA	0.05045	0.00822	0.006	1350	0.978	0.004	0.003	0.146
2013										
CDD >0°C Jan-Mar	dd	dd/100	0.18154	0.01591	0.008	1050	0.690	0.056	-0.022	0.144
CDD >0°C Apr-Jun	dd	dd/100	0.12225	0.01517	0.01	1550	0.961	0.008	-0.010	0.191
CDD >10°C Apr-Jun	dd	dd/100	0.03614	0.00459	0.01	1700	0.915	0.012	-0.007	0.210
SD wkly T Jan-Mar	°C	NA	0.06759	0.00839	0.005	1100	0.783	0.033	-0.015	0.169
SD wkly T Apr-Jun	°C	NA	0.01020	0.00114	0.01	1250	0.932	0.009	-0.006	0.247
MEAN mo mn Apr-Jun	°C	NA	0.14378	0.01511	0.01	1650	0.964	0.004	-0.008	0.201
MAX mo mn Apr-Jun	°C	NA	1.14407	0.22446	0.004	1050	0.838	0.034	-0.007	0.250
MIN mo mn Apr-Jun	°C	NA	0.16573	0.01890	0.01	1650	0.904	0.030	-0.008	0.137

APPENDIX 2.5. Results from a PCA of all vegetation structure predictor variables and box plots comparing on the ground basal area measurements to forest type (plantation vs. old-growth/mature forest) categorizations.

Principal components importance (1st 8 out of 11):

	PC1	PC2	PC3	PC4	PC5	PC6	PC7	PC8
Standard deviation	2.218	1.818	1.020	0.883	0.756	0.392	0.367	0.221
Proportion of Variance	0.447	0.300	0.095	0.071	0.052	0.014	0.012	0.004
Cumulative Proportion	0.447	0.747	0.842	0.913	0.965	0.979	0.991	0.996

Contributions of vegetation variables for 1st 8 components:

	PC1	PC2	PC3	PC4	PC5	PC6	PC7	PC8
Mn biomass	0.407	-0.190	0.076	-0.141	0.115	-0.111	-0.371	0.296
SD biomass	0.328	-0.341	0.060	0.003	0.074	-0.612	0.342	-0.167
Mn can ht	0.444	0.023	0.067	-0.045	0.012	0.195	-0.239	0.165
SD can ht	0.320	-0.372	-0.014	-0.068	-0.130	-0.055	0.222	-0.223
Mn cover >10m	0.357	0.263	0.072	0.141	-0.261	0.355	0.666	0.287
SD cover >10m	-0.110	-0.385	-0.066	0.229	-0.834	0.035	-0.232	0.058
Mn cover 2-10m	-0.115	-0.200	0.649	0.653	0.232	0.009	-0.024	0.174
SD cover 2-10m	0.144	-0.094	-0.713	0.619	0.264	0.073	-0.036	-0.020
HOME	0.440	0.080	0.055	-0.015	0.005	0.163	-0.323	0.054
CV can ht	-0.033	-0.511	0.078	-0.169	0.224	0.642	0.077	-0.383
VDR	-0.241	-0.418	-0.195	-0.250	0.164	0.026	0.175	0.736

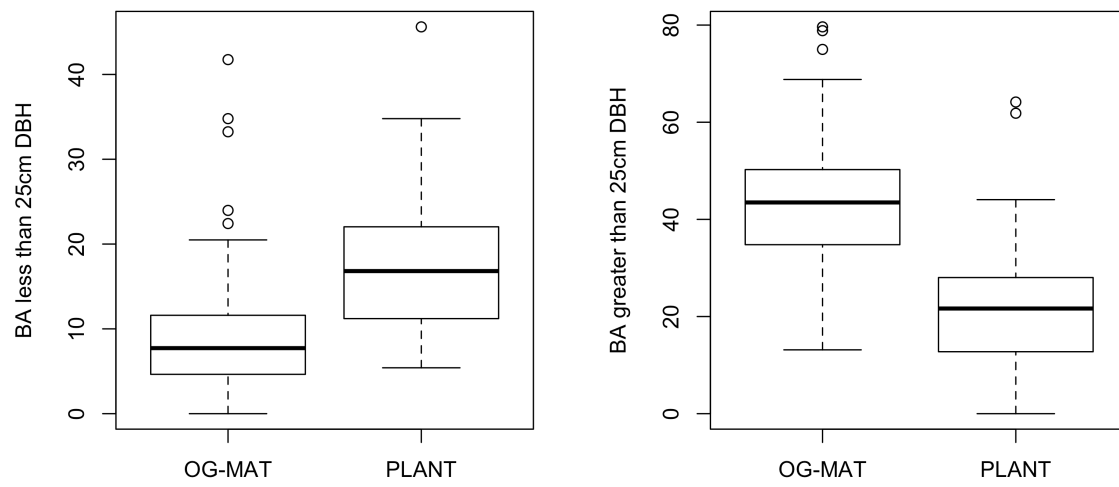
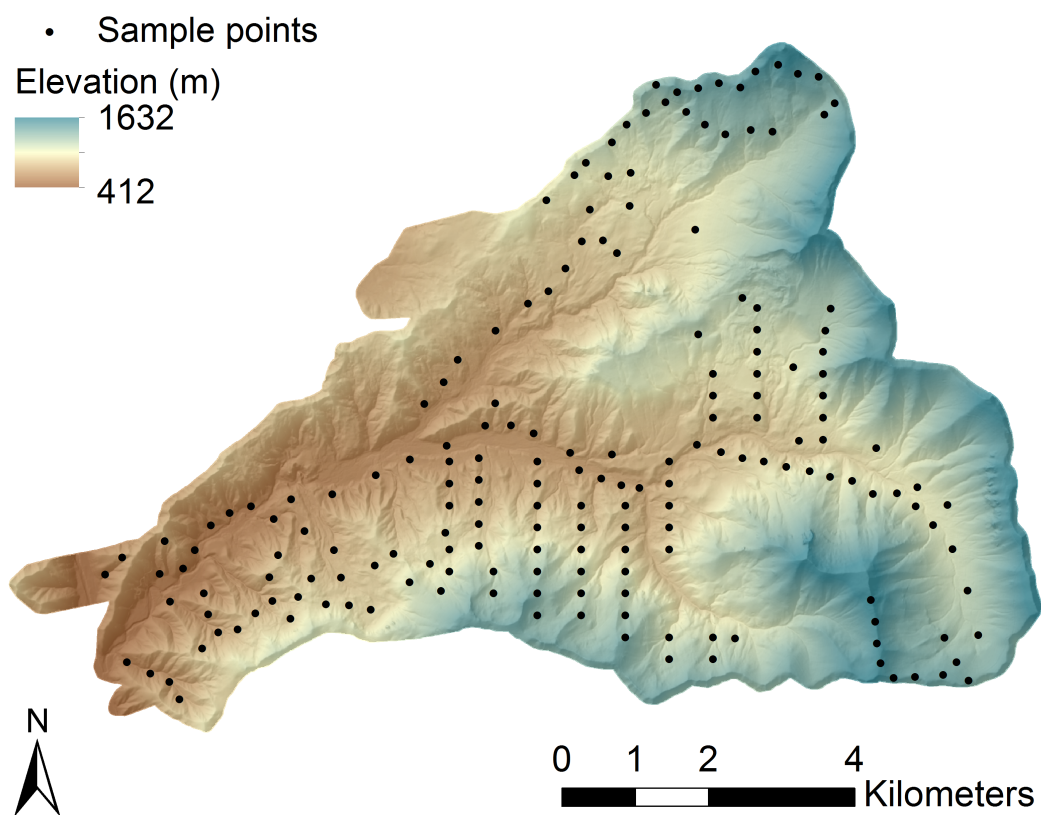


Figure S2. Box plots comparing on-the-ground basal area measurements to forest type (plantation vs. old-growth/mature forest) categorizations.



APPENDIX 3.1. Map of the H. J. Andrews Experimental Forest, Blue River, Oregon with the 183 sample locations. Sample points are for both bird and temperature data. The elevation gradient is in meters. Hillshading shows the underlying topography of the study area.

APPENDIX 3.2. Pearson's correlation coefficients between all predictor variables.

	CDD >0 J-M	CDD >10 A-J	Max T A-J	Min T A-J	Mean T A-J	Veg str (PC1)	Veg str (PC 2)	Veg comp (decid BA)
CDD >0 J-M	1	0.79	0.57	0.70	0.70	0.15	0.19	-0.01
CDD >10 A-J		1	0.90	0.87	0.96	0.14	0.21	0.15
Max T A-J			1	0.70	0.89	0.01	0.16	0.31
Min T A-J				1	0.94	0.43	0.20	0.08
Mean T A-J					1	0.26	0.21	0.20
Veg str (PC1)						1	0.00	-0.29
Veg str (PC 2)							1	0.19
Veg comp (decid BA)								1

APPENDIX 3.3. Constant rates for all parameters.

Species	Detection		Occupancy		Colonization		Extinction	
	Est	SE	Est	SE	Est	SE	Est	SE
2012								
BRCR	0.587	0.028	0.261	0.058	0.202	0.031	0.608	0.074
CBCH	0.622	0.014	0.654	0.048	0.497	0.039	0.338	0.033
GCKI	0.675	0.018	0.292	0.043	0.284	0.026	0.511	0.042
HAFL	0.665	0.026	0.352	0.050	0.057	0.016	0.259	0.061
HETH	0.752	0.022	0.206	0.077	0.216	0.032	0.576	0.070
HEWA	0.782	0.010	0.703	0.042	0.364	0.032	0.264	0.026
ORJU	0.671	0.019	0.603	0.155	0.001	0.008	0.032	0.019
PAWR	0.836	0.009	0.558	0.038	0.316	0.025	0.278	0.031
PSFL	0.742	0.013	0.398	0.041	0.309	0.028	0.346	0.032
RBNU	0.482	0.023	0.577	0.066	0.119	0.034	0.094	0.038
STJA	0.438	0.027	0.428	0.072	0.260	0.038	0.717	0.064
SWTH	0.737	0.018	0.116	0.052	0.277	0.029	0.419	0.056
VATH	0.676	0.021	0.296	0.053	0.249	0.031	0.589	0.063
WETA	0.555	0.036	0.259	0.063	0.112	0.024	0.507	0.108
WIWA	0.628	0.032	0.225	0.045	0.037	0.011	0.241	0.073
2013								
BRCR	0.588	0.025	0.302	0.056	0.211	0.029	0.495	0.077
CBCH	0.607	0.016	0.472	0.051	0.340	0.032	0.353	0.047
GCKI	0.716	0.016	0.407	0.052	0.223	0.023	0.410	0.040
HAFL	0.768	0.018	0.406	0.069	0.096	0.019	0.265	0.061
HETH	0.725	0.020	0.143	0.028	0.150	0.015	0.587	0.070
HEWA	0.799	0.009	0.776	0.037	0.449	0.036	0.293	0.021
ORJU	0.664	0.018	0.301	0.058	0.227	0.028	0.351	0.093
PAWR	0.809	0.011	0.511	0.041	0.250	0.022	0.288	0.026
PSFL	0.740	0.012	0.477	0.045	0.380	0.032	0.261	0.031
RBNU	0.686	0.013	0.738	0.055	0.391	0.067	0.204	0.038
STJA	0.462	0.025	0.731	0.129	0.002	0.021	0.058	0.026
SWTH	0.737	0.017	0.064	0.022	0.241	0.020	0.449	0.043
VATH	0.704	0.021	0.265	0.043	0.204	0.022	0.731	0.046
WETA	0.629	0.034	0.085	0.026	0.125	0.022	0.830	0.056
WIWA	0.748	0.026	0.174	0.045	0.054	0.015	0.156	0.063

APPENDIX 3.4. Coefficients and standard errors for detection probability (p) by species and year for top models. ** = significant at $P \leq 0.05$, * = significant at $P \leq 0.1$. See Appendix 8 for all model selection tables.

Species	Intercept		Vegetation						Temperature									
			Veg structure 1		Veg structure 2		Veg composition		CDD >0 Jan-Mar		CDD >10 Apr-Jun		MAX Apr-Jun		MIN Apr-Jun		MEAN Apr-Jun	
	Est	SE	Est	SE	Est	SE	Est	SE	Est	SE	Est	SE	Est	SE	Est	SE	Est	SE
2012																		
BRCR	-0.696	0.269	0.242	0.213			-0.224	0.205										
CBCH	-0.102	0.104															0.173	0.068 **
GCKI	0.163	0.149					-0.164	0.096 *			-0.388	0.111 **						
HAFL	-0.720	0.297			0.418	0.110 **	-0.070	0.100									0.377	0.128 **
HETH	-1.283	0.326											-0.594	0.153 **				
HEWA	0.560	0.160							0.284	0.074 **								
ORJU	-0.961	0.172	-0.298	0.095 **											0.068	0.105		
PAWR	1.085	0.130																
PSFL	0.377	0.131	0.474	0.110 **			0.391	0.102 **							0.035	0.111		
RBNU	-1.780	0.188	-0.088	0.108 **			-0.267	0.141 *									-0.317	0.129 **
STJA	-0.743	0.333	-0.120	0.115														
SWTH	-0.946	0.188			-0.011	0.103			-0.346	0.097 **								
VATH	-0.328	0.217	0.225	0.110 **							-0.318	0.144 **						
WETA	-0.960	0.285	-0.238	0.148	0.437	0.175 **			0.429	0.206 **								
WIWA	0.246	0.252															0.439	0.222 **
2013																		
BRCR	-0.709	0.241	0.409	0.155 **			0.060	0.252							0.377	0.147 **		
CBCH	-0.567	0.179					-0.270	0.099 **									0.210	0.088 **
GCKI	-0.140	0.198									-0.318	0.106 **						
HAFL	-0.766	0.291											0.441	0.133 **				
HETH	0.861	0.213													-0.156	0.098 *		
HEWA	0.795	0.099					-0.114	0.071 *									-0.084	0.069
ORJU	-0.257	0.172											-0.146	0.086 *				
PAWR	0.721	0.180			-0.176	0.075 **												
PSFL	0.212	0.155	0.130	0.079 *											0.249	0.093 **		
RBNU	-0.558	0.109	0.032	0.073											-0.235	0.071 **		
STJA	-1.424	0.183	-0.094	0.086									0.148	0.087 *				
SWTH	0.042	0.268	-0.306	0.107 **														
VATH	-0.181	0.215					-0.347	0.130 **					-0.140	0.121				
WETA	-0.925	0.398			0.223	0.153			0.582	0.144 **								
WIWA	-1.343	0.230	-0.347	0.140 **									-0.839	0.175 **				

Species	Intercept		Temporal autocov		Survey Time		Day of Year		Weather		Wind		Stream noise		Observer 2		Observer 3		Observer 4		Observer 5		Observer 6	
	Est	SE	Est	SE	Est	SE	Est	SE	Est	SE	Est	SE	Est	SE	Est	SE	Est	SE	Est	SE	Est	SE	Est	SE
2012																								
BRCR	-0.696	0.269	1.120	0.286 **	-0.372	0.129 **							-0.358	0.122 **										
CBCH	-0.102	0.104	0.859	0.132 **					-0.116	0.059 **	-0.189	0.070 **	-0.256	0.064 **										
GCKI	0.163	0.149	0.667	0.179 **																				
HAFL	-0.720	0.297	1.454	0.291 **			-0.538	0.125 **					0.218	0.127 *	-0.376	0.699	-0.450	0.282 *	-1.408	0.292 **	1.016	1.279	0.048	0.324
HETH	-1.283	0.326	1.828	0.364 **	-0.025	0.118	0.676	0.149 **					-1.001	0.168 **										
HEWA	0.560	0.160	1.152	0.149 **					-0.161	0.075 **			-0.589	0.081 **	0.987	0.535 *	-0.709	0.182 **	-0.018	0.186	0.797	0.814	-0.129	0.185
ORJU	-0.961	0.172	1.664	0.202 **			0.985	0.091 **																
PAWR	1.085	0.130	0.746	0.165 **	-0.398	0.074 **	0.161	0.074 **	-0.332	0.087 **														
PSFL	0.377	0.131	0.750	0.157 **					-0.399	0.081 **														
RBNU	-1.780	0.188	1.099	0.198 **			-0.448	0.088 **	-0.312	0.082 **			-1.081	0.140 **										
STJA	-0.743	0.333	0.683	0.271 **											0.921	0.442 **	-0.798	0.287 **	-0.567	0.273 **	-0.014	0.567	0.423	0.287
SWTH	-0.946	0.188	1.435	0.219 **	-0.564	0.091 **	0.946	0.148 **	-0.394	0.117 **														
VATH	-0.328	0.217	0.928	0.237 **	-0.628	0.107 **																		
WETA	-0.960	0.285	0.540	0.319 *	-0.336	0.139 **							-0.507	0.185 **										
WIWA	0.246	0.252	0.741	0.292 **									-0.239	0.159										
2013																								
BRCR	-0.709	0.241	1.155	0.255 **													0.319	0.186 *	0.405	0.188 **	0.453	0.198 **		
CBCH	-0.567	0.179	0.900	0.163 **	-0.363	0.064 **											0.714	0.252 **	0.944	0.236 **	0.659	0.228 **		
GCKI	-0.140	0.198	0.563	0.171 **			-0.250	0.084 **			0.172	0.087 **					0.714	0.252 **	0.944	0.236 **	0.659	0.228 **		
HAFL	-0.766	0.291	1.534	0.296 **			-0.329	0.133 **					0.147	0.117			1.177	0.302 **	0.765	0.351 **	0.301	0.288		
HETH	0.861	0.213	0.625	0.236 **											-0.611	0.266 **	-0.626	0.289 **	-0.123	0.433				
HEWA	0.795	0.099	0.778	0.129 **							0.103	0.065	-0.508	0.074 **										
ORJU	-0.257	0.172	1.106	0.202 **	-0.237	0.080 **	0.482	0.094 **																
PAWR	0.721	0.180	0.909	0.160 **	-0.313	0.075 **	0.297	0.085 **	-0.045	0.078					0.260	0.213	-0.196	0.225	0.474	0.225 **				
PSFL	0.212	0.155	0.813	0.140 **			-0.086	0.070							0.612	0.179 **	0.096	0.192	0.286	0.188				
RBNU	-0.558	0.109	1.204	0.140 **											-0.998	0.083 **								
STJA	-1.424	0.183	2.026	0.202 **	-0.160	0.071 **							-0.178	0.084 **	-0.236	0.165	-1.401	0.213 **	-0.900	0.192 **				
SWTH	0.042	0.268	0.906	0.248 **			0.530	0.167 **																
VATH	-0.181	0.215	1.122	0.253 **	-0.409	0.118 **							-0.366	0.122 **										
WETA	-0.925	0.398	1.614	0.451 **																				
WIWA	-1.343	0.230	2.497	0.296 **	-0.030	0.113																		

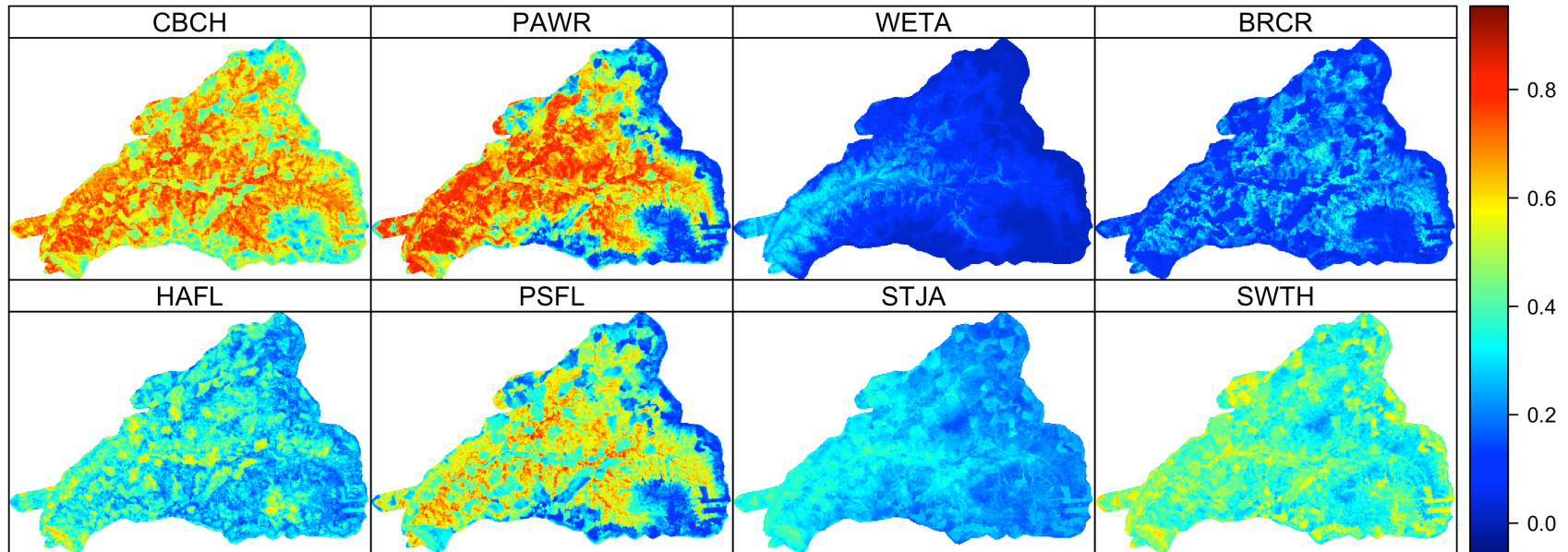
APPENDIX 3.5. Coefficients and standard errors for initial occupancy. Coefficients and standard errors for initial occupancy (ψ) by species and year for top models. ** = significant at $P \leq 0.05$, * = significant at $P \leq 0.1$. See Appendix 8 for all model selection tables.

Species	Intercept		Vegetation						Temperature											
			Veg structure 1		Veg structure 2		Veg composition		CDD >0 Jan-Mar		CDD >10 Apr-Jun		MAX Apr-Jun		MIN Apr-Jun		MEAN Apr-Jun			
	Est	SE	Est	SE	Est	SE	Est	SE	Est	SE	Est	SE	Est	SE	Est	SE	Est	SE		
2012																				
BRCR	-2.148	0.469					-1.708	0.823	**							0.603	0.300	**		
CBCH	0.585	0.211	0.298	0.219												0.409	0.213	**		
GCKI	-1.336	0.219	-0.242	0.193									-0.795	0.219	**					
HAFL	-0.784	0.240			0.425	0.205	**	0.463	0.257	*			0.179	0.222						
HETH	-1.113	0.554					0.467	0.457		0.624	0.436									
HEWA	0.841	0.203	-0.166	0.203													-0.583	0.210	**	
ORJU	2.198	2.525	-1.211	1.104												-3.246	2.636			
PAWR	0.229	0.171	0.240	0.186												0.814	0.199	**		
PSFL	-0.730	0.190	0.158	0.219	-0.627	0.189	**	-0.272	0.238							0.875	0.238	**		
RBNU	-0.127	0.266			-0.557	0.248	**	-0.566	0.337	*								-0.675	0.257	**
STJA	-0.330	0.331	-0.493	0.287	*					0.520	0.317	*								
SWTH	-2.424	0.643					0.134	0.329		-0.926	0.533	*								
VATH	-1.361	0.252	-0.195	0.251												-0.662	0.264	**		
WETA	-1.696	0.318	-0.291	0.292								0.550	0.273	**						
WIWA	-1.734	0.238	-0.448	0.228	**									-0.356	0.223					
2013																				
BRCR	-1.590	0.395			-0.404	0.259		-1.431	0.695	**			-0.576	0.317	*					
CBCH	-0.253	0.200			-0.384	0.193	**	-0.270	0.230								0.372	0.204	*	
GCKI	-1.006	0.210			-0.224	0.208											-1.459	0.242	**	
HAFL	-1.582	0.264			0.083	0.214		0.643	0.223	**							1.054	0.272	**	
HETH	-1.868	0.236					-0.384	0.320		0.156	0.224									
HEWA	1.167	0.204			-0.114	0.193											-0.440	0.213	**	
ORJU	-0.979	0.285	-0.378	0.265												-0.376	0.248			
PAWR	0.037	0.180	0.550	0.195	**											0.379	0.193	**		
PSFL	-0.489	0.186	0.395	0.199	**	-0.375	0.173	**								0.981	0.237	**		
RBNU	0.947	0.271			-0.504	0.258	**			0.302	0.258									
STJA	1.203	0.593					-0.284	0.258									0.656	0.384	*	
SWTH	-2.759	0.412			0.292	0.355		0.248	0.267											
VATH	-1.220	0.234			0.013	0.221				-0.725	0.223	**								
WETA	-3.394	0.709					1.344	0.508	**				1.251	0.617	**					
WIWA	-2.083	0.377			-0.288	0.300				-0.954	0.339	**								

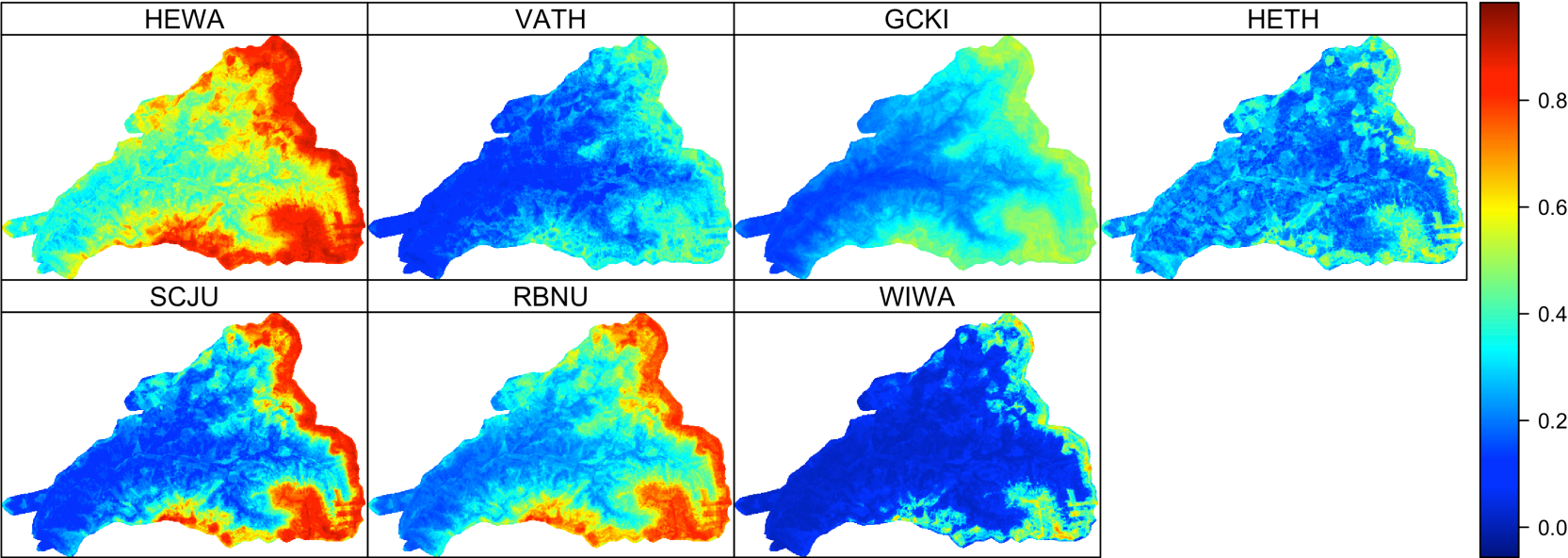
APPENDIX 3.6. Comparison of effect sizes between fine-scale temperature and vegetation for settlement and vacancy probability in the top models by species and year. See Table 3.1 for species codes.

Species	2012							
	Settlement				Vacancy			
	Veg Est/SE	Temp Est/SE	Abs diff	Larger effect	Veg Est/SE	Temp Est/SE	Abs diff	Larger effect
BRCR	3.975	0.000	3.975	Veg	1.409	0.000	1.409	Veg
CBCH	-3.013	2.131	0.882	Veg	-1.860	-1.697	0.162	Veg
GCKI	-1.184	-4.974	-3.790	Temp	0.657	2.038	-1.381	Temp
HAFL	2.107	-1.262	0.845	Veg	-1.728	-2.361	-0.633	Temp
HETH	-2.615	0.888	1.727	Veg	0.414	2.396	-1.982	Temp
HEWA	-1.147	-3.400	-2.252	Temp	1.321	2.575	-1.254	Temp
ORJU	-2.384	-2.862	-0.478	Temp	0.893	4.739	-3.846	Temp
PAWR	4.647	3.673	0.974	Veg	-2.249	-4.394	-2.145	Temp
PSFL	4.387	2.068	2.319	Veg	2.241	-1.264	0.977	Veg
RBNU	0.000	-1.160	-1.160	Temp	0.000	1.493	-1.493	Temp
STJA	-1.668	2.234	-0.566	Temp	-1.114	-0.908	0.206	Veg
SWTH	-1.942	1.807	0.134	Veg	1.074	0.000	1.074	Veg
VATH	-2.561	-4.025	-1.464	Temp	-0.144	2.615	-2.471	Temp
WETA	2.891	4.421	-1.530	Temp	1.684	-0.770	0.914	Veg
WIWA	-2.773	-2.248	0.524	Veg	0.938	3.488	-2.551	Temp
Species	2013							
	Settlement				Vacancy			
	Veg Est/SE	Temp Est/SE	Abs diff	Larger effect	Veg Est/SE	Temp Est/SE	Abs diff	Larger effect
BRCR	2.579	-1.562	1.017	Veg	1.686	-1.503	0.183	Veg
CBCH	-2.826	1.718	1.108	Veg	-2.181	-1.730	0.451	Veg
GCKI	-1.041	-6.792	-5.751	Temp	1.892	3.265	-1.374	Temp
HAFL	2.907	1.113	1.794	Veg	-2.068	-1.383	0.685	Veg
HETH	-3.933	-2.769	1.165	Veg	1.857	0.777	1.080	Veg
HEWA	-2.509	-3.921	-1.413	Temp	-0.585	3.996	-3.411	Temp
ORJU	-3.532	-3.601	-0.069	Temp	0.088	1.649	-1.560	Temp
PAWR	4.132	3.842	0.290	Veg	3.242	-3.282	-0.040	Temp
PSFL	3.452	3.459	-0.006	Temp	-2.273	-2.394	-0.121	Temp
RBNU	-2.025	-2.222	-0.197	Temp	1.071	1.581	-0.511	Temp
STJA	0.000	1.442	-1.442	Temp	0.000	1.275	-1.275	Temp
SWTH	1.780	3.413	-1.633	Temp	-2.203	-0.770	1.433	Veg
VATH	-1.713	-3.473	-1.759	Temp	-1.283	1.779	-0.495	Temp
WETA	-3.902	1.394	2.509	Veg	0.000	0.722	-0.722	Temp
WIWA	-2.490	-1.628	0.863	Veg	-1.973	-1.548	0.425	Veg

APPENDIX 3.7. Predicted occupancy probability as a function of temperature and vegetation in the final sampling session of 2012 (session 6; late June to mid-July) for the warm-associated species. See Table 3.1 for species codes.



APPENDIX 3.8. Predicted occupancy probability as a function of temperature and vegetation in the final sampling session of 2012 (session 6; late June to mid-July) for the cool-associated species. See Table 3.1 for species codes.



APPENDIX 3.9. Goodness-of-fit bootstrap results for top models of all species in 2012 and 2013.

Species	Obs	Mn BS	SD BS	Mn Obs - BS	Mn Obs - BS	P	No. sim
2012							
BRCR	3178.86	3224.03	214.97	-45.17	214.97	0.54	250
CBCH	3140.72	3293.23	22.84	-152.50	22.84	1.00	250
GCKI	3149.57	3289.50	66.60	-139.93	66.60	0.98	250
HAFL	3145.32	3303.28	257.10	-157.96	257.10	0.70	250
HETH	2929.98	3306.93	300.91	-376.94	300.91	0.94	250
HEWA	2851.23	3297.28	36.53	-446.05	36.53	1.00	250
ORJU	3160.45	3238.05	123.96	-77.60	123.96	0.78	250
PAWR	2853.67	3291.20	59.92	-437.53	59.92	1.00	250
PSFL	3085.99	3289.16	84.78	-203.18	84.78	0.99	250
RBNU	2863.99	3299.70	502.15	-435.71	502.15	0.96	250
STJA	3313.38	3296.52	50.86	16.86	50.86	0.33	250
SWTH	2753.01	3241.17	297.53	-488.16	297.53	0.99	250
VATH	3039.51	3284.69	95.67	-245.18	95.67	1.00	250
WETA	3006.59	3259.89	538.26	-253.30	538.26	0.67	250
WIWA	3025.45	3290.73	177.33	-265.28	177.33	0.94	250
2013							
BRCR	2960.58	3239.94	212.65	-279.36	212.65	0.97	250
CBCH	3176.44	3292.38	45.24	-115.94	45.24	0.98	250
GCKI	3160.40	3291.25	98.24	-130.84	98.24	0.93	250
HAFL	3146.81	3279.96	158.35	-133.15	158.35	0.78	250
HETH	3383.27	3283.91	79.92	99.36	79.92	0.10	250
HEWA	3017.91	3291.32	35.90	-273.40	35.90	1.00	250
ORJU	3180.79	3294.59	69.57	-113.80	69.57	0.94	250
PAWR	3040.74	3295.62	94.70	-254.88	94.70	1.00	250
PSFL	3083.74	3298.29	95.66	-214.55	95.66	1.00	250
RBNU	2871.31	3279.62	105.40	-408.30	105.40	1.00	250
STJA	3212.45	3307.01	143.46	-94.56	143.46	0.82	250
SWTH	2993.44	3260.54	120.80	-267.10	120.80	0.97	250
VATH	3041.48	3293.75	86.44	-252.26	86.44	1.00	250
WETA	2927.75	3227.14	397.19	-299.39	397.19	0.84	250
WIWA	2985.06	3260.00	395.22	-274.94	395.22	0.79	250

APPENDIX 3.10. Results from tests for spatial autocorrelation in the residuals from the top models for all species in 2012 and 2013.

Species	2012		2013	
	Moran's I	P	Moran's I	P
BRCR	0.003	0.244	0.010	0.203
CBCH	0.016	0.233	0.007	0.206
GCKI	0.003	0.275	-0.003	0.240
HAFL	0.002	0.251	0.001	0.328
HETH	-0.013	0.225	0.007	0.229
HEWA	-0.022	0.139	-0.009	0.244
ORJU	-0.004	0.304	-0.007	0.251
PAWR	0.002	0.264	0.007	0.215
PSFL	0.001	0.291	0.002	0.244
RBNU	-0.001	0.200	0.005	0.189
STJA	0.030	0.206	0.002	0.236
SWTH	-0.026	0.193	0.003	0.246
VATH	0.002	0.176	-0.017	0.234
WETA	-0.012	0.186	0.000	0.243
WIWA	-0.009	0.262	0.002	0.239

APPENDIX 3.11. Google docs site for AIC model selection tables.

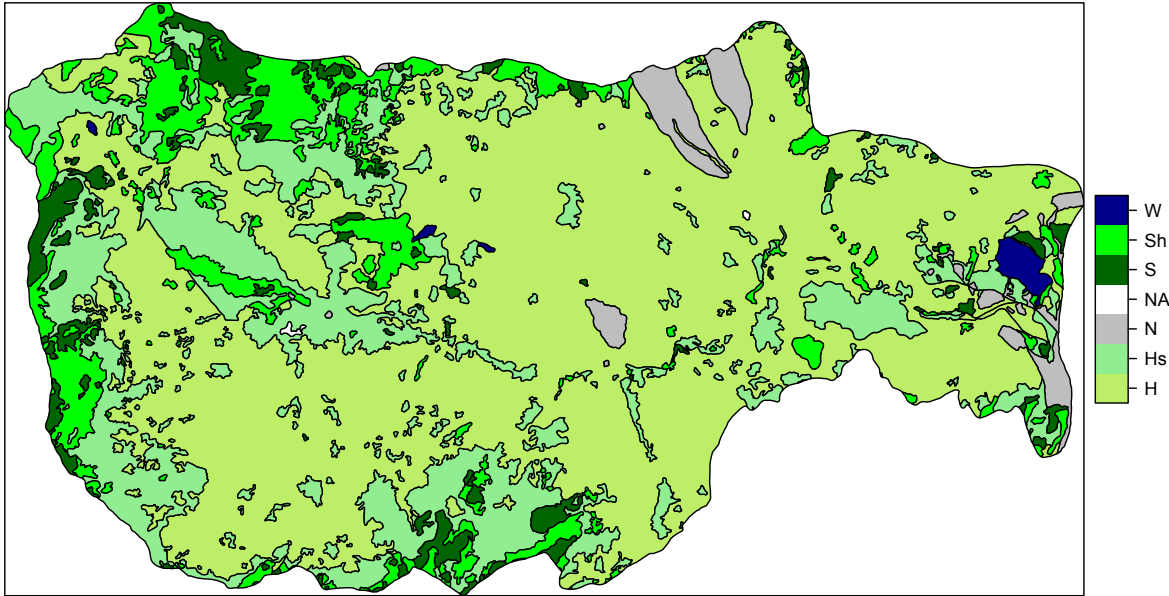
All AIC model selection tables and associated coefficients at for 2012 and 2013 for all species can be found at Google docs site:

<https://drive.google.com/folderview?id=0B-YYc7ZHIj85cnBFdHd4RzMwRUk&usp=sharing>

Column names for the model coefficients use the following notation: coefficient = parameter(covariate) and standard error = SEparameter(covariate). Parameter abbreviations are p = detection probability, psi = initial occupancy, col = colonization/settlement, ext = extinction/vacancy. Parameter(Int) refers to the intercept. 'nPars' is the number of parameters estimated in the model. Each model is ranked by its AIC score, which represents how well the model fits the data. A lower Δ AIC (delta) value is indicative of a better model. The probability that the model (of the models tested) would best explain the data is indicated by AICwt.

APPENDIX 4.1. Species list and life history traits used in analysis. Detection method and sex indicate the types of detections used for each species. Det. meth = song and Sex = male means that we only included detections of singing males. Det. meth. = any and Sex = all indicates that for a given species we included any detection (song, call, visual) and both sexes and unknown sex individuals. Prevalence is the mean proportion of sites occupies across the entire Hubbard Brook Valley for all years of the study (1999-2012). SSI = species specialization index (see methods for how this variable is calculated), low value indicates a generalist species and a high number indicates a specialist species. Mean Elv, CH, and BA refer to the mean elevation, canopy height, and basal area at which the species is most abundant. Migration: LD = long distance, SD = short distance, RES = resident. Migration, survival, reproductive output from BNA accounts. Body mass obtained from Sibley (Sibley 2000).

Species common name	Species code	Family	Scientific name	Det. Meth.	Sex	Prevalence	SSI	Mean Elv	Mean CH	Mean BA	Migration	Survival	Repro. output	Body mass
American redstart	AMRE	PARULIDAE	<i>Setophaga ruticilla</i>	song	male	0.069	0.75	587.08	30.11	40.81	LD	0.48	3.82	8.3
Black-and-white warbler	BAWW	PARULIDAE	<i>Mniotilta varia</i>	song	male	0.033	0.39	623.73	24.37	31.62	LD	0.71	5	10.7
Black-capped chickadee	BCCH	PARIDAE	<i>Poecile atricapillus</i>	any	all	0.175	0.14	785.30	31.30	42.80	RES	0.51	7	11
Blue-headed vireo	BHVI	VIREONIDAE	<i>Vireo solitarius</i>	song	male	0.166	0.21	653.01	25.07	35.31	SD	NA	4	16
Blackburnian warbler	BLBW	PARULIDAE	<i>Setophaga fusca</i>	song	male	0.533	0.14	659.59	27.89	38.37	LD	NA	4	9.8
Blue jay	BLJA	CORVIDAE	<i>Cyanocitta cristata</i>	any	all	0.042	0.14	710.30	29.22	39.18	RES	0.53	5	85
Blackpoll warbler	BLPW	PARULIDAE	<i>Setophaga striata</i>	song	male	0.084	0.60	929.04	20.55	33.57	LD	NA	8	13
Brown creeper	BRCR	CERTHIIDAE	<i>Certhia americana</i>	song	male	0.143	0.31	637.16	24.48	33.89	SD	0.44	5.8	8.4
Black-throated blue warbler	BTBW	PARULIDAE	<i>Setophaga caerulescens</i>	song	male	0.620	0.41	726.09	30.02	39.04	LD	0.87	7.6	10.2
Black-throated green warbler	BTNW	PARULIDAE	<i>Setophaga virens</i>	song	male	0.629	0.21	717.64	28.71	38.64	LD	0.67	4	8.8
Canada warbler	CAWA	PARULIDAE	<i>Cardellina canadensis</i>	song	male	0.057	0.28	730.83	24.34	31.66	LD	NA	4.8	10.3
Cedar waxwing	CEDW	BOMBYCILLIDAE	<i>Bombycilla cedrorum</i>	any	all	0.020	0.57	712.53	25.96	37.81	LD	0.45	8	32
Chimney swift	CHSW	APODIDAE	<i>Chaetura pelagica</i>	any	all	0.043	0.73	633.89	27.27	35.78	LD	0.63	4.16	23
Downy woodpecker	DOWO	PICIDAE	<i>Picoides pubescens</i>	any	all	0.010	1.77	567.68	28.31	36.73	RES	NA	4.81	27
Eastern wood-pewee	EAWP	TYRANNIDAE	<i>Contopus virens</i>	song	male	0.011	1.04	472.17	27.53	33.67	LD	NA	3	14
Golden-crowned kinglet	GCKI	REGULIDAE	<i>Regulus satrapa</i>	song	male	0.173	0.62	727.57	23.29	35.22	RES	0.11	17.2	6
Hairy woodpecker	HAWO	PICIDAE	<i>Picoides villosus</i>	any	all	0.086	0.31	659.31	27.27	36.57	RES	NA	4	66
Hermit Thrush	HETH	TURDIDAE	<i>Catharus guttatus</i>	song	male	0.103	0.57	611.32	26.23	35.04	SD	0.48	3.36	31
Magnolia warbler	MAWA	PARULIDAE	<i>Setophaga magnolia</i>	song	male	0.157	0.72	856.38	22.97	35.38	LD	0.41	4	8.7
Yellow-rumped warbler	YRWA	PARULIDAE	<i>Setophaga coronata</i>	song	male	0.260	0.48	749.63	24.00	35.36	SD	0.45	4	12.3
Nashville warbler	NAWA	PARULIDAE	<i>Oreothlypis ruficapilla</i>	song	male	0.026	0.97	835.89	20.61	33.96	LD	0.36	4.71	8.7
Ovenbird	OVEN	PARULIDAE	<i>Seiurus aurocapilla</i>	song	male	0.474	0.81	661.68	29.87	39.03	LD	0.57	4	19.5
Pileated woodpecker	PIWO	PICIDAE	<i>Dryocopus pileatus</i>	any	all	0.010	0.74	568.98	26.69	34.63	RES	0.54	4	290
Purple finch	PUFI	FRINGILLIDAE	<i>Haemorhous purpureus</i>	song	male	0.039	0.47	712.66	21.71	32.63	SD	0.71	8	25
Rose-breasted grosbeak	RBGR	CARDINALIDAE	<i>Pheucticus ludovicianus</i>	song	male	0.015	0.66	534.15	25.96	34.02	LD	0.61	4	45
Red-breasted nuthatch	RBNU	SITTIDAE	<i>Sitta canadensis</i>	any	all	0.050	0.53	770.24	23.95	35.56	RES	NA	5.8	10
Red-eyed vireo	REVI	VIREONIDAE	<i>Vireo olivaceus</i>	song	male	0.491	0.67	663.09	30.70	39.89	LD	0.53	3.1	17
Ruby-throated hummingbird	RTHU	TROCHILIDAE	<i>Archilochus colubris</i>	any	all	0.011	0.90	538.91	24.64	32.87	LD	0.31	2	3.2
Ruffed grouse	RUGR	PHASIANIDAE	<i>Bonasa umbellus</i>	any	all	0.020	0.69	694.60	24.85	32.51	RES	0.34	11.5	580
Dark-eyed junco	DEJU	EMBERIZIDAE	<i>Junco hyemalis</i>	song	male	0.119	0.60	809.01	22.47	33.63	SD	0.49	4	19
Scarlet tanager	SCTA	CARDINALIDAE	<i>Piranga olivacea</i>	song	male	0.060	1.07	474.87	25.88	34.59	LD	NA	3.8	28
Swainson's thrush	SWTH	TURDIDAE	<i>Catharus ustulatus</i>	song	male	0.161	0.34	695.94	24.38	34.89	LD	0.57	3.53	31
Veery	VEER	TURDIDAE	<i>Catharus fuscescens</i>	song	male	0.012	1.36	440.83	26.72	36.00	LD	NA	4	31
White-breasted nuthatch	WBNU	SITTIDAE	<i>Sitta carolinensis</i>	any	all	0.026	0.38	597.39	27.09	35.73	RES	0.63	6.4	21
Winter wren	WIWR	TROGLODYTIDAE	<i>Troglodytes hiemalis</i>	song	male	0.199	0.36	667.11	24.31	34.44	SD	0.39	14	9
White-throated sparrow	WTSP	EMBERIZIDAE	<i>Zonotrichia albicollis</i>	song	male	0.033	0.80	770.57	21.24	33.34	SD	0.26	4	26
Yellow-bellied flycatcher	YBFL	TYRANNIDAE	<i>Empidonax flaviventris</i>	song	male	0.064	0.73	866.63	19.21	31.52	LD	NA	9	11.5
Yellow-bellied sapsucker	YBSA	PICIDAE	<i>Sphyrapicus varius</i>	any	all	0.118	1.01	604.37	27.93	35.83	SD	NA	4.23	50



APPENDIX 4.2. Map of the Hubbard Brook Experimental Forest study area showing forest cover types. W = Water, Sh = Mixed, softwood-dominated, S = Softwood, N = non-forest, Hs = Mixed, hardwood-dominated, H = Hardwood.

Prior distributions: detection intercept (p_0) \sim uniform distribution between 0 and 1, log lambda (abundance intercept) uniform between -5 and 5, r (abundance rate of change) \sim dunif(-1,1), all covariates for detection (wind, sky, time, day) \sim dunif(-3,3).